

NN08201, 3926

**Low nitrate lettuce cultivations in greenhouses —  
optimal control in the presence of measurable disturbances**

Stefan Cornelis de Graaf

Proefschrift  
ter verkrijging van de graad van doctor  
op gezag van de rector magnificus  
van Wageningen Universiteit,  
Prof. dr. M.J. Kropff,  
in het openbaar te verdedigen  
op vrijdag 31 maart 2006  
des namiddags te half twee in de Aula

SN: 1796230

**Stefan Cornelis de Graaf**

**Optimization of greenhouse lettuce cultivations; optimal control under changing measurable uncontrollable inputs**

**Thesis Wageningen University-With references-With summary in Dutch**

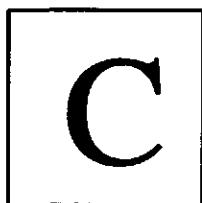
**ISBN 90-8504-378-6**



## Acknowledgement

I carried out the research described in this thesis with a lot of pleasure. The interesting contents of the research and the detailed discussions with Gerrit, Hans and a lot of other people in the Nicolet project contributed to this pleasure. The dynamic atmosphere and the support of Systems and Control group made my working conditions attractive. I am grateful to Gerard for his contribution to this thesis. Furthermore I would like to thank Jasper for his patience with me in case I was in a bad mood after doing research.

I recommend each PhD-student to join the employee's board of Wageningen University and Research Centre or the employee's board of Agrotechnolgy and Food Sciences for a while. These boards offered me some exciting distraction from my research while it settled. But above all, through these boards I had a lot of enjoyable contacts with colleagues and tight bonds with Wageningen University and Research Centre.



## C. Contents

1	Problem analysis and demarcation.....	1
1.1	Introduction.....	1
1.2	Effects of nitrate and related chemical compounds on human health .....	2
1.3	EU-directive and variations of lettuce nitrate concentrations grown in European countries.....	3
1.4	Lettuce cultivation data and relevance of solving lettuce cultivation problems in The Netherlands and Belgium.....	3
1.5	Solution direction.....	5
1.6	Quick economic evaluation of climate condition adjustment effects on nitrate concentrations .....	8
1.7	Final horticultural problem statement.....	10
2	Aspects related to solving the optimal control problem .....	15
2.1	Introduction.....	15
2.2	Mathematical formulation of general fixed-time optimal control problems .....	16
2.3	Difference between open-loop and closed-loop optimal control problems .....	17
2.4	Necessary and sufficient optimality conditions .....	18
2.5	Selection of optimisation algorithms .....	19
2.5.1	Selection of an open-loop optimisation algorithm.....	20
2.5.2	Selection of a closed-loop optimisation algorithm .....	21
2.6	Final optimal control problem statement.....	23
3	Specification of optimal control problem equations .....	25
3.1	Introduction.....	25
3.2	Dynamic lettuce growth and nitrate accumulation model .....	25
3.2.1	Mathematical outline of dynamic lettuce growth and nitrate accumulation model...25	
3.2.2	Biological interpretation of the dynamic lettuce growth and nitrate accumulation model .....	29
3.3	Dynamic climate model .....	31
3.3.1	Mathematical outline of dynamic climate model.....	31
3.3.2	Physical interpretation of dynamic climate model.....	34
3.4	Cultivation performance model .....	35
3.4.1	Mathematical outline of the cultivation performance model.....	35
3.4.2	Economical interpretation of the cultivation performance model .....	36
3.5	Fit of mathematical models in general fixed-time optimal control problem .....	39
4	Open-loop optimal control.....	41
4.1	Test of ACW-gradient optimisation algorithm in computation of an optimal control policy for achieving acceptable nitrate concentration of greenhouse lettuce .....	41

## C Contents

4.1.1	Introduction .....	41
4.1.2	The basic gradient algorithm.....	42
4.1.3	The ACW-method.....	44
4.1.4	Lettuce-greenhouse example.....	45
4.1.5	Conclusions .....	51
4.2	Optimal greenhouse climate control for achieving specified lettuce nitrate concentrations .	52
4.2.1	Introduction .....	52
4.2.2	Mathematical formulation.....	53
4.2.3	Numerical optimisation algorithm .....	58
4.2.4	Computations and results .....	60
4.2.5	Conclusion .....	72
5	Closed-loop optimal control.....	75
5.1	Closed-loop optimal control of greenhouse lettuce cultivation under measurable weather conditions .....	75
5.1.1	Introduction .....	75
5.1.2	Mathematical formulation of the optimal control problem.....	77
5.1.3	General outline of the closed-loop control algorithm .....	81
5.1.4	Design of the closed-loop control algorithm for the lettuce problem .....	82
5.1.5	Simulation and performance of the closed-loop control system.....	90
5.1.6	Conclusion .....	101
5.2	Numerical feedback laws for closed-loop singular optimal control with measurable disturbances.....	103
5.2.1	Introduction .....	103
5.2.2	Optimal control problem.....	105
5.2.3	Non-linear system representing the optimal control problem.....	106
5.2.4	Numerical static state feedback laws synthesized by MAFC .....	108
5.2.5	Synthesis and application guide of the static state feedback laws .....	110
5.2.6	Validation of static state feedback laws .....	111
5.2.7	Results .....	113
5.2.8	Discussion .....	114
5.2.9	Conclusions and implications .....	114
6	Conclusion .....	121
6.1	Introduction.....	121
6.2	Horticultural conclusion .....	121
6.3	Control theoretical interpretation of results presented in this thesis.....	122
S.	Summary .....	125
S.1	Introduction.....	125
S.2	Horticultural summary.....	125
S.3	Control summary .....	127
S	Samenvatting .....	129
S.1	Introductie .....	129
S.2	Teeltkundige samenvatting .....	129
S.3	Regeltechnische samenvatting .....	131
A.	Appendix A .....	133
A.1	Rationale of the negative correlation between lettuce nitrate concentration and the ratio of photosynthesis time-integrals and growth time-integrals .....	133
A.2	Simple procedure to estimate climate changes that lead to lettuce nitrate concentrations of ca. 3500 and 4500 ppm .....	135

**Stellingen behorende bij het proefschrift van Stefan Cornelis de Graaf, getiteld:  
Low nitrate lettuce cultivations in greenhouses—  
Optimal control in the presence of measurable disturbances**

- 1 Het closed-loop algoritme uit dit proefschrift stelt de tuinder in staat nitraatophoping in kassla te beheersen, en maakt daardoor een economisch optimale aansturing van de teelt mogelijk (dit proefschrift).
- 2 Zonder de toepassing van automatic differentiation is het onmogelijk om state feedback laws voor singuliere optimale trajecten van complexe of hoog-dimensionale systemen af te leiden (dit proefschrift).
- 3 Schalingsproblemen in de ecologie en geo-informatie wetenschappen kunnen met gelijkvormigheidstheorie opgelost worden.
- 4 Gevarieerd eten is gezonder dan het opvolgen van op onderzoek gebaseerde voedingsadviezen.
- 5 Prestatiecontracten verkleinen de kans op het bereiken van het doel waarvoor ze opgesteld zijn.
- 6 Rechtspraak heft menselijke kwetsbaarheid niet op (de Volkskrant, Forum 23 april 2003).

# 1

## 1 Problem analysis and demarcation

### 1.1 Introduction

This thesis is about optimal greenhouse lettuce cultivations such that lettuce nitrate accumulation above EU imposed maximum concentrations is prevented at maximum profits. This case is an example of two general classes of problems: firstly, crop quality improvement through adjustment of environmental conditions during cultivation and secondly, optimal control of processes that are carried out with a significant number of limitations on process variables while being affected by disturbances. Finding solutions for this problem will be interesting for people working in the area of horticulture as well as for people working in the area of optimal control.

This chapter contains an analysis and demarcation of the horticultural problem. The conclusion of this chapter is a problem statement in terms of an optimal control problem. Interesting aspects related to solving the optimal control problem are introduced and discussed in chapter 2.

This chapter starts with an explanation about effects of nitrate and related chemical compounds on human health that led to the introduction of the EU-directive. Then, maximum lettuce nitrate-concentrations mentioned in the EU-directive are compared with lettuce nitrate concentrations in European and Asian countries. Based on this comparison and also on lettuce cultivation data in different European countries a decision is made to focus on the problem of keeping Dutch and Belgian greenhouse lettuce cultivation economically feasible. Next, effects of (greenhouse) physiological and environmental conditions on lettuce nitrate concentrations and on economic feasibility are studied, because these effects constitute the basis of possible solutions. This chapter ends by phrasing the lettuce cultivation problem in terms of an optimal control problem. A quick economic evaluation shows that out of the three greenhouse climate conditions - greenhouse air temperature, greenhouse air CO<sub>2</sub>-concentration and solar light intensity- manipulation of solar light intensity is not an economically feasible option.

## 1.2 Effects of nitrate and related chemical compounds on human health

Nitrate may have harmful and beneficial effects on human health. Harmful effects consist of proposed relations between combinations of nitrate and related chemical compounds and developments of gastric cancer, urinary bladder cancer and methaemoglobinaemia. Methaemoglobinaemia is a condition that mostly affects infants up to 12 months old and is caused by reduction of nitrate to nitrite and nitric oxide that oxidize hemoglobin in red blood cells to an abnormal form known as methaemoglobin. Methaemoglobin cannot bind or transport oxygen. Beneficial effects consist of proposed relations between nitrate and pathogen killing (Addiscott and Benjamin, 2004; Lundberg, et al., 2004).

Two sources provide humans with nitrate and related chemical compounds: an exogenous source and an endogenous source. One of the exogenous sources is the consumption of vegetables and accounts for 60 through 90 percent (Lundberg, et al., 2004) of daily nitrate intakes on typical western diets. A related chemical compound, nitrite is found in some foodstuffs. For example, it is used as a food additive in meat to prevent botulism and to enhance its appearance. Other exogenous sources include cigarette smoke and car exhausts that contain volatile nitrogen oxides. Some of these are converted to nitrate or nitrite in the body. The main endogenous source is the *L*-arginine-NO pathway, which is always active throughout the body and produces NO from the amino acid *L*-arginine and oxygen. During systemic inflammatory reactions or infections, white blood cells and other cells increase nitrate concentrations considerably through another pathway.

Nitrates and nitrites from both sources mix up in the bloodstream. In case of exogenous nitrates, nitrate is ingested first and then absorbed from the gastrointestinal tract into the bloodstream. Most nitrate is ultimately excreted in the urine, some in the saliva, sweat and possibly some in the intestines. The exact fate of all nitrate in the body is still unresolved as only 60% of isotopically labelled administered nitrate is recovered in the urine (Lundberg, et al., 2004).

Harmful effects of nitrate on human health are not primarily related to nitrate ions themselves. In fact, nitrate has a remarkably low toxicity. Instead, harmful effects arise when nitrate is reduced to nitrite by bacteria in the gastrointestinal tract. Nitrite and nitrate to a smaller extent are both involved in metabolisms that can result in formation of *N*-nitrosamines, which are carcinogenic. Individuals can also be exposed to preformed *N*-nitrosamines, for example from the diet and tobacco products, and in certain working environments (Lundberg, et al., 2004).

Although carcinogenic properties of *N*-nitroso compounds were proved in cell cultures and animal experiments, relations between nitrate intake and gastric cancer in humans have not been proved. In fact, many studies show either no effects or inverse effects.

Nitrite may also have beneficial effects (Lundberg, et al., 2004). It may help killing ingested pathogens in the stomach and improve gastric mucosal blood flow and mucus secretion. Dental caries, skin infections, urinary tract infections may be inhibited by growth-inhibition or self-destruction of harmful bacteria that are exposed to acidified nitrite. Research also showed that



physiological concentrations of nitrite can dilate blood vessels, thereby possibly affecting the vascular tone in ischaemic tissues, platelet function and leukocyte adhesion (Lundberg, et al., 2004).

### **1.3 EU-directive and variations of lettuce nitrate concentrations grown in European countries**

Concerned about harmful effects of nitrate, nitrite and *N*-nitrosamines on human health and despite the fact that 50% of nitrate is produced endogenously from the *L*-arginine-NO pathway, the European Union tries to minimize accumulation of these chemical compounds in the environment and food by imposing maximum vegetable nitrate-concentrations in a directive. By doing this, lettuce nitrate concentrations have become a quality mark. In case of greenhouse grown Butterhead lettuce, maximum allowable nitrate concentrations of lettuce harvested in winter (1 October to 31 March) are 4500 ppm (or mg kg<sup>-1</sup> fresh product) and in summer (1 April to 30 September) 3500 ppm. In case of outdoor grown lettuce, maximum nitrate concentration of lettuce harvested in summer (1 May to 31 August) are 2500 ppm (Siomos and Dogras, 1999).

Whether imposed maximum nitrate concentrations are met depends on geographic locations and climatic conditions of lettuce cultivations. Data about nitrate concentrations in Butterhead lettuce samples in different European and Asian countries in summer, winter and all year round are shown in table 1. This table roughly shows three relationships between nitrate concentrations, geographic locations and climatic conditions. Firstly, nitrate concentrations tend to be higher and therefore tend to exceed imposed maximum nitrate concentrations more likely in samples from northern European countries than those from southern European countries. Secondly, higher nitrate concentrations are found in winter than in summer. Thirdly, nitrate concentrations of lettuce cultivated in greenhouses are usually considerably higher than those cultivated outdoors in seasons and regions where both methods of cultivation are feasible.

### **1.4 Lettuce cultivation data and relevance of solving lettuce cultivation problems in The Netherlands and Belgium**

Lettuce cultivated in northern European countries tend to have nitrate concentrations that exceed imposed maximum concentrations. The extent of this problem and the need to solve this problem is discussed with the help of data on total lettuce cultivation and protected lettuce cultivation in European countries (table 2).

Table 1: Nitrate concentrations in Butterhead lettuce samples in different European and Asian countries in summer, winter and all year round

latitude	country	winter			summer			all year round			references
		nitrate concentration range [ppm]	mean nitrate concentration [ppm]	cultivation conditions	nitrate concentration range [ppm]	mean nitrate concentration [ppm]	cultivation conditions	nitrate concentration range [ppm]	mean nitrate concentration [ppm]	cultivation conditions	
55°-58°	Denmark		2900-4300	a.p.		1400-2700	a.p.	110-5300	2440-2760	a.p.	1
54°-55°	Northern Ireland					1880	p				2
53°-55°	north England								3270	p	2, 3
51°-55°	Ireland	2200-5500	3200-4500	u	900-4700	2200-2800	u				4
51°-55°	England and	430-5310	3120	p	200-4600	2170-2610	p				2, 3
51°-55°	Northern Ireland										3
51°-55°	England and	270-3980	1240-1790	o	20-3060	350-1350	o				2
51°-53°	Northern Ireland										
51°-53°	south England								2680	p	5
51°-53°	Netherlands	310-4710	3080	p	270-5090	2510	p				6
48°-55°	Germany							230-3290	1560 - 2070	u	7
48°-50°	Germany (Bavaria)							210-4040	2060	u	8
51°	Germany (Erfurt)	2350-4550		p	1100-2300		p				9
47°-49°	Austria	<2500-4000		p	<1500-2500		o				10
46°-48°	Switzerland	1300-4300	1400-3600	u	300-3000	700-2500	u		1420	u	11
43°-51°	France							220-2430	1180	u	12
37°-42°	Turkey							140-5540	260	u	13
39°	Spain (Valencia)										14
35°-42°	Greece				470-1950		o	100-510	220-250	u	15
30°-34°	Jordan	5-100	30	o							
p.	all lettuce cultivated on soil, under glass (protected)				o			all lettuce cultivated on soil, outdoors			
a.p.	almost all lettuce cultivated under glass (protected)				u			lettuce cultivated on soil, under glass or outdoors			
1	Petersen and Stoltze (1999)				9			Elmadfa and Burger (1999)			
2	Ysart, <i>et al.</i> (1999)				10			Roorda van Eysinga (1984)			
3	anonymous (2001b, 2004a)				11			L'hironde and L'hironde (2002)			
4	Byrne, <i>et al.</i> (year unknown)				12			Tosun and Ustun (2004)			
5	Van der Schee and Speek (2000, 2002)				13			Domínguez Gento and Domínguez Gento (1994)			
6	anonymous (2004b), Schuddeboom (1995)				14			Storros and Dogras (1999)			
7	anonymous (year unknown)				15			Amr and Hadidi (2001)			
8	Drews, <i>et al.</i> (1995b)										

Table 2: Data on total lettuce cultivation and protected lettuce cultivation in some European countries (anonymous, 2001a; anonymous, 2005; Georges, Van Lierde and Verspecht, 2003)

<i>country name</i>	<i>total lettuce cultivation (kg)</i>	<i>protected lettuce cultivation (kg)</i>
25 countries of European Union	2614·10 <sup>6</sup>	
Spain	990·10 <sup>6</sup>	31·10 <sup>6</sup>
Italy	479·10 <sup>6</sup>	
France	383·10 <sup>6</sup>	
Germany	181·10 <sup>6</sup>	
United Kingdom	154·10 <sup>6</sup>	24·10 <sup>6</sup>
Belgium	93·10 <sup>6</sup>	47·10 <sup>6</sup>
Greece	81·10 <sup>6</sup>	
Netherlands	72·10 <sup>6</sup>	43·10 <sup>6</sup>
Austria	55·10 <sup>6</sup>	
Portugal	51·10 <sup>6</sup>	
Sweden	22·10 <sup>6</sup>	
Hungary	12·10 <sup>6</sup>	
Denmark	9·10 <sup>6</sup>	
Ireland	9·10 <sup>6</sup>	

There are two opinions about this issue. The first opinion is to concentrate lettuce cultivation in southern European countries because these countries currently cultivate low nitrate concentration lettuce that accounts for approximately 75% of total lettuce cultivation in the European Union. This production may be increased easily. The second opinion is to maintain lettuce cultivation and even stimulate low nitrate content lettuce cultivation in northern European countries because lettuce cultivation in these countries is economically feasible (Georges, Van Lierde and Verspecht, 2003).

The second opinion is supported in this thesis. Furthermore, there is a focus on protected, soil bound lettuce cultivation in The Netherlands and Belgium, which have comparable climatic conditions. So, the problem of keeping a low nitrate content in conjunction with an economically feasible lettuce cultivation in The Netherlands and Belgium is assumed relevant enough to offer a solution and is therefore chosen as an example of problems about crop quality improvement.

### 1.5 Solution direction

Solutions to this problem require considerations of two effects: effects of (greenhouse) physiological and environmental conditions on nitrate concentrations and on economic feasibility. These effects have been studied in literature. Table 3 lists studies about effects of physiological conditions and environmental conditions on lettuce nitrate concentrations and table 4 lists studies about effects of physiological conditions and environmental conditions on economic feasibility of lettuce and other vegetable cultivations.

Table 3: Studies about effects of physiological conditions and environmental conditions on lettuce nitrate concentrations

<i>conditions</i>	<i>references</i>
<i>physiological</i>	
concentrations of glucose, fructose, and malate	Behr and Wiebe (1988), anonymous (2002), Drews, et al. (1995a), Drews et al. (1995b), Seginer, Buwalda and Van Straten (1998)
concentrations of potassium, chloride, phosphate, sulfur	Behr and Wiebe (1988), anonymous (2002), Drews, et al. (1995a), Drews et al. (1995b), Corré and Breimer (1979), Maynard (1976), Van der Boon, et al. (1990)
concentrations of other chemical compounds	Drews, et al. (1995a), Drews et al. (1995b), anonymous (2002)
nitrate reductase activity	Chadjaâ, et al. (1999), Gaudreau, et al. (1995)
lettuce fresh weight and various parts of lettuce plants	anonymous (2002), Drews, et al. (1995a), Maynard (1976), Van der Boon, et al. (1990), Abu-Rayyan, et al. (2004), Hanafy Ahmed (2000), Amr and Hadidi (2001), Seginer, Buwalda and Van Straten (1998), anonymous (2002)
lettuce species	Amr and Hadidi (2001), Behr and Wiebe (1988), Drews, et al. (1995a), Drews et al. (1995b), Escobar-Gutiérrez, et al. (2002), Roorda van Eysinga (1984), Maynard (1976), anonymous (2002)
<i>environmental</i>	
solar radiation intensity	anonymous (anonymous, 2002), Chadjaâ, et al. (1999), Corré and Breimer (1979), Dapoigny, et al. (2000), Dapoigny, et al. (1996), Drews et al. (1995b), Maynard (1976), Van der Boon, et al. (1990), Roorda van Eysinga (1984), Steingröver et al. (1993), Seginer, Buwalda and Van Straten (1998), anonymous (anonymous, 2002)
air temperature	Corré and Breimer (1979), Dapoigny, et al. (2000), Drews et al. (1995b), Maynard (1976), Van der Boon, et al. (1990), Roorda van Eysinga (1984), Steingröver et al. (1993), Seginer, Buwalda and Van Straten (1998), anonymous (2002)
CO <sub>2</sub> -concentration in the air	anonymous (2002), Corré and Breimer (1979), Seginer, Buwalda and Van Straten (1998)
fertilization levels	Corré and Breimer (1979), Maynard (1976), Hanafy Ahmed (2000), Van der Boon, et al. (1990), Roorda van Eysinga (1984), Dapoigny, et al. (2000), Dapoigny, et al. (1996), Domínguez Gento and Domínguez Gento (1994)
irrigation levels	Abu-Rayyan, et al. (2004), Aggelides, et al. (1999), Corré and Breimer (1979), Maynard (1976)
storage conditions	Chung, et al. (2004), Dapoigny, et al. (1996), Corré and Breimer (1979)

Table 4: Studies about effects of physiological conditions and environmental conditions on economic feasibility of lettuce and other vegetable cultivations

<i>conditions</i>	<i>references</i>
<i>lettuce cultivation</i>	
environmental conditions	van Henten (1994)*, Dueck, <i>et al.</i> (2004a; 2004b), Ferentinos, <i>et al.</i> (2000)*, anonymous (1998), Ioslovich and Seginer (2000; 2002)*, Stigter and van Straten (2000)*, Seginer, <i>et al.</i> (1991)*
lettuce quality	van Henten (1994)*, Seginer, <i>et al.</i> (1991)*
non-environmental conditions such as labour, renting, etc	anonymous (1998), Ioslovich and Seginer (2000; 2002)*, Seginer, <i>et al.</i> (1991)*, Georges <i>et al.</i> (2003)
<i>other vegetable cultivations</i>	
solar radiation intensity	Dueck, <i>et al.</i> (2004a; 2004b), Tap (2000)*, Zwart (2002), Ferentinos, <i>et al.</i> (2000)*, anonymous (1998)
air temperature	Dueck, <i>et al.</i> (2004a; 2004b), Tap (2000)*, Zwart (2002), Seginer and Sher (1993)*, Alscher, <i>et al.</i> (2001)*, Pohlheim and Heißner (1996)*
CO <sub>2</sub> -concentration in the air	Dueck, <i>et al.</i> (2004a; 2004b), Tap (2000)*, Zwart (2002), Ferentinos, <i>et al.</i> (2000)*, anonymous (1998), anonymous (1992), Alscher, <i>et al.</i> (2001)*, Aikman (1996)*, Pohlheim and Heißner (1996)*
fertilization levels	anonymous (1998)
irrigation levels	anonymous (1998)
storage conditions	anonymous (1998)
non-environmental conditions such as labour, renting, etc	anonymous (2000), anonymous (1998), Seginer and Sher (1993)*, Verhaegh and de Groot (2000), Calatrava-Requena, and Cañero and Javier (2001), Taragola and van Lierde (2000), Georges <i>et al.</i> (2003)

\* Studies about computing optimal cultivation conditions

Greenhouse lettuce growers can use the knowledge about these effects at three moments during lettuce cultivation: at the moment of planting, during cultivation and after the moment of harvesting. At the moment of planting they can do this by choosing a lettuce cultivar and fertilization levels. During lettuce cultivation they can do this by controlling the air temperature, CO<sub>2</sub>-concentration in the air, supplementary solar radiation, irrigation levels and sometimes fertilization levels. After the moment of harvesting they can do this by controlling storage conditions.

Most studies in table 3 are about qualitative effects except for studies carried out by Seginer, Buwalda and Van Straten (1998). They built the only mathematical model that is able to predict dynamics of lettuce nitrate concentration and lettuce fresh weight quantitatively. These predictions are based on data of solar or artificial radiation intensity values, greenhouse air temperatures and greenhouse air CO<sub>2</sub>-concentrations during lettuce cultivations. Most studies in table 4 apply models describing effects of physiological conditions and environmental conditions on cultivation costs or profits of lettuce or other vegetable cultivations. Half of these is about sensitivities of costs or profits to changes of cultivation conditions. The other half is about computing cultivation conditions such that costs are minimized or profits are maximized. These studies belong to the class of optimal control problems.

The horticultural problem about greenhouse lettuce cultivation will be solved as an optimal control problem here. The objective is to compute optimal climate conditions such that the profit is maximized while preventing lettuce nitrate accumulation above EU imposed maximum concentrations. To compute these cultivation conditions a model presented by Seginer, Buwalda and Van Straten and models describing effects of physiological conditions and environmental conditions on cultivations profits are used.

Climate conditions that affect nitrate concentrations effectively will be chosen in the next section.

### 1.6 Quick economic evaluation of climate condition adjustment effects on nitrate concentrations

Three climate conditions can be adjusted to affect nitrate concentrations: solar radiation intensity values, greenhouse air temperatures and greenhouse air CO<sub>2</sub>-concentrations. Not all of these adjustments are economically feasible however. To analyse this, a quick evaluation is made based on results presented by Vanthoor (2002) and some economic rules of thumb.

Results of Vanthoor presented in figure 1 show decreasing lettuce nitrate concentrations with increasing ratio of the time-integral of photosynthesis and time-integral of growth. These ratios can be interpreted as dimensionless numbers that combine effects of global solar radiation intensity, temperatures and CO<sub>2</sub>-concentrations during the last 14 cultivation days ( $1.2 \cdot 10^6$  s) on lettuce nitrate concentrations at harvest time. They were calculated according to the equation:

$$R = \int_0^{t_f} \frac{el\sigma_{Ca}}{el + \sigma_{Ca}} dt \cdot \left( \int_0^{t_f} vke^{c(\bar{t}_s - \bar{r}^*)} dt \right)^{-1} \quad (1)$$

Parameters and inputs in this equation are specified in table 5. The rationale of this relationship is explained in appendix A.

This equation and figure 1 were used to estimate quantitative changes of global solar radiation intensity, CO<sub>2</sub>-concentration and temperature that each lead to typical nitrate concentration decreases of 200 through 500 ppm, depending on the lettuce variety and the required nitrate concentration at harvest. These estimations were done according to a simple estimation procedure developed for greenhouse growers. This procedure is explained in Appendix A. Results of estimations and related costs are in table 6.

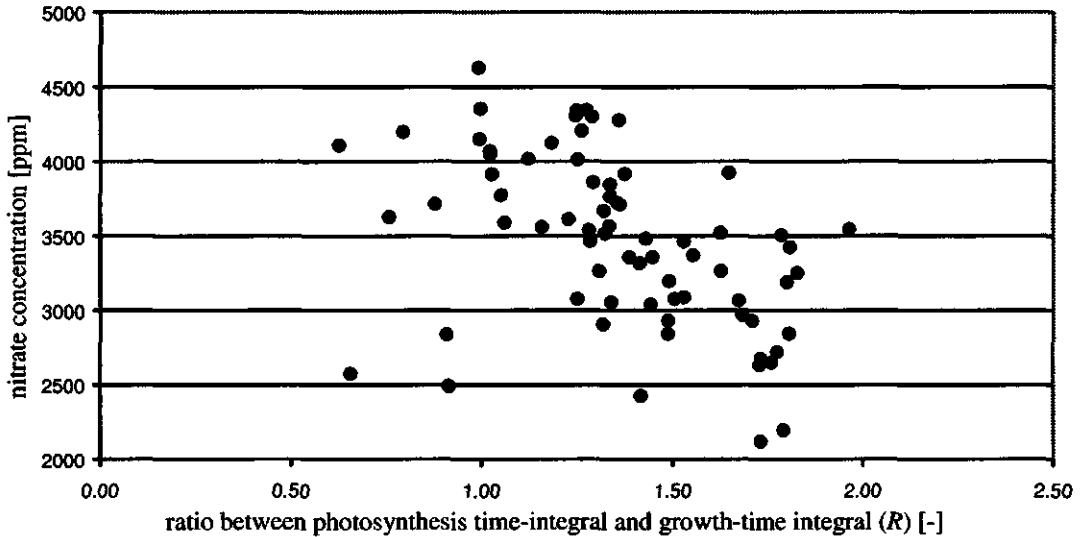


Figure 1: Lettuce nitrate concentration plotted against ratio of the time-integral of photosynthesis and time-integral of growth

Table 5: Specification of parameter and inputs used in equation 1

name	symbol	value	units
<i>parameters</i>			
final time	$t_f$	$1.2 \cdot 10^6$	s
photosynthesis efficiency	$\varepsilon$	0.07	mol [C]·mol <sup>-1</sup> PAP
leaf conductance of CO <sub>2</sub>	$\sigma$	$1.2 \cdot 10^{-3}$	m·s <sup>-1</sup>
growth yield	$\nu$	18.7	mol [C]·m <sup>-2</sup>
specific maintenance rate coefficient	$k$	$0.25 \cdot 10^{-6}$	s <sup>-1</sup>
temperature effect parameter	$c$	0.0693	°C <sup>-1</sup>
reference temperature	$T^*$	20	°C
<i>inputs</i>			
solar radiation intensity	$I$		mol [C]·mol <sup>-1</sup> PAP·m <sup>-2</sup> ·s <sup>-1</sup>
CO <sub>2</sub> -concentration in the greenhouse air	$C_{Ca}$		mol·m <sup>-3</sup>
greenhouse air temperature	$T_a$		°C

Table 6: Estimated changes of global solar radiation intensity, CO<sub>2</sub>-concentration and temperature required to reduce nitrate concentrations by 200 to 500 ppm. Also shown are the associated costs (estimated from anonymous (1992), anonymous (1998), Zwart (2002), Georges, Van Lierde and Verspecht (2003))

	<i>estimated changes</i>	<i>related costs</i>
global solar radiation intensity	$+2 \cdot 10^7 \text{ J} \cdot \text{m}^{-2}$	$+1 \text{ €} \cdot \text{m}^{-2}$
temperature	$-3^\circ\text{C}$	$-6 \cdot 10^{-2} \text{ €} \cdot \text{m}^{-2}$
CO <sub>2</sub> -concentration	$+361 \text{ ppm} \cdot \text{m}^{-2}$	$+3 \cdot 10^{-3} \text{ €} \cdot \text{m}^{-2}$

To define whether these changes are economically feasible, related costs need to be compared with lettuce cultivation profits which are approximately  $-1$  to  $1 \text{ €} \cdot \text{m}^{-2}$  (anonymous, 1998). The costs related to the required estimated temperature changes are two orders of magnitude smaller than the profits. This means that temperature adjustments hardly affect profits and therefore are economically feasible. The same is true for CO<sub>2</sub>-concentration changes, because related costs are three orders of magnitude smaller than profits. Solar radiation intensity adjustments are not economically feasible, because related costs are in the same order of magnitude as profits.

Concluding, in this thesis only optimal trajectories of temperature and CO<sub>2</sub>-concentrations are computed, because these adjustments are economically feasible.

## 1.7 Final horticultural problem statement

The problem of keeping a low nitrate content and an economically feasible lettuce cultivation in the Netherlands and Belgium is studied in this thesis. This problem belongs to the general class of horticultural problems about crop quality improvement through adjustment of environmental conditions during cultivation. It will be solved as an optimal control problem through the computation of optimal greenhouse air temperatures and greenhouse air CO<sub>2</sub>-concentrations such that the profit is maximized while lettuce nitrate accumulation above EU imposed maximum concentrations is prevented. To compute these conditions a model presented by Seginer, Buwalda and Van Straten (1998) and models describing effects of physiological conditions and environmental conditions on cultivations profits are used.

## References

- Abu-Rayyan, A., B. H. Kharawish and K. Al-Ismail (2004). Nitrate content in lettuce (*Lactuca sativa* L) heads in relation to plant spacing, nitrogen form and irrigation level. *Journal of the science of food and agriculture*, 84, 931-936.
- Addiscott, T. M. and N. Benjamin (2004). Nitrate and human health. *Soil Use and Management*, 20, 98-104.



- Aggelides, S., I. Assimakopoulos, P. Kerkides and A. Skondras (1999). Effects of soil water potential on the nitrate content and the yield of lettuce. *Communications in soil science and plant analysis*, 30, 235-243.
- Aikman, D. P. (1996). A procedure for optimizing carbon dioxide enrichment of a glasshouse tomato crop. *Journal agricultural engineering research*, 63, 171-184.
- Alscher, G., H. Krug and H.-P. Liebig (2001). Optimisation of CO<sub>2</sub> and temperature control in greenhouse crops by means of growth models at different abstraction levels 1. control strategies, growth models and input data. *Gartenbauwissenschaft*, 66, 105-114.
- Amr, A. and N. Hadidi (2001). Effect of cultivar and harvest date on nitrate (NO<sub>3</sub>) and nitrite (NO<sub>2</sub>) content of selected vegetables grown under open field and greenhouse conditions in Jordan. *Journal of food composition and analysis*, 14, 59-67.
- anonymous (1992). *Beslissingsmodel voor CO<sub>2</sub> in de glastuinbouw investeringsselectie & doseertechniek: Aanvullend CO<sub>2</sub> doseren en warmteopslag; kwantitatieve informatie (Report)*, Nederlandse Onderneming voor Energie en Milieu, Proefstation voor Tuinbouw onder Glas, Sittard, Naaldwijk, The Netherlands.
- anonymous (1998). *Kwantitatieve informatie voor de glastuinbouw 1998-1999*, Proefstation voor Bloemmisterij en Glasgroente, Naaldwijk, The Netherlands.
- anonymous (2000). *Land- en tuinbouwcijfers 2000*, Landbouw-economisch Instituut, Centraal Bureau voor de Statistiek, 's Gravenhage, The Netherlands.
- anonymous (2001a). *Anuario de estadística agroalimentaria, Anexo 2001*, Ministerio de Agricultura, Pesca y Alimentación,
- anonymous (2001b). *UK monitoring programme for nitrate in lettuce and spinach (number 16/01) (Report)*, Food Standards Agency, London.
- anonymous (2002). *Optimal control of nitrate accumulation in greenhouse lettuce and other leafy vegetables; Fair project CT 98-4362 (Report)*, Haifa, Israel. Wageningen, The Netherlands. Ghent, Belgium. Rumbek, Belgium, Aalsmeer, The Netherlands.
- anonymous (2004a). *UK monitoring programme for nitrate in lettuce and spinach 2000-2002 (Report)*, Food Standards Agency, London.
- anonymous (2004b). *Lebensmittel-Monitoring; Ergebnisse des bundesweiten Lebensmittel-Monitorings des Jahre 1995 bis 2002 (Report)*, Bundesamt für Verbraucherschutz und Lebensmittelsicherheit, Berlin.
- anonymous (2005). *Eurostat*, [www.europa.eu.int/comm/eurostat/](http://www.europa.eu.int/comm/eurostat/), Luxembourg.
- anonymous (year unknown). *Jahresbericht 2001 (Report)*, Bayerisches Landesamt für Gesundheit und Lebensmittelsicherheit, Erlangen, Germany.
- Behr, U. and H.-J. Wiebe (1988). Beziehung zwischen dem Gehalt an Nitrat und anderen Osmotica des Zellsaftes bei Kopfsalatsorten (*Lactuca sativa* L.). *Gartenbauwissenschaft*, 53, 206-210.
- Byrne, C., M. J. Maher, M. J. Hennerty, M. J. Mahon and P. A. Walshe (year unknown). *Reducing the nitrate content of protected lettuce (Report)*, Irish Agriculture and Food Development Authority, Dublin.
- Calatrava-Requena, J., R. Cañero and J. Ortega (2001). Productivity and cultivation costs analysis in plastic greenhouses in the Nijar (Almería) area. *Acta Horticulturae*, 559, 737-744.
- Chadjaâ, H., L.-P. Vézina and A. Gosselin (1999). Effets d'un éclairage d'appoint sur la croissance et le métabolisme azoté primaire de la laitue mâche et de l'épinard cultivés en serre. *Canadian journal of plant science*, 79, 421-426.
- Chung, J.-C., S.-S. Chou and D.-F. Hwang (2004). Changes in nitrate and nitrite of four vegetables during storage at refrigerated and ambient temperatures. *Food additives and contaminants*, 21, 317-322.
- Corré, W. J. and T. Breimer (1979). *Nitrate and nitrite in vegetables*, Centre for Agricultural Publishing and Documentation, Wageningen, The Netherlands.

- Dapigny, L., S. de Tourdonnet, J. Roger-Estrade, M.-H. Jeuffroy and A. Fleury (2000). Effect of nitrogen nutrition on growth and nitrate accumulation in lettuce (*Lactuca sativa* L.) under various conditions of radiation and temperature. *Agronomie*, 20, 843-855.
- Dapigny, L., P. Robin, C. Raynal-Lacroix and A. Fleury (1996). Relation entre la vitesse relative de croissance et la teneur en azote chez laitue (*Lactuca sativa* L.). Effets de l'ombrage et du niveau de l'alimentation minérale. *Agronomie*, 16, 529-539.
- Domínguez Gento, P. and A. Domínguez Gento (1994). Nitratos en lechugas procedentes de cultivos convencionales y ecológicos en la provincia de Valencia. In: *Proceedings of the Congreso de la sociedad española de agricultura ecológica*. Toledo.
- Drews, M., I. Schonhof and A. Krumbein (1995a). Gehalt und Verteilung von Inhaltsstoffen in Kopfsalat. *Gartenbauwissenschaft*, 60, 287-293.
- Drews, M., I. Schonhof and A. Krumbein (1995b). Nitrat-, Vitamin C-,  $\beta$ -Carotin- und Zuckergehalt von Kopfsalat im Jahresverlauf beim Anbau im Gewächshaus (*Lactuca sativa* L.). *Gartenbauwissenschaft*, 60, 180-187.
- Dueck, T., A. Elings, F. Kempkes, P. Knies, N. Van de Braak, N. Garcia, G. Heij, J. Janse, R. Kaarsemaker, P. Korsten, R. Maaswinkel, M. Ruijs, C. Reijnders and R. Van der Meer (2004a). *Energie in kentallen: zoek naar een nieuwe balans, nota 312 (Report)*, Plant research international B.V., Wageningen.
- Dueck, T., A. Elings, F. Kempkes, P. Knies, N. Van de Braak, N. Garcia, G. Heij, J. Janse, R. Kaarsemaker, P. Korsten, R. Maaswinkel, M. Ruijs, C. Reijnders and R. Van der Meer (2004b). *Energie in kentallen: zoek naar een nieuwe balans, nota 313 (Report)*, Plant research international B.V., Wageningen.
- Elmadfa, I. and P. Burger (1999). *Expertengutachten zur Lebensmittelsicherheit Nitrat (Report)*, Institut für Ernährungswissenschaften der Universität Wien, Wien.
- Escobar-Gutiérrez, A. J., I. G. Burns, A. Lee and R. N. Edmondson (2002). Screening lettuce cultivars for low nitrate content during summer and winter production. *Journal of Horticultural Science & Biotechnology*, 77, 232-237.
- Ferentinos, K. P., L. D. Albright and D. V. Ramani (2000). Optimal light integral and carbon dioxide concentration combinations for lettuce in ventilated greenhouses. *Journal of agricultural engineering research*, 77, 309-315.
- Gaudreau, L., J. Charbonneau, L.-P. Vezina and A. Gosselin (1995). Effects of photoperiod and photosynthetic photon flux on nitrate content and nitrate reductase activity in greenhouse-grown lettuce. *Journal of plant nutrition*, 18, 437-453.
- Georges, H., D. Van Lierde and A. Verspecht (2003). *De Vlaamse glastuinbouw en zijn concurrenten (Report)*, Centrum voor Landbouweconomie, Ministerie van de Vlaamse Gemeenschap, Brussels, Belgium.
- Hanafy Ahmed, A. H., J. F. Mishriky and M. K. Khalil (2000). Reducing nitrate accumulation in lettuce (*Lactuca sativa* L.) plants by using different biofertilizers. In: *Proceedings of ICEHM2000* pp. 509-517. Cairo University, Egypt.
- Ioslovich, I. and I. Seginer (2000). Acceptable nitrate concentration of greenhouse lettuce: an optimal control policy for temperature, plant spacing and nitrate supply. In: *Preprints of Agricontrol 2000; International conference on modelling and control in agriculture, horticulture and post-harvested processing* pp. 89-94. IFAC, Wageningen University & Research Centre, Royal Dutch Institute of Engineers, Wageningen, The Netherlands.
- Ioslovich, I. and I. Seginer (2002). Acceptable nitrate concentration of greenhouse lettuce: two optimal control policies. *Biosystems Engineering*, 83, 199-215.
- L'hirondel, J. L. and J. L. L'hirondel (2002). *Nitrate and man*, CABI Publishing, Oxon, United Kingdom.
- Lundberg, J. O., E. Weitzberg, J. A. Cole and N. Benjamin (2004). Nitrate, bacteria and human health. *Nature Reviews*, 2, 593-602.

- Maynard, D. N., A. V. Barker, P. L. Minotti and N. H. Peck (1976). Nitrate accumulation in vegetables. In: *Advances in agronomy* (Brady, N. C. (Ed)), pp. 71-118. Academic Press, New York.
- Petersen, A. and S. Stoltze (1999). Nitrate and nitrite in vegetables on the Danish market: content and intake. *Food additives and contaminants*, 16, 291-299.
- Pohlheim, H. and A. Heißner (1996). *Optimale Steuerung des Klimas im Gewächshaus mit Evolutionären Algorithmen: Grundlagen, Verfahren und Ergebnisse (Report)*, Technische Universität Ilmenau, Ilmenau, Germany.
- Roorda van Eysinga, J. P. N. L. (1984). Nitrate and glasshouse vegetables. *Fertilizer research*, 5, 149-156.
- Schuddeboom, L. J. (1995). *A survey of the exposure to nitrate and nitrite in foods (including drinking water)*, Council of Europe Press, Bilthoven, Netherlands.
- Seginer, I., F. Buwalda and G. van Straten (1998). Nitrate concentration in greenhouse lettuce: a modelling study. *Acta Horticulturae*, 456, 189-197.
- Seginer, I. and A. Sher (1993). Optimal greenhouse temperature trajectories for a multi-state-variable tomato model. In: *The computerized greenhouse* (Hashimoto, Y., G. P. A. Bot, W. Day, H.-J. Tantau and H. Nonami. (Ed)), pp. 153-172. Academic press, San Diego, California.
- Seginer, I., G. Shina, L. D. Albright and L. S. Marsh (1991). Optimal temperature setpoints for greenhouse lettuce. *Journal of agricultural engineering research*, 49, 209-226.
- Siomos, A. S. and C. C. Dogras (1999). Nitrates in vegetables produced in Greece. *Journal of vegetable crop production*, 5, 3-13.
- Steingröver, E. G., J. W. Steenhuizen and J. Van der Boon (1993). Effects of low light intensities at night on nitrate accumulation in lettuce grown on a recirculating nutrient solution. *Netherlands Journal of Agricultural Science*, 41, 13-21.
- Stigter, J. D. and G. van Straten (2000). Nitrate control of leavy vegetables; a classical dynamic optimization approach. In: *Preprints of Agricontrol 2000; International conference on modelling and control in agriculture, horticulture and post-harvested processing* pp. 95-99. IFAC, Wageningen University & Research Centre, Royal Dutch Institute of Engineers, Wageningen, the Netherlands.
- Tap, F. (2000). *Economics-based optimal control of greenhouse tomato crop production (PhD-thesis)*, Wageningen University, Wageningen, The Netherlands.
- Taragola, N. and D. Van Lierde (2000). Competitive strategies in the sector of greenhouse tomato production in Belgium. *Acta Horticulturae*, 514, 149-155.
- Tosun, I. and N. S. Ustun (2004). Nitrate content of lettuce grown in the greenhouse. *Bulletin of environmental, contamination and toxicology*, 72, 109-113.
- Van der Boon, J., J. W. Steenhuizen and E. G. Steingröver (1990). Growth and nitrate concentration of lettuce as affected by total nitrogen and chloride concentration,  $\text{NH}_4/\text{NO}_3$  ratio and temperature of the recirculating nutrient solution. *Journal of horticultural science*, 65, 309-321.
- van der Schee, H. A. and A. J. Speek (2000). *Report of nitrate monitoring results concerning Regulation EU 194/97; The Netherlands 2000 (Report)*, Inspectorate for health protection and veterinary public health (KVV), Amsterdam.
- van der Schee, H. A. and A. J. Speek (2002). *Report of nitrate monitoring results concerning Regulation EU 194/97; The Netherlands 2001 (Report)*, Inspectorate for health protection and veterinary public health (KVV), Amsterdam.
- van Henten, E. J. (1994). *Greenhouse climate management: an optimal control approach (PhD-thesis)*, Landbouwniversiteit Wageningen, Wageningen, The Netherlands.
- Vanthoor, E. (2002). Relation photosynthesis, growth and nitrate in Beitem experiments. In: *Final report of Nicolet-project FAIR6-CT98-4362 (Report)*. Wageningen University, Wageningen.

- Verhaegh, A. P. and N. S. P. de Groot (2000). Chain production costs of fruit vegetables: a comparison between Spain and the Netherlands. *Acta Horticulturae*, 514, 177-180.
- Ysart, G., R. Clifford and N. Harrison (1999). Monitoring for nitrate in UK-grown lettuce and spinach. *Food additives and contaminants*, 16, 301-306.
- Zwart (2002). *Analyzing energy-saving options in greenhouse cultivation using a simulation model (PhD-thesis)*, Wageningen University, Wageningen, The Netherlands.

# 2

## 2 Aspects related to solving the optimal control problem

### 2.1 Introduction

This chapter is an introduction about aspects related to solving the optimal control problem presented in chapter 1. Most of these aspects will be elaborated upon in next chapters. The aspects are:

- Mathematical formulation of general fixed-time optimal control problems
- Difference between open-loop and closed-loop optimal control problems
- Necessary and sufficient optimality conditions
- Selection of a suitable open-loop optimisation algorithm
- Selection of a suitable closed-loop optimisation algorithm

These aspects will be discussed because the optimal control problem cannot be solved directly from the models about effects of greenhouse air temperatures and  $\text{CO}_2$ -concentrations on lettuce nitrate concentrations and economic feasibility. These models describe effects of *all possible* temperature and  $\text{CO}_2$ -concentration trajectories on nitrate concentrations and economic feasibility. They do not describe *optimal* temperature and  $\text{CO}_2$ -concentration trajectories.

These models can be fit in a mathematical formulation of optimal control problems so that general equations exist which these trajectories need to fulfil in order to be optimal. These equations are called necessary and sufficient optimality conditions and are actually used to compute the optimal trajectories. These trajectories can be solutions of either open-loop or closed-loop optimal control problems as will be explained in this chapter. The computations are often too complex to be made analytically, so numerical algorithms need to be used.

The numerical computations presented in this thesis are interesting for people working in the area of optimal control because they incorporate solving optimal control problems with non-linear differential algebraic equations, affected by high frequency disturbances and end-constraints.

## 2.2 Mathematical formulation of general fixed-time optimal control problems

In this thesis the model is cast in the form of a general fixed-time optimal control problem. For convenience this problem is stated using the so-called *Mayer-formulation* (Bryson, 1999; Stengel, 1994).

Given the augmented system

$$\dot{\underline{x}} = \begin{bmatrix} \dot{\underline{x}}^m \\ \dot{\underline{x}}^L \end{bmatrix} = \begin{bmatrix} \underline{m}(\underline{x}^m, \underline{z}, \underline{u}, \underline{d}) \\ \underline{L}(\underline{x}^m, \underline{u}) \end{bmatrix} = \underline{f}(\underline{x}, \underline{z}, \underline{u}, \underline{d}) \quad (2)$$

and the constraints

$$\underline{Q} = \underline{n}(\underline{x}, \underline{z}, \underline{d}, \underline{u}) \quad (3)$$

$$\underline{Q} \geq \underline{c}(\underline{u}) \quad (4)$$

$$\underline{Q} \geq \underline{s}(\underline{z}) \quad (5)$$

$$\underline{Q} \leq \underline{\psi}(\underline{x}_f) \quad \underline{x}_f = \underline{x}(t_f) \quad (6)$$

maximise

$$J = \phi(\underline{x}_f) \quad (7)$$

where

$$\begin{array}{llllll} \underline{x} \in \mathbb{R}^{n_x} & \underline{x}^m \in \mathbb{R}^{n_x^m} & \underline{x}^L \in \mathbb{R}^{n_x^L} & \underline{u} \in \mathbb{R}^{n_u} & \underline{z} \in \mathbb{R}^{n_z} & \underline{d} \in \mathbb{R}^{n_d} \\ \underline{m} \in \mathbb{R}^{n_m} & \underline{L} \in \mathbb{R}^{n_L} & \underline{n} \in \mathbb{R}^{n_n} & \underline{\psi} \in \mathbb{R}^{n_\psi} & \underline{c} \in \mathbb{R}^{n_c} & \underline{s} \in \mathbb{R}^{n_s} \end{array}$$

Furthermore  $\underline{x}^m(t)$  is the system state vector  $\underline{x}^L(t)$  is the running costs and  $\underline{d}(t)$  the high-frequency disturbance vector and  $\underline{u}(t)$  the control input vector. The vector  $\underline{z}(t)$  is a vector of quasi steady states, which originates from the assumption that the rate of change of these variables is so fast as compared to that of other states that these variables always reach a quasi steady state. The

function  $\underline{m}(\underline{x}^m, \underline{z}, \underline{d}, \underline{u})$  is the system state function,  $\underline{n}(\underline{x}, \underline{z}, \underline{d}, \underline{u})$  an algebraic constraint function for the calculation of the quasi steady states and  $L(\underline{x}^m, \underline{u})$  the running cost function. Equations 4, 5 and 6 represent inequality constraints on  $\underline{c}(\underline{u})$ ,  $\underline{s}(\underline{z})$  and  $\underline{\psi}(\underline{x}_f)$  that are functions of the inputs, quasi steady states and final value of the states, respectively. The function  $\phi(\underline{x}_f)$  that is maximized is a measure for economic feasibility of lettuce cultivations. The functions  $\underline{m}$ ,  $L$ ,  $\underline{n}$ ,  $\underline{c}$ ,  $\underline{s}$ ,  $\underline{\psi}$ , and  $\phi$  are assumed to be differentiable with respect to  $\underline{x}$ ,  $\underline{u}$ ,  $\underline{z}$ ,  $\underline{x}_f$  and  $\underline{d}$ .

The system state function  $\underline{m}$  in this thesis consists of equations from the model presented by Seginer, Buwalda and Van Straten and a model describing dynamics of greenhouse environmental or climate conditions. The algebraic constraint function,  $\underline{n}$  consists of equations from the last model. Both models are discussed in chapter 3. Details on the constraints with respect to the inputs and quasi steady states presented by equations 4 and 5 are also discussed there.

Note that the optimal control problem is written in the *Mayer-formulation* (Bryson, 1999; Stengel, 1994), which means that the problem is an *end-point optimal control problem*. This is not a restrictive class of optimal control problems because any optimal control problem where the running costs function  $L$  is part of the performance index (equation 8) can be cast in equations 2 to 7. This is done by introducing an additional state equation for the running costs function.

$$J = \phi'(\underline{x}_f) + \int_{t_0}^{t_f} L(\underline{x}^m, \underline{u}) dt \quad (8)$$

$$\text{where } \phi'(\underline{x}_f) = \phi(\underline{x}_f) - x_f^L = \phi(\underline{x}_f) - \int_{t_0}^{t_f} L(\underline{x}^m, \underline{u}) dt$$

A fixed final time is assumed in the performance index. This and other details of the performance index are discussed in chapter 3.

### 2.3 Difference between open-loop and closed-loop optimal control problems

It is essential to know whether optimal control problems are solved in open-loop or in closed-loop. Solving optimal control problems in open-loop means that observed state values are assumed to evolve according to the system state function  $\underline{m}$  and that disturbance values  $d(t)$  evolve along known trajectories so that there are no unforeseen changes in state and disturbance values. Solving optimal control problems in open-loop produces control trajectories that are optimal for these assumptions. Solving optimal control problems in closed-loop produces control trajectories that respond optimally to observed unforeseen changes in state and disturbance values.

In this thesis, the optimal control problem is solved both in open-loop (chapter 4) as well as in closed-loop (chapter 5). Characteristics of the open-loop computed control trajectories are used for solving the optimal control problem in closed-loop.

## 2.4 Necessary and sufficient optimality conditions

Control input trajectories need to fulfil equations in order to be optimal. These equations are called necessary and sufficient optimality conditions and are actually used to compute the optimal trajectories.

The necessary conditions are:

$$\frac{\partial H(\underline{x}, \underline{\lambda}, \underline{u}, \underline{d})}{\partial \underline{u}} = \underline{\lambda}^T \left[ \frac{\partial \underline{f}(\underline{x}, \underline{z}, \underline{u}, \underline{d})}{\partial \underline{u}} \right] = \underline{0}^T \quad (9a)$$

If admissible values for the control  $\underline{u}$  cannot fulfill this condition then the control is set to the maximal admissible value for  $\underline{u}$  if:

$$\left. \frac{\partial H(\underline{x}, \underline{\lambda}, \underline{u}, \underline{d})}{\partial \underline{u}} \right|_{\underline{u}_{\max}} = \underline{\lambda}^T \left[ \frac{\partial \underline{f}(\underline{x}, \underline{z}, \underline{u}, \underline{d})}{\partial \underline{u}} \right] \Big|_{\underline{u}_{\max}} > \underline{0}^T \quad \text{where } \underline{u} = \underline{u}_{\max} \quad (9b)$$

or the control is set to the minimal admissible values for  $\underline{u}$  if:

$$\left. \frac{\partial H(\underline{x}, \underline{\lambda}, \underline{u}, \underline{d})}{\partial \underline{u}} \right|_{\underline{u}_{\min}} = \underline{\lambda}^T \left[ \frac{\partial \underline{f}(\underline{x}, \underline{z}, \underline{u}, \underline{d})}{\partial \underline{u}} \right] \Big|_{\underline{u}_{\min}} < \underline{0}^T \quad \text{where } \underline{u} = \underline{u}_{\min} \quad (9c)$$

In these equations  $H$  is the Hamiltonian(-function) and  $\underline{u}(t)$  the control input vector:

$$H(\underline{x}, \underline{\lambda}, \underline{u}, \underline{d}) = \underline{\lambda}^T \underline{f}(\underline{x}, \underline{u}, \underline{d}) \quad (10)$$

The state and costate dynamics are described by:

$$\dot{\underline{x}} = \frac{\partial H}{\partial \underline{x}} = \underline{f}(\underline{x}, \underline{z}, \underline{u}, \underline{d}) \quad \underline{x}(t_0) = \underline{x}_0 \quad (11)$$

$$\dot{\underline{\lambda}} = -\frac{\partial H}{\partial \underline{x}} = -\underline{\lambda}^T \frac{\partial \underline{f}(\underline{x}, \underline{z}, \underline{u}, \underline{d})}{\partial \underline{x}} \quad \underline{\lambda}(t_f) = \frac{\partial \phi}{\partial \underline{x}} \Big|_{t=t_f} + \left( \frac{\partial \psi}{\partial \underline{x}} \Big|_{t=t_f} \right)^T \underline{v} \quad (12)$$



The conditions in equations 11 and 12 that fix state values at the initial time and costate values at the final time are called boundary conditions.

Equations 9a, 11 and 12 are derived from the variation of the performance equation that is set equal to zero ( $dJ = 0$ ) when the variations in  $\underline{x}$ ,  $\underline{\lambda}$  and  $\underline{u}$  are unequal to zero and the higher-order terms assumed sufficiently close to zero (Bryson and Ho, 1975; Kirk, 1970; Lewis and Syrmos, 1995; Stengel, 1994):

$$\delta J' = \left( \frac{\partial \phi}{\partial \underline{x}} + \left( \frac{\partial \psi}{\partial \underline{x}} \right)^T \underline{v} - \underline{\lambda} \right)^T d\underline{x} \Big|_{t=t_f} + \int_0^t \left\{ \left( \frac{\partial H}{\partial \underline{x}} + \underline{\dot{\lambda}} \right)^T \delta \underline{x} + \frac{\partial H}{\partial \underline{u}} \delta \underline{u} + \left( \frac{\partial H}{\partial \underline{\lambda}} - \underline{\dot{x}} \right) \delta \underline{\lambda} \right\} dt + \text{higher-order terms} = 0 \quad (13)$$

Extra conditions are derived from second-order terms (Jönsson, Trygger and Ögren, 2002):

$$\frac{\partial^2 \phi}{\partial \underline{x}^2} \Big|_{t_f} \geq 0 \quad (14)$$

$$\frac{\partial^2 H}{\partial \underline{u}^2} > 0 \quad (15)$$

$$\begin{bmatrix} \frac{\partial^2 H}{\partial \underline{x}^2} & \frac{\partial^2 H}{\partial \underline{u} \partial \underline{x}} \\ \frac{\partial^2 H}{\partial \underline{x} \partial \underline{u}} & \frac{\partial^2 H}{\partial \underline{u}^2} \end{bmatrix} \geq 0 \quad (16)$$

Equations 9a, 9b, 9c and 15 can also be derived from Pontryagin's minimum principle (Lewis and Syrmos, 1995). These equations and equations 14 and 16 are called sufficient conditions for a local minimum value of  $J'$ . In this thesis, only necessary conditions will be fulfilled by the algorithms presented in chapters 4 and 5.

## 2.5 Selection of optimisation algorithms

The necessary conditions presented in section 2.4 are used to compute optimal trajectories. Analytical computations may be difficult because equations 9a, 11 and 12 are complex equations and equations 11 and 12 need to fulfil split boundary conditions: one boundary condition at  $t_0$  and one boundary condition at  $t_f$ . Therefore, numerical optimisation algorithms are used.

Numerical optimisation algorithms for solving open-loop optimal control problems are distinguished from numerical optimisation algorithms for solving closed-loop optimal control problems. Both types of algorithms are discussed separately.

### 2.5.1 *Selection of an open-loop optimisation algorithm*

Open-loop numerical optimisation algorithms consist of series of improvements of state, costate or control trajectories. These improvements are based on error-data that are created by substituting guessed state, costate and control trajectories into equations 9a, 9b, 9c, 11 and 12 for the first improvement and substituting improved state, costate and control trajectories for other improvements. The series ends when the mismatch or the improvement is considered small enough. The final improved state, costate and control trajectories are considered optimal.

Open-loop optimisation algorithms can be subdivided into four classes: parametric optimization, dynamic programming, gradient optimization and linear quadratic methods. The class of parametric optimization algorithms includes algorithms that use Chebychev polynomials or penalty function methods (Stengel, 1994) and the class of linear quadratic optimization includes model predictive control algorithms. Neighboring optimal control algorithms, quasilinearization algorithms and shooting method algorithms are not considered here because these algorithms rely on good initial trajectories derived from the other algorithms (Stengel, 1994).

Each algorithm is suitable for solving open-loop problems with certain relevant characteristics. To choose an algorithm that is suitable for the open-loop problem in this thesis, all algorithms need to be evaluated based on specific characteristics of this problem. These characteristics are:

- The problem is nonlinear because it contains a nonlinear function  $m$ .
- The problem is non-quadratic because the function  $L$  is non-quadratic.
- The problem has constraints on states and inputs.
- The optimality of computed optimal trajectories needs to be as accurate as possible.

Table 7 shows a suitability evaluation based upon these characteristics. This table also includes relevant references.

This table shows gradient optimization algorithms are suitable to solve the open-loop optimal control problem in this thesis, and therefore such an algorithm will be studied and applied in this thesis.

Table 7: Suitability evaluation of open-loop optimisation algorithms on characteristics of the open-loop optimal control problem and relevant references

		<i>characteristics of open-loop optimal control problem</i>				<i>references</i>
		<i>non-linear</i>	<i>non-quadratic</i>	<i>constraints on states and inputs</i>	<i>exact optimal trajectories</i>	
<i>open-loop optimisation algorithms</i>	parametric optimization	+	+	+	-	Stengel (1994), Balakrishnan (1968)
	dynamic programming	--	--	+	+	Stengel (1994), Lewis (1995), Kirk (1970), Nevistic (1997)
	gradient optimization	+	+	+	+	Bryson (1999; 1975), Mehra and Davis (1972), Kirk (1970), Stengel (1994)
	linear quadratic methods	-	--	+	+	Lewis (1995), Nevistic (1997), Morari (1999)
--	unsuitable	-	hardly suitable	+	suitable	

Note that dynamic programming is unsuitable to solve nonlinear optimal control problems. This is because partial differential equations need to be solved in dynamic programming and no efficient algorithm is available to do this except for optimal control problems with ordinary linear differential equations and quadratic performance equations (Nevistic, 1997; Stengel, 1994).

### 2.5.2 Selection of a closed-loop optimisation algorithm

Closed-loop optimisation algorithms can roughly be divided into seven types of algorithms. These types and relevant references are in table 8.

Each algorithm is suitable for solving closed-loop problems with certain relevant characteristics. To choose an algorithm that is at least suitable for the closed-loop problem in this thesis, all algorithms need to be evaluated on characteristics of this problem. These characteristics are:

- The problem is nonlinear because it consists of a nonlinear function  $m$
- Costate equations may be such that forward integration of these equations to compute costates lead to undesired costate values. This topic is discussed by Kalman (1966).
- The problem is non-quadratic because the function  $L$  is non-quadratic.
- The problem contains path constraints because of the algebraic equations.
- Closed-loop control input trajectories computations should be fast.
- The optimality of computed optimal trajectories need to be as exact as possible.

The algorithms were also evaluated on their ability to deal with singular optimal trajectories because, in general, a lot of optimal control problems are input-affine and so their optimal trajectories consist of singular optimal trajectories. Although the problem in this thesis is not input-affine (see chapter 3), this characteristic is still evaluated to choose a closed-loop optimal control algorithm that is suitable for the general class of problems presented in section 2.2.

Table 9 shows a suitability evaluation based on these characteristics. It shows closed-loop algorithms based on sub-optimal control algorithms and neural networks (incl. parametric optimisation) are equally suitable to solve the closed-loop problem in this thesis. Sub-optimal control algorithms will be studied and applied in this thesis.

Table 8: Types of closed-loop optimisation algorithms and relevant references

<i>types</i>	<i>references</i>
receding horizon (incl. some MPC)	Tap (2000), Mayne, <i>et al.</i> (2000), and Mayne and Rawlings (2001)
neighbouring optimal control	Lee and Bryson (1989)
sub-optimal control algorithm	Palanki, <i>et al.</i> (1993), Rahman and Palanki (1996), Srinivasan, <i>et al.</i> (2002), van Henten (1994), Friedland and Sarachik (1966)
linear quadratic methods (incl. some MPC)	Nevistic (1997), Mayne, <i>et al.</i> (2000), and Mayne and Rawlings (2001)
neural networks (incl. parametric optimisation)	Seginer and Sher (1993), Stengel (1994)
dynamic programming	Stengel (1994)

Table 9: Suitability evaluation of open-loop optimisation algorithms on characteristics of the open-loop optimal control problem

		characteristics of the closed-loop optimal control problem						
		non-linear	undesired costate-values	non-quadratic	path constraints	fast computations	exact optimal trajectories	singular control
closed-loop optimisation algorithms	receding horizon (incl. some MPC)	+	+	+	+	--	+	+
	neighbouring optimal control	+	-	+	-	+	-	--
	suboptimal control algorithm	+	-	+	+	+	+	+
	linear quadratic methods (incl. some MPC)	-	+	--	+	+	+	+
	neural networks (incl. parametric optimisation)	+	+	+	+	+	-	+
	dynamic programming	--	+	--	+	+	+	+
		-- unsuitable	- hardly suitable	+	suitable			

2.6 Final optimal control problem statement

Concluding the problem of computing optimal greenhouse air temperatures and greenhouse air CO<sub>2</sub>-concentrations belongs to the general class of optimal control problems with non-linear differential algebraic equations affected by measurable, high-frequency disturbances and end-constraints. This problem is going to be solved both in open-loop and in closed-loop, using algorithms that are able to deal with all problem characteristics properly. A gradient optimization algorithm will be studied and applied to solve the problem in open-loop and an suboptimal control algorithm to solve the problem in closed-loop.

References

Balakrishnan, A. V. (1968). On a new computing technique in optimal control theory and the maximum principle. *Siam Journal of Control*, 6, 149-173.

Bryson, A. E. (1999). *Dynamic optimization*, Addison-Wesley Longman, Inc., Menlo Park.

Bryson, A. E. and Y.-C. Ho (1975). *Applied optimal control; optimization, estimation and control*, Hemisphere, New York.

Friedland, B. and P. E. Sarachik (1966). A unified approach to suboptimum control. *Proceedings of the 3rd Congress of IFAC*, 1, 13A.11-13A.18.

- Jönsson, U., C. Trygger and P. Ögren (2002). *Lectures on optimal control (course-notes)*, Royal Institute of Technology, Stockholm.
- Kalman, R. E. (1966). Toward a theory of difficulty of computation in optimal control. *Proceedings of fourth IBM scientific computing symposium*, 25-43.
- Kirk, D. E. (1970). *Optimal control theory; an introduction*, Prentice-Hall, Inc., Englewood Cliffs, New Jersey.
- Lee, A. Y. and A. E. Bryson (1989). Neighbouring extremals of dynamic optimization problems with parameter variations. *Optimal control applications & methods*, 10, 39-52.
- Lewis, F. L. and V. L. Syrmos (1995). *Optimal control*, John Wiley & Sons, Inc., New York.
- Mayne, D. Q. and J. B. Rawlings (2001). Correction to "Constrained model predictive control: stability and optimality". *Automatica*, 37, 483.
- Mayne, D. Q., J. B. Rawlings, C. V. Rao and P. O. M. Scokaer (2000). Constrained model predictive control: stability and optimality. *Automatica*, 36, 789-814.
- Mehra, R. K. and R. E. Davis (1972). A generalized gradient method for optimal control problems with inequality constraints and singular arcs. *IEEE Transactions on automatic control*, AC-17, 69-79.
- Morari, M. and J. H. Lee (1999). Model predictive control: past, present and future. *Computers and chemical engineering*, 23, 667-682.
- Nevistic, V. (1997). *Constrained control of nonlinear systems (PhD-thesis)*, Swiss Federal Institute of Technology, Zurich.
- Palanki, S., C. Kravaris and H. Y. Wang (1993). Synthesis of state feedback laws for end-point optimization in batch processes. *Chemical Engineering Science*, 48, 135-152.
- Rahman, S. and S. Palanki (1996). On-line optimization of batch processes in the presence of measurable disturbances. *American Institute of chemical engineering journal*, 42, 2869-2882.
- Seginer, I. and A. Sher (1993). Optimal greenhouse temperature trajectories for a multi-state-variable tomato model. In: *The computerized greenhouse* (Hashimoto, Y., G. P. A. Bot, W. Day, H.-J. Tantau and H. Nonami. (Ed)), pp. 153-172. Academic press, San Diego, California.
- Srinivasan, B., S. Palanki and D. Bonvin (2002). Dynamic optimization of batch processes: II. Role of measurements in handling uncertainty. *Computers and chemical engineering*, 27, 27-44.
- Stengel, R. F. (1994). *Optimal control and estimation*, Dover publications, Inc., New York.
- Tap, F. (2000). *Economics-based optimal control of greenhouse tomato crop production (PhD-thesis)*, Wageningen University, Wageningen, The Netherlands.
- van Henten, E. J. (1994). *Greenhouse climate management: an optimal control approach (PhD-thesis)*, Landbouwniversiteit Wageningen, Wageningen, The Netherlands.

# 3

## 3 Specification of optimal control problem equations

### 3.1 Introduction

Equations 2 to 7 of the general fixed-time optimal control problem presented in section 2.2 are specified in this chapter. This is done by presenting three models: firstly the model presented by Seginer, Buwalda and Van Straten (Seginer, Buwalda and van Straten, 1998) describing the effects of solar or artificial radiation intensity values, greenhouse air temperatures and greenhouse air CO<sub>2</sub>-concentrations on lettuce nitrate concentrations and lettuce fresh weights, secondly a model presented by Seginer and Van Straten (2001) describing dynamics of greenhouse climate conditions affected by outside weather conditions and thirdly a cultivation performance model.

Each model is explained twice: first mathematically then either biologically, physically or economically. Each explanation can be read without reading the other thereby offering the possibility to read the most interesting explanation only. In section 3.5 all models are cast in the general variables  $\underline{x}(t)$ ,  $\underline{z}(t)$ ,  $\underline{u}(t)$ ,  $\underline{d}(t)$  and general functions  $\underline{f}(\underline{x}, \underline{z}, \underline{u}, \underline{d})$ ,  $\underline{n}(\underline{x}, \underline{z}, \underline{u}, \underline{d})$ ,  $\underline{c}(\underline{u})$ ,  $\underline{s}(\underline{z})$ ,  $\underline{\psi}(\underline{x}_f)$  and  $\phi(\underline{z}_f)$  of the general fixed-time optimal control problem.

### 3.2 Dynamic lettuce growth and nitrate accumulation model

#### 3.2.1 Mathematical outline of dynamic lettuce growth and nitrate accumulation model

Seginer, Buwalda and Van Straten (1998) developed a model that describes effects of solar or artificial radiation intensity values, greenhouse air temperatures and greenhouse air CO<sub>2</sub>-concentrations on lettuce nitrate concentrations and lettuce fresh weights. According to this model, assimilates are produced by photosynthesis and are converted into lettuce structure material and energy that is needed for growth (fresh weight increase) and maintenance. These processes also affect nitrate concentrations through assimilate concentrations: If, at constant fresh weight, assimilate concentrations are high, then nitrate concentrations are low and vice versa. This means

that if assimilate production rates exceed assimilate conversion rates then assimilate concentrations will increase and nitrate concentration will decrease.

The model consists of two state equations:

$$\frac{dM_{Cv}}{dt} = F_{Cav}(S_0, C_{Ca}, M_{Cs}, M_{Cv}) - F_{Cm}(M_{Cs}, T_a) - (1 + \theta) F_{Cvs}(M_{Cs}, M_{Cv}, T_a) \quad (17)$$

$$\frac{dM_{Cs}}{dt} = F_{Cvs}(M_{Cs}, M_{Cv}, T_a) \quad (18)$$

where  $M_{Cv}$  (mol [C]·m<sup>-2</sup>) is the mass of assimilates in lettuce vacuoles,  $M_{Cs}$  (mol [C]·m<sup>-2</sup>) mass of lettuce structural material,  $S_0$  (mol photo-synthetically active photons·m<sup>-3</sup>·s<sup>-1</sup>) the solar radiation intensity,  $C_{Ca}$  (mol [C]·m<sup>-3</sup>) the greenhouse air carbon dioxide concentration and  $T_a$  (°C) the greenhouse air temperature.

The fluxes in equations 17 and 18 are summarized in two tables. Equations, units and descriptions of fluxes are in table 10. Equations, units and descriptions of functions used in the equations of table 10 are in table 11. Some functions were changed in the course of time because of better scientific insight. Numbers of sections in which specific secondary functions were used are also in table 11.

Outputs of the model are lettuce fresh weight  $y_1$  (g·plant<sup>-1</sup>) and lettuce nitrate concentration  $y_2$  (ppm):

$$y_1 = \frac{\beta\kappa\eta_{OMC}(M_{Cv} + M_{Cs}) + \eta_{MMN}(\Pi_v M_{Cs} - \gamma\kappa M_{Cv})}{\beta\kappa N_p} \quad (19)$$

$$y_2 = \frac{\eta_{ppm}\eta_{NO3N}(\Pi_v M_{Cs} - \gamma\kappa M_{Cv})}{(\beta\kappa\eta_{OMC}(M_{Cv} + M_{Cs}) + \eta_{MMN}(\Pi_v M_{Cs} - \gamma\kappa M_{Cv}))} \quad (20)$$

Equation 20 shows the mentioned relationship between assimilate concentrations and nitrate concentrations: If, at constant fresh weight, assimilate concentrations are high then nitrate concentrations are low and vice versa.

Values, units and descriptions of parameters are in table 12. Constraints related to the fresh weight  $y_1$  and lettuce nitrate concentration  $y_2$  are in table 13. Note, constraints related to the nitrate concentration  $y_2$  stem from the EU-directive about maximum lettuce nitrate concentrations, which is mentioned in chapter 1.



Table 10: Equations, units and descriptions of fluxes in equations 17 and 18

fluxes	equations	units	descriptions
$F_{car}(S_0, C_{ca}, M_{cs}, M_{cv})$	$= P(I, C_{ca}) f_1(M_{cs}) h_p(M_{cv}, M_{cs})$	$\text{mol [C]} \cdot \text{m}^{-2} \cdot \text{s}^{-1}$	photosynthesis
$F_{cm}(M_{cs}, T_a)$	$= e(T_a) f_2(M_{cs})$	$\text{mol [C]} \cdot \text{m}^{-2} \cdot \text{s}^{-1}$	maintenance
$F_{cs}(M_{cs}, M_{cv}, T_a)$	$= g(T_a) f_1(M_{cs}) h_g(M_{cv}, M_{cs})$	$\text{mol [C]} \cdot \text{m}^{-2} \cdot \text{s}^{-1}$	growth

Table 11: Equations, units and descriptions of functions used in the equations of table 10

functions	units	section no.	description
$P(I, C_{ca}) = \frac{\varepsilon S_0 \sigma (C_{ca} - C_{cs})}{\varepsilon S_0 + \sigma (C_{ca} - C_{cs})}$	$\text{mol [C]} \cdot \text{m}^{-2} \cdot \text{s}^{-1}$	all	uninhibited gross photosynthesis of closed canopy
$f_1(M_{cs}) = 1 - e^{-\alpha I}$	-	all	light interception of the canopy
$f_2(M_{cs}) = \begin{cases} M_{cs} \\ 1 - e^{-\alpha I} \end{cases}$	-	section 4.1 all but section 4.1	light interception of the canopy
$h_p(M_{cv}, M_{cs}) = \begin{cases} 1 - \frac{1}{1 + e^{-\left(\frac{M_{cv}}{M_{cs}} \frac{\gamma}{\Pi_v} - b_p\right)}} \\ 1 - \frac{1}{1 + \left(\frac{b_g \Pi_v M_{cs}}{\gamma M_{cv}}\right)^{t_g}} \end{cases}$	-	section 4.1 all but section 4.1	photosynthesis inhibition
$h_g(M_{cv}, M_{cs}) = \begin{cases} \frac{1}{1 + e^{-\left(\frac{M_{cv}}{M_{cs}} \frac{\gamma}{\Pi_v} - b_g\right)}} \\ 1 - \frac{1}{1 + \left(\frac{(1 - b_p) \Pi_v M_{cs}}{\Pi_v M_{cs} - \gamma M_{cv}}\right)^{t_g}} \end{cases}$	-	section 4.1 all but section 4.1	growth inhibition
$e(T_a) = k e^{c(T_a - T^*)}$	$\text{mol [C]} \cdot \text{m}^{-2} \cdot \text{s}^{-1}$	all	specific respiration maintenance
$g(T_a) = m k e^{c(T_a - T^*)}$	$\text{mol [C]} \cdot \text{m}^{-2} \cdot \text{s}^{-1}$	all	uninhibited growth

Table 12: Values, units and descriptions of parameters

Parameter values marked with \* are from Vanthoor (2001). Other parameter values are from Van Straten, et al. (1999)

parameters	value	units	description
$a$	0.70 *	$\text{m}^2 \cdot \text{mol} [\text{C}]^{-1}$	leaf area closure parameter
$\epsilon$	$7 \cdot 10^{-2}$	$\text{mol} [\text{C}] \cdot \text{mol PAP}^{-1}$	apparent light use efficiency
$\sigma$	$1.2 \cdot 10^{-3}$	$\text{m} \cdot \text{s}^{-1}$	$\text{CO}_2$ transport coefficient
$c^*$	$1.1 \cdot 10^{-3}$	$\text{mol} [\text{C}] \cdot \text{m}^3$	$\text{CO}_2$ compensation point
$k$	$2.5 \cdot 10^{-7}$	$\text{s}^{-1}$	specific maintenance rate coefficient
$T^*$	20	$^{\circ}\text{C}$	reference temperature
$c$	$6.9 \cdot 10^{-2}$	$^{\circ}\text{C}^{-1}$	temperature effect parameter
$m$	18.7 *	$\text{mol} \cdot \text{m}^{-2}$	growth parameter
$\theta$	0.3	-	growth respiration loss function
$s_p$	30	-	slope parameter
$s_g$	30	-	slope parameter
$b_p$	0.8	-	threshold parameter
$b_g$	0.2	-	threshold parameter
$\Pi_v$	$5.3 \cdot 10^5$	Pa	constant turgor pressure
$\beta$	$6.0 \cdot 10^3$	Pa	regression parameter of C/N ratio in vacuoles
$\gamma$	$6.1 \cdot 10^2$	Pa	regression parameter of C/N ratio in vacuoles
$\kappa$	$1.3 \cdot 10^3$	$\text{mol} [\text{C}] \cdot \text{m}^{-3}$	structural C per unit vacuole volume
$\eta_{\text{OMC}}$	$30 \cdot 10^{-3}$	$\text{kg} \cdot \text{mol} [\text{C}]^{-1}$	mass of organic matter per mol [C]
$\eta_{\text{MMN}}$	$148 \cdot 10^{-3}$	$\text{kg} \cdot \text{mol} [\text{N}]^{-1}$	mass of minerals per mol N in vacuoles
$\eta_{\text{DMFM}}$	0.05	$\text{kg} \cdot \text{kg}^{-1}$	dry matter to fresh matter ratio
$\eta_{\text{NO}_3\text{N}}$	$62 \cdot 10^{-3}$	$\text{kg NO}_3^- \cdot \text{mol} [\text{N}]^{-1}$	mass of nitrate per mol [N]
$\eta_{\text{SH}}$	0.180	$\text{kg hexose} \cdot \text{mol hexose}^{-1}$	mass of assimilates (hexose) per mol hexose
$\eta_{\text{C}_{\text{hex}}}$	14	$\text{mol} [\text{C}] \cdot \text{mol hexose}^{-1}$	moles of [C] per mol hexose
$\eta_{\text{ppm}}$	$1 \cdot 10^6$	$\text{ppm} \cdot \text{kg} \cdot \text{kg}^{-1}$	conversion factor between ppm and $\text{kg} \cdot \text{kg}^{-1}$
$N_p$	18	$\text{plant} \cdot \text{m}^{-2}$	plant density

Table 13: Constraints related to lettuce growth and lettuce nitrate concentration

	lower bound values	upper bound values	units
$y_1$	300	-	$\text{g} \cdot \text{head}^{-1}$
$y_2$	-	3500 (summer) 4500 (winter)	ppm

### 3.2.2 *Biological interpretation of the dynamic lettuce growth and nitrate accumulation model*

Seginer, Buwalda and Van Straten (1998) developed a model that describes effects of solar or artificial radiation intensity values, greenhouse air temperatures and greenhouse air CO<sub>2</sub>-concentrations on lettuce nitrate concentrations and lettuce fresh weights. According to this model, assimilates are produced by photosynthesis out of CO<sub>2</sub> and water and are converted into lettuce structure material and energy that is needed for growth (fresh weight increase) and maintenance. These processes also affect nitrate concentrations through assimilate concentrations: If, at constant fresh weight, assimilate concentrations are high then nitrate concentrations are low and vice versa. This means that if photosynthesis rates exceed conversion rates then assimilate concentrations will increase and nitrate concentration will decrease.

All processes are affected by solar radiation intensity, greenhouse air CO<sub>2</sub>-concentration, greenhouse air temperature, assimilate mass and structural material mass. These effects are in table 14.

Measured variables during lettuce cultivation are assumed to be lettuce fresh weight and lettuce nitrate concentration. Fresh weights are approximately proportional to mass sums of assimilate, lettuce structure material and nitrate. Nitrate concentrations are approximately inversed proportional to ratios between assimilates mass and fresh weight.

The combination of effects presented in table 14 constitutes the model and effectively supports the idea that if the solar radiation intensity is high, the greenhouse air temperature is low and the greenhouse air CO<sub>2</sub>-concentration in the greenhouse air is high then the photosynthesis rate is high compared to the assimilate conversion rates. This leads to high assimilate concentrations, low nitrate concentrations and relative low fresh weight increases. On the other hand, if the solar radiation intensity is low, the greenhouse air temperature is high and the greenhouse air CO<sub>2</sub>-concentration in the greenhouse air is low then photosynthesis rates are low compared to assimilate conversion rates. This leads to low assimilate concentrations, high nitrate concentrations and relative high fresh weight increases. Table 15 shows both situations.

Five basic assumptions are part of the model:

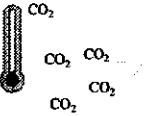

1. There is no distinction between shoots, roots and stem.
2. Storage pools of compounds related to assimilates that affect lettuce growth and nitrate content, such as starch pools do not exist.
3. Vacuole volumes constitute a fixed fraction of the total volume in lettuce plants.
4. Lettuce plants grow by building new cells with exactly the same proportions as existing cells.
5. The model is applicable for lettuce cultivation processes in which abnormalities, like tipburn or bolting are not present.

Table 14: Effects of increasing values of solar radiation intensity, greenhouse air CO<sub>2</sub>-concentration, greenhouse air temperature, assimilate mass and structural material mass on photosynthesis and conversion rates

	<i>photosynthesis rate</i>	<i>conversion rate related to maintenance</i>	<i>conversion rate related to growth</i>
<i>solar radiation intensity</i>	saturated increase	none	none
<i>greenhouse air CO<sub>2</sub>-concentration</i>	saturated increase	none	none
<i>greenhouse air temperature</i>	none	saturated increase	saturated increase
<i>assimilate mass</i>	saturated decrease	none	saturated increase
<i>structural material mass</i>	{ saturated increase if ratio of assimilate mass to structural material mass is constant or decreases.	proportional increase (section 4.1)	saturated increase if ratio of assimilate mass to structural material mass is constant or increases.
	{ saturated increase if ratio of assimilate mass to structural material mass is constant or decreases.	saturated increase (other sections)	saturated decrease if ratio of assimilate mass to structural material mass decreases.

increasing values of:

Table 15: Effects of solar radiation intensity, greenhouse air temperature and greenhouse air CO<sub>2</sub>-concentration on nitrate concentrations and fresh weight increases in lettuce plants

<i>weather condition</i>	<i>relation between photosynthesis and conversion rates</i>	<i>relative fresh weight increase</i>	<i>NO<sub>3</sub><sup>-</sup> concentration</i>
	<b>photosynthesis rate &gt; conversion rate</b>	High	increases
	<b>photosynthesis rate &lt; conversion rate</b>	Low	decreases

### 3.3 Dynamic climate model

#### 3.3.1 Mathematical outline of dynamic climate model

Seginer and Van Straten (2001) presented a model that describes dynamics of greenhouse climate conditions affected by outside weather conditions. This model consists of one state equation and three algebraic equations. A modified version of this model is presented here. The modifications are related to the heating flux and the specific ventilation rate. The model equations are:

$$\frac{dT_g}{dt} = \frac{F_{Sog}(S_o) - F_{Lga}(M_{Sc}, RH_a, T_a, S_o) - F_{Hga}(T_{ga}, T_a)}{K} \quad (21)$$

$$0 = F_{Hea}(T_a, T_p) - F_{Hga}(T_g, T_a) - F_{Hao}^c(T_a, T_o) - F_{Hao}^v(T_a, T_o, Q) \quad (22)$$

$$0 = F_{Lga}(M_{Sc}, RH_a, T_a, S_o) - F_{Lao}^v(RH_a, T_a, RH_o, T_o, Q) \quad (23)$$

$$0 = F_{Cea} - F_{Cao}^v(C_{Ca}, C_{Co}, Q) + F_{Cm}(M_{Cs}, T_a) - \theta F_{Cvs}(M_{Sc}, M_{Cv}, T_a, C_{Ca}) - F_{Cav}(M_{Sc}, M_{Cv}, C_{Ca}, S_o) \quad (24)$$

Equation 21 is a differential equation for the heat balance of the virtual unit of soil and apparatus. Equations 22, 23 and 24 are algebraic equations (quasi steady state equations) for the sensible heat balance of the greenhouse air, the latent heat balance of the greenhouse air and the  $CO_2$ -mass balance of the greenhouse air respectively. Units and descriptions of states, quasi steady states, controllable and disturbances in these equations are in table 16.

Equations, units and descriptions of the functions  $F_{Sog}$ ,  $F_{Lga}$ ,  $F_{Hga}$ ,  $F_{Hea}$ ,  $F_{Hao}^c$ ,  $F_{Hao}^v$ ,  $F_{Lao}^v$  and  $F_{Cao}^v$  are in table 17. Equations, units and descriptions of the functions  $F_{Cm}$ ,  $F_{Cvs}$  and  $F_{Cav}$  are in table 10. Other symbols are symbols for parameters. Values, units and descriptions of these parameters are in table 18.

The function  $\hat{w}_a(T_a)$  and  $\hat{w}_a(T_o)$  in table 17 are saturated relative humidities (kg [vapour]-kg air<sup>-1</sup>) of the greenhouse air and outside air. The equation for both functions are:

$$\hat{w}_a(T_*) = \frac{M_{H_2O}(1 + c_{s1}T_*)}{\rho_0 R_g (T_* + c_{s2})} c_{s3} e^{\frac{c_{s4}T_*}{c_{s5} + T_*}} \quad (25)$$

where  $T_*$  is either  $T_a$  or  $T_o$ .

Table 16: Units and descriptions of states, quasi steady states, controllable and disturbances in equations 21 to 24

<i>symbol</i>	<i>units</i>	<i>description</i>
<i>states</i>		
$T_g$	°C	temperature of the virtual unit of soil and apparatus
<i>quasi steady states</i>		
$T_a$	°C	greenhouse air temperature
$RH_a$	kg [vapour]·kg air <sup>-1</sup>	greenhouse air mixing humidity ratio
$C_{Ca}$	mol [C]·m <sup>-3</sup>	greenhouse air carbon dioxide concentration
<i>control inputs</i>		
$T_p$	°C	heating pipe temperature
$Q^v$	m <sup>3</sup> ·m <sup>-2</sup>	specific ventilation rate
$F_{Cca}$	mol [C]·m <sup>-2</sup> ·s <sup>-1</sup>	CO <sub>2</sub> transfer by injection into the greenhouse air
<i>disturbances</i>		
$T_o$	°C	outside air temperature
$S_o$	mol PAP·m <sup>-3</sup> ·s <sup>-1</sup>	the light intensity
$RH_o$	kg [vapour]·kg air <sup>-1</sup>	outside air mixing humidity ratio
$C_{Co}$	mol [C]·m <sup>-3</sup>	outside air carbon dioxide concentration

Table 17: Process descriptions, underlying functions and units of functions in equations 21 to 24

	<i>functions</i>	<i>units</i>	<i>description</i>
$F_{Sog}(S_o)$	$= \epsilon \tau S_o$	J·s <sup>-1</sup>	solar radiation absorbance
$F_{Lga}(M_{sc}, RH_a, T_a, S_o)$	$= q\lambda [A\tau S_o + B\hat{w}_a(T_a)(1 - RH_a)] f(M_{cs})$	J·s <sup>-1</sup>	latent heat transfer by evapotranspiration from virtual unit to greenhouse air
$F_{Hga}(T_{ga}, T_a)$	$= v_{ga} A_{ga} (T_g - T_a)$	J·s <sup>-1</sup>	heat transfer from the virtual unit to greenhouse air
$F_{Hpa}(T_a, T_p)$	$= v_{pa} A_{pa} (T_p - T_a)$	J·s <sup>-1</sup>	heat transfer from heating pipes to greenhouse air
$F_{Hao}^c(T_a, T_o)$	$= v_{ao} A_{ao} (T_a - T_o)$	J·s <sup>-1</sup>	heat transfer by diffusion from greenhouse air to outside air
$F_{Hao}^v(T_a, T_o, Q^v)$	$= \rho c Q^v (T_a - T_o)$	J·s <sup>-1</sup>	heat transfer by ventilation from greenhouse air to outside air
$F_{Lao}^v(RH_a, T_a, RH_o, T_o, Q^v)$	$= \rho\lambda Q^v (RH_a \hat{w}_a(T_a) - RH_o \hat{w}_a(T_o))$	J·s <sup>-1</sup>	latent heat transfer by ventilation from greenhouse air to outside air
$F_{Cao}^v(C_{Ca}, C_{Co}, Q^v)$	$= Q^v (C_{Ca} - C_{Co})$	mol CO <sub>2</sub> s <sup>-1</sup>	CO <sub>2</sub> transfer by ventilation from greenhouse air to outside air

Table 18: Greenhouse parameter values and description

markers	references	markers	references
#	Estimated from Breugelmans (2000)	-	Von Elsner (2000)
&	Defant and Defant (1958)	*	guess values not corrected by calibration
'	Seginer and Van Straten (2001)	%	guess values corrected by calibration
\$	Lide (2003)	@	Van Henten (1994)

parameters	value	units	description	
$A$	daylight night	$1.2 \cdot 10^{-7}$ $0.6 \cdot 10^{-7}$	$\text{kg}[\text{vapour}] \cdot \text{J}^{-1}$	coefficient in the Penman-Monteith formula
$A_{sa}$	1.0	#	$\text{m}^2[\text{contact area}] \cdot \text{m}^{-2}[\text{ground}]$	contact area between the greenhouse air and the virtual unit of soil, crop and apparatus
$A_{pa}$	0.33	#	$\text{m}^2[\text{contact area}] \cdot \text{m}^{-2}[\text{ground}]$	contact area between the heating tubes and the virtual unit of soil, crop and apparatus
$A_{ao}$	1.9	#	$\text{m}^2[\text{contact area}] \cdot \text{m}^{-2}[\text{ground}]$	contact area between the greenhouse air and the outside air.
$B$	daylight night	$1.3 \cdot 10^{-3}$ $0.7 \cdot 10^{-3}$	$\text{kg}[\text{air}] \cdot \text{m}^{-2}[\text{ground}] \cdot \text{s}^{-1}$	coefficient in the modified Penman-Monteith formula
$C$		$1.0 \cdot 10^3$	$\text{J} \cdot \text{kg}^{-1}[\text{air}] \cdot \text{K}^{-1}$	specific heat of air at constant pressure
$c_{s1}$		$3.8 \cdot 10^{-3}$	$^{\circ}\text{C}^{-1}$	saturated humidity ratio parameter
$c_{s2}$		$2.7 \cdot 10^2$	$^{\circ}\text{C}$	saturated humidity ratio parameter
$c_{s3}$		$6.1 \cdot 10^2$		saturated humidity ratio parameter
$c_{s4}$		17		saturated humidity ratio parameter
$c_{s5}$		$2.4 \cdot 10^2$	$^{\circ}\text{C}$	saturated humidity ratio parameter
$K$		$1.9 \cdot 10^4$	$\text{J} \cdot \text{m}^{-2}[\text{ground}] \cdot \text{K}^{-1}$	heat capacity
$M_{H_2O}$		18	$\text{g} \cdot \text{moles H}_2\text{O}$	mass of water
$q$		1		Penman-Monteith formula tuning factor
$R_g$		$8.3 \cdot 10^3$		gas constant
$v_{sa}$		5	$\text{W} \cdot \text{m}^{-2}[\text{contact area}] \cdot \text{K}^{-1}$	overall heat transfer coefficient between the greenhouse air and the virtual unit of soil, crop and apparatus
$v_{pa}$		5	$\text{W} \cdot \text{m}^{-2}[\text{contact area}] \cdot \text{K}^{-1}$	overall heat transfer coefficient between the heating tubes and the greenhouse
$v_{ao}$		2.8	$\text{W} \cdot \text{m}^{-2}[\text{contact area}] \cdot \text{K}^{-1}$	overall heat transfer coefficient between the greenhouse air and the outside air.
$\epsilon$		1		greenhouse heating efficiency of solar radiation
$\lambda$		$2.5 \cdot 10^6$	$\text{J} \cdot \text{kg}^{-1}[\text{vapour}]$	latent heat of vaporisation of water
$\rho$		1.2	$\text{kg}[\text{air}] \cdot \text{m}^{-3}$	air density
$\tau$		0.6		cover transmissivity to solar radiation

Realistic constraints related to states, quasi steady states and control inputs are in table 19. Lower bound constraints on  $F_{Cea}$ ,  $RH_a$ ,  $C_{Ca}$  are physical constraints. Other constraints are from literature or are guessed values

Table 19: Realistic constraints related to quasi steady states and control inputs

Constraint values marked with <sup>#</sup> are from Von Elsner (2000). Constraint values marked with <sup>&</sup> are physical constraints. Constraint values marked with <sup>!</sup> were estimated from Van Henten (1994). For estimating the lower bound a wind speed of  $0 \text{ m}\cdot\text{s}^{-1}$  was assumed and to obtain a conservative estimate of the upper bound a wind speed of  $1 \text{ m}\cdot\text{s}^{-1}$  and window apertures of 100% were assumed. The upper bound is a realistic value because a windspeed of  $1 \text{ m}\cdot\text{s}^{-1}$  or larger is present in the Netherlands 93% of a year. Other constraint values are guessed values.

	lower bound		upper bound		units
quasi steady states					
$T_a$	5.0	#	40	#	°C
$RH_a$	0.0	&	0.9	#	-
$C_{Ca}$	0.0	&	-		mol·m <sup>-3</sup>
control inputs					
$T_p$	$T_a$	&	70		°C
$Q$	$7.5\cdot 10^{-5}$	!	$7.7\cdot 10^{-3}$	!	m·s <sup>-1</sup>
$F_{Ca}$	0.0	&	-		mol·m <sup>-2</sup> ·s <sup>-1</sup>

### 3.3.2 Physical interpretation of dynamic climate model

Seginer and Van Straten (2001) presented a model that describes fluctuations of four climate conditions: temperature of a virtual unit of soil and apparatus, greenhouse air temperature, greenhouse air relative humidity ratio and greenhouse air  $\text{CO}_2$ -concentration. Each fluctuation is modelled by a balance: a heat balance of the virtual unit of soil and apparatus, a sensible heat balance of the greenhouse air, a latent heat balance of the greenhouse air and a greenhouse air  $\text{CO}_2$ -mass balance.

Thirteen processes affect these fluctuations. Table 20 shows which processes affect which fluctuations directly. These processes are themselves functions of outside climate conditions (solar radiation intensity, outside air temperature, outside air  $\text{CO}_2$ -concentration, outside relative humidity ratio), inside climate conditions (greenhouse air  $\text{CO}_2$ -concentration, greenhouse air temperature, greenhouse air relative humidity ratio, heating pipe temperature), mass of assimilates in vacuoles and mass of lettuce structural material.

Fluctuations of the greenhouse air temperature, greenhouse air relative humidity ratio and greenhouse air  $\text{CO}_2$ -concentration are at least 10 times faster than fluctuations of temperature of the virtual unit of soil. This difference in fluctuation rates leads to instant adjustments of the first three variables and slow convergence of the fourth variable to new values upon changes of outside climate conditions, inside climate conditions or masses.



Table 20: Direct effects of processes on fluctuations of the temperature of a virtual unit of soil and apparatus, the greenhouse air temperature, greenhouse air relative humidity ratio and greenhouse air CO<sub>2</sub>-concentration

	<div style="text-align: center;"> <i>fluctuation of greenhouse air CO<sub>2</sub>-concentration</i>  <i>fluctuation of greenhouse air relative humidity</i>  <i>fluctuation of the greenhouse air temperature</i>  <i>fluctuation of temperature of a virtual unit of soil and apparatus</i> </div>			
solar radiation absorbance	•			
latent heat transfer by evapotranspiration from virtual unit to greenhouse air	•		•	
heat transfer from the virtual unit to greenhouse air	•	•		
heat transfer from heating pipes to greenhouse air		•		
heat transfer from heating pipes to greenhouse air		•		
heat transfer by diffusion from greenhouse air to outside air		•		
heat transfer by ventilation from greenhouse air to outside air		•		
latent heat transfer by ventilation from greenhouse air to outside air				•
CO <sub>2</sub> -enrichment flow				•
CO <sub>2</sub> -transfer by ventilation from greenhouse air to outside air				•
CO <sub>2</sub> -production by maintenance of lettuce plants				•
CO <sub>2</sub> -production by growth of lettuce plants				•
CO <sub>2</sub> -intake by photosynthesis of lettuce plants				•

### 3.4 Cultivation performance model

#### 3.4.1 Mathematical outline of the cultivation performance model

A cultivation performance model that consists of a state equation for the running costs  $R$  and a function  $\phi(\underline{x}_f)$  was developed. This is explained in the next section. The state equation summates accumulation rates of control-dependent running costs ( $\text{€}\cdot\text{m}^{-2}\cdot\text{s}^{-1}$ ) and the function  $\phi(\underline{x}_f)$  represents cultivation profits ( $\text{€}\cdot\text{m}^{-2}$ ):

$$\frac{dR}{dt} = c_h F_{H_{ea}}(T_a, T_p) + c_c F_{C_{ea}} \quad (26)$$

$$\phi(\underline{x}_f) = c_s y_{1,f} - R_f \quad (27)$$

where  $c_h$ ,  $c_c$ ,  $c_s$  are parameters which names, values, units and references are in table 21,  $F_{Hea}(T_a, T_p)$  and  $F_{Cea}$  are heat and CO<sub>2</sub> transfer functions (see section 3.2.1),  $y_{1,f}$  the lettuce fresh weight at harvest time (see section 3.2.1) and  $R_f$  the running costs state at harvest time.

Note that in Belgium heating costs are lower ( $3 \cdot 10^{-9}$  €·J<sup>-1</sup>) according to Georges, Van Lierde and Verspecht (2003). However, Dutch heating costs are used in this thesis.

### 3.4.2 Economical interpretation of the cultivation performance model

In this section the cultivation performance model is developed on an economical basis. This model includes the assumption that the optimal control problem consists of a fixed final time. This assumption will also be discussed.

The assumed final cultivation goal for fruit and vegetable growers is to improve their total profits. This goal has to be achieved by achieving deduced goals that fit in fruit and vegetable market situations and other optimisation goal affecting situations. These deduced goals by fruit and vegetable market situation and other situations that affect these goals are in table 22.

In the case of lettuce cultivations in the Netherlands and Belgium, area limitation is not laid on lettuce greenhouse growers, but a kind of quota limitation is. Greenhouse growers often have fixed planting densities because lettuce cultivation is soil bound. Also, they have fixed annual cultivation schemes and cultivation durations. This leads to fixed amounts of cultivated lettuce per year, which is the same as quota limitation.

Table 21: Names, symbols, values and references of parameters used in equations 26 and 27

The value of  $c_s$  is a product of 18 lettuce heads per m<sup>2</sup> and additional prices per unit head weight presented by van Henten (1994).

symbol	name	value	units	references
$c_h$	dutch heating costs	$4 \cdot 10^{-9}$	€·J <sup>-1</sup>	Georges, et al. (2003).
$c_c$	CO <sub>2</sub> -injection costs	$9 \cdot 10^{-2}$	€·kg <sup>-1</sup>	anonymous (1992)
$c_s$	net lettuce sales price	in spring and summer: $-8 \cdot 10^{-3}$ in autumn and winter: $6 \cdot 10^{-2}$	€·m <sup>-2</sup> ·g <sup>-1</sup> plant	van Henten (1994)

Table 22: Deduced optimisation goals by fruit and vegetable market situation and other situations that affect these goals

<i>fruit and vegetable market situation</i>			
		<i>saturated market, leading to small differences between sales revenues and costs, called profits</i>	<i>non-saturated market, leading to huge sales revenues that make costs insignificant low</i>
<i>other optimisation goal affecting situations</i>	<i>Unlimited fruit and vegetable cultivation</i>	Maximisation of profits per unit product and per unit time	Maximisation of sales revenues per unit product and per unit time
	<i>Amount of cultivated fruits or vegetables is limited. (quota limitation).</i>	Maximisation of profits per unit product <sup>a</sup>	Maximisation of sales revenues per unit product
	<i>Amount of fruit or vegetable cultivation area is limited (area limitation).</i>	Maximisation of profits per unit area and per unit time <sup>a</sup>	Maximisation of sales revenues per unit area and per unit time

<sup>a</sup> Seginer and Ioslovich (1999)

Whether the present lettuce market situation in The Netherlands and Belgium is saturated or not is indicated by data about sales revenues, costs and profits of greenhouse vegetable cultivation. These data are in table 23 as percentages of the total costs for the Netherlands in years 1991, 1995, 1997, 1998 and 1999 and for Belgium in years 2000, 2001 and 2002. Explanations of costs mentioned in this table are in table 24.

Table 23 shows that profit percentages are between -10% and +7%. These are low profit margins, indicating that the lettuce market is saturated. Combined with the presence of quota limitation, this market situation leads to the conclusion that the deduced goal is: calculating optimal control trajectories that lead to maximum profits per unit lettuce with fixed final time and fixed planting density.

Two more statements are included in this conclusion. Firstly, table 23 also shows that the profit percentages are equal to the lowest cost percentages. This means that even reducing costs that contribute only little to the total costs can still be beneficial in increasing profits. Secondly, costs and parts of sales revenues that are dependent on fixed final time and fixed planting density, but independent of controls or states that need to be optimised are fixed themselves. This means that they do not have to be considered when calculating optimal control trajectories leading to maximum profits, but only need to be considered when calculating the maximum profits themselves.

Table 23: Costs, sales revenues and profits of greenhouse vegetable cultivation as percentages of the total costs for the Netherlands in years 1991, 1995, 1997, 1998 and 1999 and for Belgium in years 2000, 2001 and 2002 (anonymous, 2000; anonymous, 2004)

		Netherlands					Belgium		
		1991	1995	1997	1998	1999	2000	2001	2002
FIXED COSTS	assets	20	18	16	16	17	20	20	21
	labour	34	38	38	39	39	33	34	35
	general	6	7	7	8	8	6	6	6
VARIABLE COSTS	energy	18	17	18	18	17	20	20	17
	seed/seedling	7	6	7	7	7	9	9	9
	fertilizer	3	2	2	2	2	3	3	3
	pesticide	1	2	1	1	1	2	2	2
	other materials	4	3	3	3	3	3	2	3
	delivery	6	7	7	6	6	4	4	4
total costs		100	100	100	100	100	100	100	100
total sales revenues		103	90	105	103	99	107	98	96
profit		+3	-10	+5	+3	-1	+7	-2	-4

Table 24: Explanation of the costs mentioned in table 23 (anonymous, 2000; anonymous, 2004)

costs	explanation
assets	Sum of costs for depreciation, maintenance and interest of buildings and machinery. Sum of costs for depreciation, maintenance and interest of the land on which greenhouses are situated are not included in general.
labour	Sum of wages paid to all personal of the greenhouse, including wage for third party work that is not related to other cost factors.
general	Sum of costs for magazine subscription, administration, breeding assistance, soil research, bank provision, electricity, soil/polder general expenses, plant/hardware insurance, water, car, gas minimum costs.
energy	Sum of costs related to heating of greenhouse.
seed/seedling	Sum of costs for seeds and seedlings.
fertilizer	Sum of costs for organic and non-organic fertilizers.
pesticides	Sum of costs for pesticides and labour costs related to soil disinfection.
other materials	Sum of costs for other cultivation materials, such as: pots, potting compost, soil cover for steaming.
delivery	Sum of costs for auction and packaging.

Energy costs, CO<sub>2</sub>-injection costs and sales revenues are control-dependent or state-dependent according to anonymous (1998), anonymous (1992), Georges, Van Lierde and Verspecht (2003) and Zwart (2002). So these costs and revenues are only considered when maximising profits.

This leads to the overall conclusion that the goal of greenhouse lettuce cultivation is to maximise profits per unit lettuce for which optimal control trajectories should be calculated. A fixed final time, fixed planting density, energy costs, CO<sub>2</sub>-injection costs and sales revenues need to be taken into account when computing optimal control trajectories.

### 3.5 Fit of mathematical models in general fixed-time optimal control problem

All three models are cast in the general variables  $\underline{x}$ ,  $\underline{z}$ ,  $\underline{u}$ ,  $\underline{d}$  (table 25) and general functions  $\underline{f}(\underline{x}, \underline{z}, \underline{u}, \underline{d})$ ,  $\underline{n}(\underline{x}, \underline{z}, \underline{u}, \underline{d})$ ,  $\underline{c}(\underline{u})$ ,  $\underline{s}(\underline{z})$ ,  $\underline{\psi}(\underline{x}_f)$ ,  $\underline{\phi}(\underline{x}_f)$  (table 26) of the general fixed-time optimal control problem presented in section 2.2.

Table 25: Fit of the specific variables in the general variables

names of variables	specific variables	general variables
states	$[M_{cv} \ M_{ca} \ T_g \ R]^T$	$= \underline{x}$
pseudo steady states	$[T_o \ RH_o \ C_{co}]^T$	$= \underline{z}$
control inputs	$[T_r \ Q \ F_{co}]^T$	$= \underline{u}$
disturbances	$[T_o \ S_o \ RH_o \ C_{co}]^T$	$= \underline{d}$

Table 26: Fit of the specific functions in the general functions

names of functions	specific functions	general functions
system state function	right hand side of equations 17, 18, 21 and 26	$= \underline{f}(\underline{x}, \underline{z}, \underline{u}, \underline{d})$
algebraic constraint function	right hand side of equations 22, 23 and 24	$= \underline{n}(\underline{x}, \underline{z}, \underline{u}, \underline{d})$
inequality constraint function related to control inputs	$[-\underline{u} + \text{lower bound values mentioned in table 19,}$ $\underline{u} - \text{upper bound values mentioned in table 19}]^T$	$= \underline{c}(\underline{u})$
inequality constraint function related to pseudo steady states	$[-\underline{z} + \text{lower bound values mentioned in table 19,}$ $\underline{z} - \text{upper bound values mentioned in table 19}]^T$	$= \underline{s}(\underline{z})$
inequality constraint function related to state final values	$[-\underline{y}_f + \text{lower bound values mentioned in table 13,}$ $\underline{y}_f - \text{upper bound values mentioned in table 13}]^T$  $\underline{y}_f = \underline{y}(t_f) \text{ of equations 19 and 20}$	$= \underline{\psi}(\underline{x}_f)$
final value function	right hand side of equation 27	$= \underline{\phi}(\underline{x}_f)$

## References

- anonymous (1992). *Beslissingsmodel voor CO<sub>2</sub> in de glastuinbouw investeringsselectie & doseertechniek: Aanvullend CO<sub>2</sub> doseren en warmteopslag; kwantitatieve informatie (Report)*, Nederlandse Onderneming voor Energie en Milieu, Proefstation voor Tuinbouw onder Glas, Sittard, Naaldwijk, The Netherlands.
- anonymous (1998). *Kwantitatieve informatie voor de glastuinbouw 1998-1999*, Proefstation voor Bloemmisterij en Glasgroente, Naaldwijk, The Netherlands.
- anonymous (2000). *Land- en tuinbouwcijfers 2000*, Landbouw-economisch Instituut, Centraal Bureau voor de Statistiek, 's Gravenhage, The Netherlands.
- anonymous (2004). *De rendabiliteit van het tuinbouwbedrijf (Report)*, Centrum voor Landbouweconomie, Ministerie van de Vlaamse Gemeenschap, Brussel.
- Breugelmans, M. (2000). *Optimal control of nitrate accumulation in greenhouse lettuce and other leavy vegetables, Nicolet; Technical report on four greenhouse growth experiments during year 1*, Ghent Univeristy, Provincial Research and Advisory Centre for Agriculture and Horticulture, Ghent, Rumbeke (Beitem), Belgium.
- Defant, A. and F. Defant (1958). *Physikalische dynamik der atmosphäre*, Akademische Verlagsgesellschaft, Frankfurt, Germany.
- Georges, H., D. Van Lierde and A. Verspecht (2003). *De Vlaamse glastuinbouw en zijn concurrenten (Report)*, Centrum voor Landbouweconomie, Ministerie van de Vlaamse Gemeenschap, Brussels, Belgium.
- Lide, D. R. (2003). *Handbook of chemistry and physics*, CRC Press, Boca Raton.
- Seginer, I., F. Buwalda and G. van Straten (1998). Nitrate concentration in greenhouse lettuce: a modelling study. *Acta Horticulturae*, 456, 189-197.
- Seginer, I. and I. Ioslovich (1999). Optimal spacing and cultivation intensity for an industrialized crop production system. *Agricultural systems*, 62, 143-157.
- Seginer, I. and G. van Straten (2001). *Simple Geenhouse Model + annotations (Report)*, Wageningen University, Wageningen.
- van Henten, E. J. (1994). *Greenhouse climate management: an optimal control approach (PhD-thesis)*, Landbouwwuniversiteit Wageningen, Wageningen, The Netherlands.
- van Straten, G., I. Lopez Cruz, I. Seginer and F. Buwalda (1999). Calibration and sensitivity analysis of a dynamic model for control of nitrate in lettuce. *Acta Horticulturae*, 507,
- Vanthoor, E. (2001). *Calibration of a lettuce model and a computation of an optimal lettuce growth strategy (MSc-thesis)*, Wageningen University, Wageningen.
- von Elsner, B., D. Briassoulis, D. Waaijenberg, A. Mistriotis, C. von Zabeltitz, J. Gratraud, G. Russo and R. Suay-Cortes (2000). Review of structural and functional characteristics of greenhouses in European union countries: part 1, design requirements. *Journal of agricultural engineering research*, 75, 1-16.
- Zwart (2002). *Analyzing energy-saving options in greenhouse cultivation using a simulation model (PhD-thesis)*, Wageningen University, Wageningen, The Netherlands.

# 4

## 4 Open-loop optimal control

### 4.1 Test of ACW-gradient optimisation algorithm in computation of an optimal control policy for achieving acceptable nitrate concentration of greenhouse lettuce

This section is a copy of the paper:

De Graaf, S.C., J.D. Stigter and G. van Straten (2004). Test of ACW-gradient optimisation algorithm in computation of an optimal control policy for achieving acceptable nitrate concentration of greenhouse lettuce. *Mathematics and computers in simulation*, 65, 117-126

**Abstract:** The ACW-gradient method proposed by Weinreb (1985) is put to the test in finding optimal control laws for an optimisation problem with bounds on the inputs and terminal state constraints, presented by Ioslovich and Seginer (2000). By making certain assumptions they derived properties of the solution in an analytic way. Here, it is shown that the numerical ACW-gradient algorithm is capable of finding solutions without making additional assumptions.

#### 4.1.1 Introduction

Often (non-) linear optimisation problems have to be simplified by making certain assumptions if the purpose is to find optimal control laws analytically. There is no need of these assumptions when iterative numerical computation algorithms are used. The suitability of a particular algorithm however, depends upon the type of problem. A particularly difficult class of problems is obtained when there are bounds on the inputs in conjunction with terminal constraints, which often appear in agriculture, (bio)chemical industry and robotics. The ACW-gradient algorithm (Weinreb, 1985; Weinreb and Bryson, 1985) has been proposed for this situation. In this paper the ACW-gradient algorithm is put to the test on a problem presented by Ioslovich and Seginer (2000). This problem was selected because they provided an analytical derived control policy under certain assumptions, to which the numerical results without using their assumptions can be compared.

The basic gradient algorithm and the ACW-algorithm will be explained in sections 4.1.2 and 4.1.3. In section 4.1.4 the optimisation problem and (one of) its solution(s) will be explained. Section 4.1.5 summarises the paper.

#### 4.1.2 The basic gradient algorithm

The optimisation problem written in the *Mayer*-formulation (Bryson, 1999; Stengel, 1994), considered here is:

$$\dot{\underline{x}} = \begin{bmatrix} \dot{\underline{x}}^m \\ \dot{\underline{x}}^L \end{bmatrix} = \begin{bmatrix} m(\underline{x}^m, \underline{u}) \\ L(\underline{x}^m, \underline{u}) \end{bmatrix} = \underline{f}(\underline{x}, \underline{u}) \quad \begin{array}{ll} \underline{x}^m(0) = \underline{x}_0^m & \underline{x}^m \in \mathbb{R}^{n_x}, \quad \underline{u} \in \mathbb{R}^{n_u} \\ \underline{x}^L(0) = 0 & \underline{x}^L \in \mathbb{R} \end{array} \quad (28)$$

$$\underline{\psi}(\underline{x}_f) = \underline{0} \quad \underline{x}_f = \underline{x}(t_f) \quad \underline{\psi} \in \mathbb{R}^{n_\psi} \quad (29)$$

The augmented performance index that has to be minimised is:

$$J' = \phi(\underline{x}_f) + \underline{x}_f^L + \underline{v}^T \underline{\psi}(\underline{x}_f) + \int_0^{t_f} \underline{\lambda}^T \underline{f}(\underline{x}, \underline{u}) dt = \phi'(\underline{x}_f) + \underline{v}^T \underline{\psi}(\underline{x}_f) + \int_0^{t_f} \underline{\lambda}^T \underline{f}(\underline{x}, \underline{u}) dt \quad (30)$$

where  $\underline{x}^m(t)$  is the system state vector,  $\underline{x}^L$  is the running costs state,  $\underline{u}(t)$  is the control vector and  $\underline{\psi}(\underline{x}_f)$  is the constraint vector applied to the final state. The function  $m(\underline{x}^m, \underline{u})$  is the system state function,  $L(\underline{x}^m, \underline{u})$  is the running costs function and  $\underline{f}(\underline{x}^m, \underline{u})$  is the vector with both functions  $m$  and  $L$ ,  $\phi(\underline{x}_f)$  is the final weighting function in the *Bolza*-formulation and  $\phi'(\underline{x}_f)$  is the final weighting function in the *Mayer*-formulation (Bryson, 1999; Stengel, 1994).  $\underline{\lambda}$  and  $\underline{v}$  are *Lagrange* multipliers for respectively the state equations and for the final constraints. The functions  $m$ ,  $\underline{\psi}$ ,  $\phi$  and  $L$  are assumed to be differentiable with respect to  $\underline{x}$ ,  $\underline{u}$  and  $\underline{x}_f$ .

Bryson (1999) developed a MATLAB-version of the gradient algorithm to solve optimisation problems with terminal constraints. In this algorithm the optimal solution is considered to be found when the increment of  $J'$  is almost equal to zero:

$$dJ' = \left( \frac{d\phi'}{d\underline{x}} + \underline{v}^T \frac{d\underline{\psi}}{d\underline{x}} - \underline{\lambda}^T \right)^T d\underline{x}_f + \int_0^{t_f} \left[ \left( \left( \frac{\partial \underline{f}}{\partial \underline{x}} \right)^T \underline{\lambda} + \frac{d\underline{\lambda}}{dt} \right)^T \delta \underline{x} + \left( \left( \frac{\partial \underline{f}}{\partial \underline{u}} \right)^T \underline{\lambda} \right)^T \delta \underline{u} \right] dt = 0 \quad (31)$$



Setting to zero the coefficients of the independent increments  $d\underline{x}|_t$ ,  $\delta\underline{x}$ ,  $\delta\underline{u}$  yields necessary conditions for an optimal solution:

$$\left( \frac{d\phi}{d\underline{x}} + \underline{v}^T \frac{d\psi}{d\underline{x}} - \underline{\lambda}^T \right) \Big|_t = 0 \quad -\frac{d\underline{\lambda}}{dt} = \left( \frac{\partial f}{\partial \underline{x}} \right)^T \underline{\lambda} \quad \left( \frac{\partial f}{\partial \underline{u}} \right)^T \underline{\lambda} = 0 \quad (32)$$

Bryson showed that  $\underline{\lambda}$  and  $\underline{v}$  for the optimal control trajectories are related according to the following set of equations, in which  $\underline{\lambda}^*$  and  $\underline{\lambda}^v$  are adjoint variables.

$$\underline{\lambda} = \underline{\lambda}^* + \underline{v}^T \underline{\lambda}^v \quad (33)$$

$$\underline{\lambda}^* \Big|_t = \frac{d\phi}{d\underline{x}} \Big|_t \quad -\frac{d\underline{\lambda}^*}{dt} = \left( \frac{\partial f}{\partial \underline{x}} \right)^T \underline{\lambda}^* \quad (34)$$

$$\underline{\lambda}^v \Big|_t = \frac{d\psi}{d\underline{x}} \Big|_t \quad -\frac{d\underline{\lambda}^v}{dt} = \left( \frac{\partial f}{\partial \underline{x}} \right)^T \underline{\lambda}^v \quad (35)$$

This relation leads to the following equations for calculating the variation of  $\underline{u}$ , which eventually leads to the optimal solution:

$$Q = \int_0^t \left[ \left( \frac{\partial f}{\partial \underline{u}}(t) \right)^T \underline{\lambda}^v(t) \right]^T K \left( \frac{\partial f}{\partial \underline{u}}(t) \right)^T \underline{\lambda}^v(t) dt \quad (Q \text{ is non-singular}) \quad (36)$$

$$g = \int_0^t \left[ \left( \frac{\partial f}{\partial \underline{u}}(t) \right)^T \underline{\lambda}^v(t) \right]^T K \left( \frac{\partial f}{\partial \underline{u}}(t) \right)^T \underline{\lambda}^*(t) dt \quad (37)$$

$$\underline{v} = -Q^{-1}g \quad (38)$$

$$\delta\underline{u}(t) = -K \left\{ \left[ \left( \frac{\partial f}{\partial \underline{u}} \right)^T \underline{\lambda}^* + \underline{v}^T \left( \frac{\partial f}{\partial \underline{u}} \right)^T \underline{\lambda}^v \right]^T + \eta \left( \frac{\partial f}{\partial \underline{u}} \right)^T \underline{\lambda}^v Q^{-1} \underline{v} \right\} \quad (39)$$

where  $K$  is a positive preselected control variation matrix and  $\eta$  is a positive preselected constant reciprocal amount of steps in reaching the final state constraints.

The algorithm consists of the following steps, based on the equations above:

- Guess  $\underline{u}(t)$  for  $t \in [0, t_f]$
- integrate  $\dot{\underline{x}} = \underline{f}(\underline{x}, \underline{u})$  with  $\underline{x}(0)$ ,  $\underline{u}(t)$ . Store  $\underline{x}(t)$ ,  $\underline{u}(t)$  and  $\underline{\psi}(\underline{x}(t_f))$
- integrate backward to compute  $\underline{\lambda}^s$ ,  $\underline{\lambda}^v$  (from  $\left(\frac{\partial f}{\partial \underline{x}}\right)^T \underline{\lambda}^s$ ,  $\left(\frac{\partial f}{\partial \underline{x}}\right)^T \underline{\lambda}^v$ ),  $Q$  and  $g$
- calculate  $\underline{v}$ ,  $\delta \underline{u}$  and the new  $\underline{u}$
- repeat b to d until  $\left\| \int_0^{t_f} \delta \underline{u}(t) dt \right\| < \varepsilon$  and  $\sum_{i=1}^k |\psi_i| < \varepsilon$ , where  $\varepsilon$  is a preselected small positive value relative to  $\phi'(\underline{x}_f)$

#### 4.1.3 The ACW-method

Weinreb (1985) introduced the adjustable control-variation weight (ACW) method to incorporate control bounds in the optimal control laws calculated by the gradient algorithm. According to Weinreb the ACW-method overcomes problems inherent to the penalty function method, the slack variable method and the switch-times parameter optimisation method. The inputs are normalised with respect to the bounds such that:

$$|\mu_i| \leq 1 \quad i = 1, \dots, m \quad (40)$$

In the basic gradient algorithm the control weight  $K$  is independent of the control. In the ACW gradient algorithm  $K$  is dependent on the distance between the control and its control bounds, such that it becomes zero when one of the bounds is reached.  $K$  is the following matrix:

$$K = \begin{bmatrix} c^{u_1} k^{u_1}(u_1) & & & 0 \\ & c^{u_2} k^{u_2}(u_2) & & \\ & & \ddots & \\ 0 & & & c^{u_m} k^{u_m}(u_m) \end{bmatrix} \quad (41)$$

where  $k^{u_i}$  is in between 0 and 1 and  $c^{u_i}$  is a positive weighting constant.

For the calculation of  $v$  (equations 36 to 38) the following equation for  $k^{u_i}(u_i)$  is used:

$$k^{u_i}(u_i) = 1 - |\mu_i| \quad (42)$$

So,  $k^{u_i}(u_i)$  approaches zero as the control approaches one of its bounds.

For the calculation of  $\delta u$  (equation 39) the following equations for  $k^u(u_i)$  are used

$$k^u(u_i) = \begin{cases} 1 - \omega & \text{if } |u_i| \geq \omega \text{ and } \operatorname{sgn}\left(u_i \frac{\partial f}{\partial u_i} \underline{\lambda}\right) = +1 \\ 1 - |u_i| & \text{otherwise} \end{cases} \quad (43)$$

where  $\omega$  is a design value, close to but smaller than +1. Here,  $k^u(u_i)$  approaches zero when moving towards a bound in the optimal control direction, or  $k^u(u_i)$  is equal to  $1 - \omega$  when moving towards a bound in the non-optimal direction.

#### 4.1.4 Lettuce-greenhouse example

##### 4.1.4.1 Problem formulation

The ACW-gradient algorithm was used to compute optimal control laws for an optimisation problem described by Ioslovich and Seginer (2000). They analytically found optimal control policies for temperature, nitrate flux and plant spacing for the growth of greenhouse lettuce. These optimal control policies lead to minimal costs while assuring that the nitrate concentration of the greenhouse lettuce at the end of the growing period is equal to or below a specified level. The latter is important because maximum nitrate levels in lettuce are set by the European Union so as to protect people from health risks.

In this problem, growth of greenhouse lettuce is depicted as a change of the carbon content of the lettuce structure per plant ( $m_{Cs}$ ). As the carbon content of the lettuce structure increases monotonically with the independent cultivation time, it can be taken as the independent variable. The carbon content in lettuce vacuoles, ( $m_{Cv}$ ) is the state, for which the following state equation is defined:

$$\frac{dm_{Cv}}{dm_{Cs}} = \frac{F_{Cav} - F_{Cm} - (1 + \theta)F_{Cvs}}{F_{Cvs}} \quad (44)$$

$F_{Cav}$ ,  $F_{Cm}$ ,  $F_{Cvs}$  are the photosynthesis, the maintenance and the growth, i.e. conversion from vacuoles to structure, respectively. The parameter  $\theta$  is the growth respiration expressed as a fraction of growth. The equations for the photosynthesis and the maintenance are:

$$F_{Cav} = p(I, C_{Ca}) f\left(\frac{m_{Cs}}{a}\right) h_p\left(\frac{m_{Cs}}{a}, \frac{m_{Cv}}{a}\right) \quad (45)$$

$$F_{Cm} = \frac{m_{Cs}}{a} e(T) \quad (46)$$

where  $p$  is a carbon photosynthesis function,  $f$  a light interception function,  $h_p$  a photosynthesis inhibition function and  $e$  a specific maintenance respiration function. The inputs are the light intensity  $I$ , the carbon dioxide concentration  $C_{Ca}$  of the greenhouse air, the temperature  $T$  and the plant space  $a$ .

A linear relationship between the nitrate concentration in vacuoles ( $C_{Nv}$ ),  $m_{Cv}$  and  $m_{Cs}$  is specified in an output equation (Seginer and Straten, 1999):

$$C_{Nv} = \frac{\Pi_v}{\beta} - \frac{\gamma \cdot \kappa}{\beta} \frac{m_{Cv}}{m_{Cs}} \quad (47)$$

where  $\gamma$ ,  $\beta$  and  $\kappa$  are coefficients and,  $\Pi_v$ , the osmotic pressure in the lettuce vacuoles.

Based on a nitrogen balance of the lettuce vacuoles (Seginer and Straten, 1999) and this equation, the nitrogen uptake of the lettuce plants  $F_{Nrv}$  can be considered as control input when it is confined between the following bounds:

$$\max\left(0, -\frac{\gamma}{\beta}(F_{Cav} - F_{Cm})\right) \leq F_{Nrv} \leq \frac{\left(\frac{\Pi_v}{\kappa} + \gamma(1 + \theta) + \beta r\right)F_{Cvs}^d - \gamma(F_{Cav} - F_{Cm})}{\beta} \quad (48)$$

where  $r$  is the ratio of nitrogen to carbon in the structure and

$$F_{Cvs}^d = g(T) f\left(\frac{m_{Cs}}{a}\right) h_g\left(\frac{m_{Cs}}{a}, \frac{m_{Cv}}{a}\right) \quad (49)$$

which is the growth demand of the lettuce plant.

The right hand side of equation 48 is the nitrogen uptake by the lettuce plants when the nitrogen supply is abundant. The lower bound has to be larger than zero because it is assumed that it is only possible to supply and not to extract nitrogen.

When  $F_{Nrv}$  acts as a control, according to equation 48  $F_{Cvs}$  is restricted:

$$0 \leq F_{Cvs} \leq F_{Cvs}^d \quad (50)$$

Note, the change of the lower bound on  $F_{Cvs}$  compared to Ioslovich and Seginer (2000).

$F_{Cvs}^d$  depends on the temperature, which is also a bounded input control:

$$T_L \leq T \leq T_U \quad (51)$$

where  $T_L$  and  $T_U$  are the lower and the upper bounds on the temperature. This dependency of the upper bound on the temperature can be removed by writing:

$$F_{Cvs} = \left( \frac{\alpha + 1}{2} \right) F_{Cvs}^d \quad \text{and} \quad -1 \leq \alpha \leq 1 \quad (52)$$

where  $\alpha(t)$  is a new control variable, which can be viewed according to equation 48 as a dimensionless nitrogen supply.

The plant space  $a$  is assumed an unbounded control input. Furthermore, there is an end-constraint  $\psi$  on  $m_{Cs}$ , which via equation 47 is in accordance with the maximum nitrate level in lettuce set by the European Union.

The optimisation problem is formulated in the *Mayer*-formulation (Bryson, 1999; Stengel, 1994). Written in this formulation, the cost-state equation and the augmented cost criterion, which has to be minimised are:

$$\frac{dx^L}{dm_{Cs}} = \frac{(\max\{0, P_H (T - T_S)\}) + P_R}{F_{Cvs}} \quad (53)$$

$$\text{Minimise } J' = x_f^L + v^T \psi + \int_{m_{Cs,i}}^{m_{Cs,f}} \left( \lambda^m \frac{F_{Cav} - F_{Cm} - (1 + \theta) F_{Cvs}}{F_{Cvs}} + \lambda^L \frac{(\max\{0, P_H (T - T_S)\}) + P_R}{F_{Cvs}} \right) dm_{Cs} \quad (54)$$

The associated Hamiltonian is:

$$H = \lambda^m \frac{F_{Cav} - F_{Cm} - (1 + \theta) F_{Cvs}}{F_{Cvs}} + \lambda^L \frac{(\max\{0, P_H (T - T_S)\}) + P_R}{F_{Cvs}} \quad (55)$$

where  $z$  is the cost-state,  $z_f$  the final cost-state,  $m_{Cs,i}$  and  $m_{Cs,f}$  the initial and final carbon content in the lettuce structure,  $P_R$  the cost of renting and  $P_H$  is the cost of heating the greenhouse above a specified temperature  $T_S$ , which is the temperature in an unheated and unventilated greenhouse. The variable  $v$  is a *Lagrange*-multiplier and  $\lambda^m$ ,  $\lambda^L$  are adjoint variables. The cost-criterion represents the total costs of heating and renting over cultivation time. Further details of the problem are presented in Seginer, *et al.* (1998).

#### 4.1.4.2 Calculations

Optimal trajectories for  $T$  and  $\alpha$  ( $F_{Cvs}$ ) are calculated while  $a$  was kept constant. The parameters of the goal function, the bounds and the tuning parameter  $\varpi$  were set to realistic values in table 27.

Note that the environmental conditions  $T_s$ ,  $I$  and  $C_{Ca}$  are assumed constant throughout. The value of  $m_{Cv, \text{end-constraint}}$  is in accordance with a maximum winter nitrate level of 4500 ppm, set by the European Union.

#### 4.1.4.3 Results

Figures 2 to 7 show optimal trajectories of the state, inputs and other relevant variables. Using the ACW-gradient algorithm, an Intel Pentium III, 500 MHz, 256 MB RAM system required  $10^2$  iterations (less than 10 minutes) to converge to these optimal trajectories. It should be noted that these trajectories critically depend upon the statement of the optimisation problem.

The optimal trajectory for  $m_{Cv}a^{-1}$  is plotted against  $m_{Cs}a^{-1}$  in figure 2. This figure shows that the carbon content in the vacuoles starts at the given initial value and ends at its end-constraint.

The optimal control laws for  $T$  and  $\alpha$  are plotted against  $m_{Cs}a^{-1}$  in figures 3 and 4. Figure 3 shows that the optimal temperature trajectory is first on the lower temperature bound of 8 °C and switches via a singular trajectory to the upper temperature bound of 20 °C. The optimal value for  $\alpha$  increases from 0.975 to 0.998, which means that at the given fixed  $CO_2$  and light levels there is a minor need to limit the nitrate supply in order to meet the end-constraint.

Table 27: Realistic parameter values of the goal function, bounds and the tuning parameter  $\varpi$

parameters	values	parameters	values
$P_H$	$1.7 \cdot 10^{-8} \text{ €} \cdot \text{s}^{-1} \cdot \text{°C}^{-1} \cdot \text{m}^{-2}$	$\varpi$	0.8
$P_R$	$1.4 \cdot 10^{-6} \text{ €} \cdot \text{s}^{-1} \cdot \text{m}^{-2}$	$m_{Cs,i}$	$3.8 \cdot 10^{-1} \text{ mol C} \cdot \text{plant}^{-1}$
$T_s$	10 °C	$m_{Cs,f}$	$4.4 \cdot 10^{-1} \text{ mol C} \cdot \text{plant}^{-1}$
$T_U$	20 °C	$m_{Cv,i}$	$6.0 \cdot 10^{-2} \text{ mol C} \cdot \text{plant}^{-1}$
$T_L$	8 °C	$m_{Cv, \text{end-constraint}}$	$6.0 \cdot 10^{-2} \text{ mol C} \cdot \text{plant}^{-1}$
$I$	$1.1 \cdot 10^{-4} \text{ mol PAP} \cdot \text{m}^{-2} \cdot \text{s}^{-1}$	$a$	$5.5 \cdot 10^{-2} \text{ m}^2 \cdot \text{plant}^{-1}$ (18 plants $\cdot \text{m}^{-2}$ )
$C_{Ca}$	$2.0 \cdot 10^{-2} \text{ mol CO}_2 \cdot \text{m}^{-3}$		

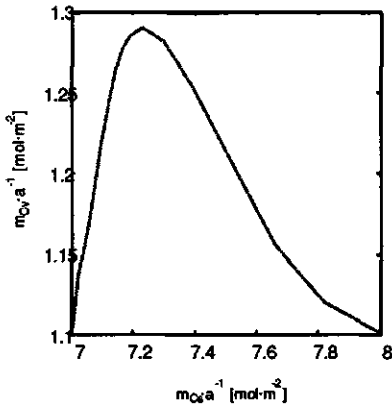


Figure 2: optimal  $m_{C_s} a^{-1}$ -trajectory

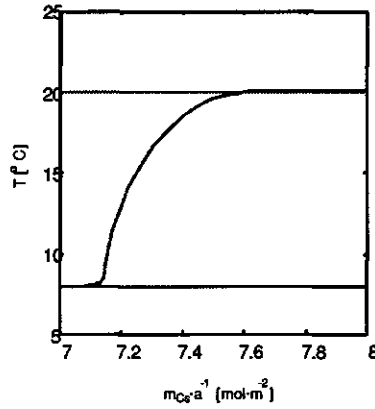


Figure 3: optimal  $T$ -trajectory

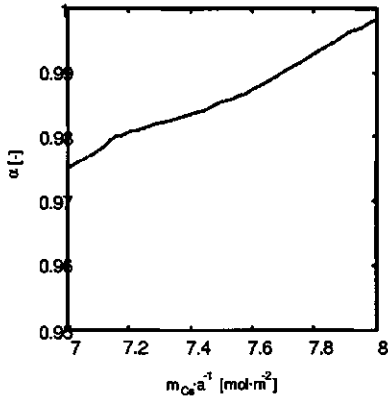


Figure 4: optimal  $\alpha$ -trajectory

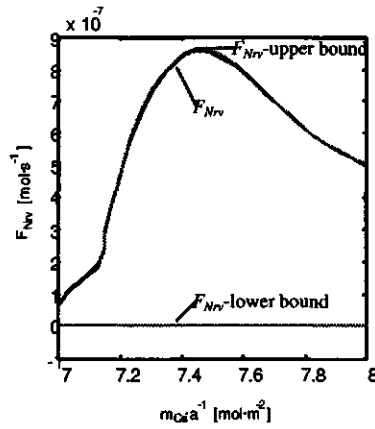


Figure 5: optimal  $F_{Nrv}$ -trajectory

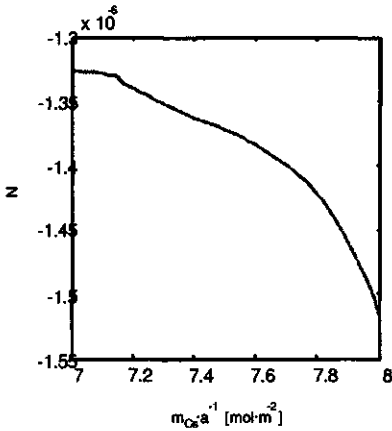


Figure 6: optimal  $N$ -trajectory

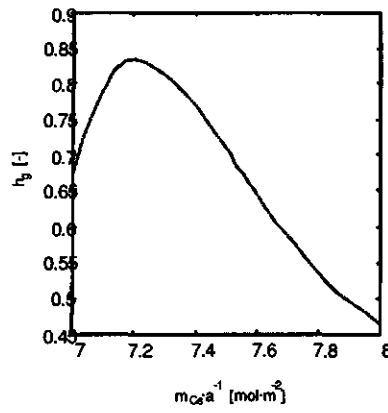


Figure 7: optimal  $h_g$ -trajectory

In figure 5  $F_{Nrv}$  is plotted against  $m_{Cs}a^{-1}$ . From this figure it is clear that  $F_{Nrv}$  is larger than 0 and smaller than the  $F_{Nrv}$ -upper bound for all values of  $m_{Cs}a^{-1}$ , which is in accordance with the confinement for  $F_{Nrv}$ .

The minimal costs  $J$  are:  $2.5 \cdot 10^{-2} \text{ €} \cdot \text{m}^{-2}$  or equivalently  $1.4 \cdot 10^{-3} \text{ €} \cdot \text{plant}^{-1}$ .

Ioslovich and Seginer (2000) proposed a strategy to determine the optimal value of  $F_{Cvs}$ , based on maximizing a Hamiltonian which had an opposite sign compared to the Hamiltonian given by equation 28. In this strategy the calculation of the numerator of this Hamiltonian is needed:

$$N = -\frac{\lambda^g}{\lambda^l} \left( p(I, C_{Co}) f\left(\frac{m_{Cs}}{a}\right) h_p\left(\frac{m_{Cs}}{a}, \frac{m_{Cv}}{a}\right) - \frac{m_{Cs}}{a} e(T) \right) - (\max\{0, P_H(T - T_s)\}) - P_R \quad (56)$$

$F_{Cvs}$  is determined by the following equations:

$$N < 0 \text{ then } F_{Cvs} = F_{Cvs}^d \quad \text{that is } \alpha = 1 \quad (57)$$

$$N = 0 \text{ then } 0 \leq F_{Cvs} \leq g\{T\} f\left(\frac{m_{Cs}}{a}\right) h_g\left(\frac{m_{Cs}}{a}, \frac{m_{Cv}}{a}\right) \quad \text{that is } -1 \leq \alpha \leq 1 \quad (58)$$

$$N > 0 \text{ then } F_{Cvs} \text{ approaches } 0 \quad \text{that is } \alpha = -1 \quad (59)$$

In figure 6  $N$  is plotted against  $m_{Cs}a^{-1}$ . From this figure it is clear that  $N$  is negative and increases in absolute values over time. This means that  $\alpha$  increases to 1, which is confirmed by figure 4. So the optimal control strategies for  $F_{Cvs}$  calculated by the ACW-gradient method support the analytically found optimal control policy by Ioslovich and Seginer.

In the equation for calculating  $N$  it is assumed by Ioslovich and Seginer that  $h_p$  is equal to 1. The numerically calculated optimal trajectory of  $h_p$  during the cultivation is approximately equal to 1 which confirms that the assumption is justified.

In deriving the optimal control policy analytically, Ioslovich and Seginer had to assume that  $h_g$  is equal to 1. Figure 7 shows that under certain conditions optimal solutions exist for which  $h_g \neq 1$ .

Concluding, the results of figures 2 to 7 show that the numerical ACW-gradient algorithm is capable of finding solutions of a complex optimisation problem without the need for additional assumptions.



#### 4.1.5 Conclusions

The ACW-gradient method proposed by Weinreb (1985) has been explained and is put to the test in finding optimal control laws for an optimisation problem with bounds on the inputs, presented and solved analytically by Ioslovich and Seginer (2000). It has been shown that the numerical ACW-gradient algorithm is capable of finding solutions for this problem without the need for additional assumptions.

#### References

- Bryson, A. E. (1999). *Dynamic optimization*, Addison-Wesley Longman, Inc., Menlo Park.
- Ioslovich, I. and I. Seginer (2000). Acceptable nitrate concentration of greenhouse lettuce: an optimal control policy for temperature, plant spacing and nitrate supply. In: *Preprints of Agricontrol 2000; International conference on modelling and control in agriculture, horticulture and post-harvested processing* pp. 89-94. IFAC, Wageningen University & Research Centre, Royal Dutch Institute of Engineers, Wageningen, The Netherlands.
- Seginer, I., F. Buwalda and G. van Straten (1998). Nitrate concentration in greenhouse lettuce: a modelling study. *Acta Horticulturae*, 456, 189-197.
- Seginer, I. and v. G. Straten (1999). Lettuce growth limited by nitrate supply. *Acta Horticulturae*, 507, 141-148.
- Stengel, R. F. (1994). *Optimal control and estimation*, Dover publications, Inc., New York.
- Weinreb, A. (1985). *Optimal control with multiple bounded inputs (PhD-thesis)*, Stanford University, Stanford.
- Weinreb, A. and A. E. Bryson (1985). Optimal control of systems with hard control bounds. *IEEE Transactions on automatic control*, 30, 1135-1138.

## 4.2 Optimal greenhouse climate control for achieving specified lettuce nitrate concentrations

This section is an extended version of the paper:

De Graaf, S.C., J.D. Stigter and G. van Straten (2005). Optimal greenhouse climate control for achieving specified lettuce nitrate concentration. in: *Preprints of IFAC Workshop on control applications of optimisation* (Ed: Bars, R., E. Gyurkovics), Viségrad, Hungary

**Abstract:** Characteristics of computed optimal open-loop control trajectories for growing low nitrate content lettuce in Dutch and Belgian greenhouses are presented, interpreted and compared with current climate control setpoints. These trajectories are computed because greenhouse lettuce growers in the Netherlands and Belgium are often not able to comply with European maximum nitrate concentrations levels. To compute them a mathematical optimal control problem is formulated that consists of a dynamic lettuce growth and nitrate accumulation model, dynamic greenhouse climate model, realistic constraints and climate data. This problem is solved by means of the adjustable control-variation weight (ACW) gradient algorithm. Physical, biological and economical interpretations show that the trajectory characteristics make sense. The comparison reveals a correspondence between these characteristics and current climate control setpoints. However, increasing CO<sub>2</sub>-concentrations and relative humidity values may improve lettuce cultivations with respect to final nitrate concentrations and sales revenues, without increasing running costs too much.

### 4.2.1 Introduction

Cultivating low nitrate content lettuce in greenhouses belongs to a class of agricultural and (bio)chemical processes that are carried out with a significant number of limitations on process variables while being affected by disturbances. Computing open-loop optimal control trajectories for these processes often implies solving optimal control problems with non-linear differential algebraic equations, affected by high frequency disturbances, possibly conflicting path constraints and end-constraints.

Such computations were carried out for climate conditions that prevail in the Netherlands and Belgium and results are presented and discussed in this paper. These results are interesting for lettuce greenhouse growers in both countries because they are often not able to comply with European maximum nitrate concentration standards despite the fact that their greenhouses offer possibilities to control lettuce cultivations through sophisticated greenhouse climate control (von Elsner, et al., 2000a).

Optimal trajectories of greenhouse air temperatures, ventilation rates, CO<sub>2</sub>-concentrations, CO<sub>2</sub>-enrichment flows, relative humidities and heating pipe temperatures are computed and compared with current common setpoints of climate control. To compute these trajectories a mathematical

formulation of the optimal control problem and a numerical optimisation algorithm are needed. These are explained first in this paper. In the formulation outline two dynamic models are discussed: a lettuce growth and nitrate accumulation model (Seginer, Buwalda and van Straten, 1998), and a dynamic greenhouse climate model (Seginer and van Straten, 2001). The explanation of the algorithm is about the MATLAB adjustable control-variation weight (ACW) gradient algorithm.

This paper differs from papers by Ioslovich and Seginer (2002) and by De Graaf (2004) in two respects. Firstly, outside and greenhouse climate conditions are taken into account in this paper and not in the other papers. Secondly, ventilation rates and CO<sub>2</sub>-enrichment flows are considered as control inputs beside the greenhouse air temperature in this paper instead of the nitrate flux and plant spacing. In this way results are obtained that are believed to be of more interest in practice, in particular when lettuce is cultivated on soil.

#### 4.2.2 Mathematical formulation

The lettuce cultivation problem is stated as an optimal control problem in the *Mayer*-formulation (Bryson, 1999; Stengel, 1994).

Given the system

$$\dot{\underline{x}} = \begin{bmatrix} \dot{\underline{x}}^m \\ \dot{\underline{x}}^L \end{bmatrix} = \begin{bmatrix} \underline{m}(\underline{x}^m, \underline{z}, \underline{u}, \underline{d}) \\ \underline{L}(\underline{x}^m, \underline{u}) \end{bmatrix} = \underline{f}(\underline{x}, \underline{z}, \underline{u}, \underline{d}) \quad \underline{x}(t_0) = \underline{x}_0 \quad (60)$$

and the constraints

$$0 = \underline{n}(\underline{x}, \underline{z}, \underline{d}, \underline{u}) \quad (61)$$

$$0 \geq \underline{c}(\underline{u}) \quad (62)$$

$$0 \geq \underline{s}(\underline{z}) \quad (63)$$

$$0 \leq \underline{\psi}(\underline{x}_f) \quad \underline{x}_f = \underline{x}(t_f) \quad (64)$$

maximize the augmented performance index

$$J' = \phi(\underline{x}_f) + \underline{v}^T \underline{\psi}(\underline{x}_f) + \int_{t_0}^{t_f} \underline{\lambda}^T \underline{f}(\underline{x}, \underline{z}, \underline{u}, \underline{d}) dt \quad (65)$$

where

$$\begin{array}{lllll} x \in \mathbb{R}^n & u \in \mathbb{R}^m & z \in \mathbb{R}^p & d \in \mathbb{R}^q & m \in \mathbb{R}^r \\ L \in \mathbb{R} & q \in \mathbb{R}^s & \psi \in \mathbb{R}^r & c \in \mathbb{R}^s & s \in \mathbb{R}^n \end{array} \quad (66)$$

Furthermore  $\underline{x}^m(t)$  is the system state vector,  $\underline{x}^L(t)$  is the running costs,  $\underline{d}(t)$  the disturbance vector and  $\underline{u}(t)$  the control input vector. The vector  $\underline{z}(t)$  is a vector of quasi steady states, which originates from the assumption that the rate of change of these variables is so fast as compared to that of other states that these variables always reach a quasi steady state. The function  $\underline{m}(\underline{x}^m, \underline{z}, \underline{u}, \underline{d})$  is the system state function,  $L(\underline{x}^m, \underline{u})$  is the running costs function and  $\underline{n}(\underline{x}, \underline{z}, \underline{u}, \underline{d})$  is an algebraic constraint function for the calculation of the quasi steady states. Equations 62, 63 and 64 represent inequality constraints on  $\underline{c}(\underline{u})$ ,  $\underline{s}(\underline{z})$  and  $\underline{\psi}(\underline{x}_f)$ , which are functions of the states, quasi steady states and final values of the states, respectively. The function  $\phi(\underline{x}_f)$  represents the profit at final time and is maximised. The vectors  $\underline{\lambda}$  and  $\underline{v}$  contain *Lagrange* multipliers for the state equations and for the final constraints, respectively. The functions  $\underline{m}$ ,  $L$ ,  $\underline{n}$ ,  $\underline{c}$ ,  $\underline{s}$ ,  $\underline{\psi}$ , and  $\phi$  are assumed to be differentiable with respect to  $\underline{x}$ ,  $\underline{z}$ ,  $\underline{u}$  and  $\underline{x}_f$ .

#### 4.2.2.1 Outline of dynamic lettuce growth and nitrate accumulation model

The system state function  $\underline{m}$  in equation 60 partly consists of a dynamical model, developed by Seginer, Buwalda and Van Straten (1998) in which growth of lettuce and nitrate accumulation in lettuce is related to greenhouse air temperature, CO<sub>2</sub>-concentration and solar radiation. The basis of this model is a negative correlation between sugars and nitrate in lettuce vacuoles. Sugars are produced by the photosynthesis process and are converted into lettuce structure material and energy, needed for growth and maintenance. This means that a higher production of sugars compared to conversion of sugars will lead to an increase of the sugar concentration and a decrease of the nitrate concentration in lettuce.

The model consists of two state differential equations 67, 68. The states are the carbon content in lettuce vacuoles  $M_{Cv}$  and the carbon content in the lettuce structure  $M_{Cs}$ .

$$\frac{dM_{Cv}}{dt} = F_{Cav}(S_0, C_{Ca}, M_{Cs}, M_{Cv}) - F_{Cm}(M_{Cs}, T_a) - (1 + \theta) F_{Cvs}(M_{Cs}, M_{Cv}, T_a) \quad (67)$$

$$\frac{dM_{Cs}}{dt} = F_{Cvs}(M_{Cs}, M_{Cv}, T_a) \quad (68)$$

$F_{Cav}$ ,  $F_{Cm}$ ,  $F_{Cvs}$  are non-linear functions for photosynthesis, maintenance and growth, i.e. sugar conversion from vacuoles to structure, respectively. The parameter  $\theta$  is the growth respiration expressed as a fraction of growth.  $S_0$  is the light intensity, which is an uncontrollable weather input (disturbance), depending on  $t$ . The dynamics of the greenhouse air carbon dioxide concentration  $C_{Ca}$  (quasi steady state) and the greenhouse air temperature  $T_a$  (quasi steady state) are described by the dynamic climate model, explained below.

The outputs of the lettuce growth and nitrate accumulation model are the fresh weight per head  $y_{fw}$  and the nitrate content per head  $y_{NO_3^-}$ , which depend on  $M_{Cs}$  and  $M_{Cv}$ .

$$\begin{bmatrix} y_{fw} \\ y_{NO_3^-} \end{bmatrix} = \underline{h}(M_{Cs}, M_{Cv}) \quad (69)$$

The negative correlation between sugars and nitrate is part of the function  $\underline{h}$ .  $\underline{\psi}$  in equation 64 is a function of  $\underline{h}$  and by substitution of equation 69, a function of the states  $M_{Cs}$  and  $M_{Cv}$ .

#### 4.2.2.2 Outline of dynamic climate model

Beside equations 67 and 68, the system state function in equation 60 consists of one additional state differential equation, which is part of a dynamic climate model, developed by Seginer and Van Straten (2001).

$$\frac{dT_g}{dt} = F_{Sog}(S_0) - F_{Lga}(M_{Cs}, RH_a, T_a, S_0) - F_{Hga}(T_g, T_a) \quad (70)$$

Equation 70 is a differential equation for the temperature  $T_g$  of the virtual unit of soil, crop and apparatus in a greenhouse. Associated to this equation there are three algebraic equations captured by equation 61.

$$0 = F_{Hea}(T_a, T_p) + F_{Hga}(T_g, T_a) - F_{Hao}^c(T_a, T_o) - F_{Hao}^v(T_a, T_o, Q^v) \quad (71)$$

$$0 = F_{Lga}(M_{Cs}, RH_a, T_a, S_0) - F_{Lao}^v(RH_a, T_a, RH_o, T_o, Q^v) \quad (72)$$

$$0 = P - F_{Cao}^v(C_{Ca}, C_{Co}, Q^v) + F_{Cm}(M_{Cs}, T_a) - \theta F_{Cvs}(M_{Cs}, M_{Cv}, T_a, C_{Ca}) - F_{Cav}(M_{Cs}, M_{Cv}, C_{Ca}, S_0) \quad (73)$$

These equations describe quasi steady state assumptions for  $C_{Ca}$ ,  $T_a$  and  $RH_a$  being the carbon dioxide concentration, air temperature and relative humidity in the greenhouse. They are algebraic equations for the sensible heat balance of the greenhouse air, for the latent heat balance of the greenhouse air and for the  $CO_2$ -balance of the greenhouse air respectively. They originate from the assumption that the rate of change of these states is so fat compared to that of  $T_g$  that these states always reach a quasi steady state. Furthermore  $Q^v$  (control input) is the specific ventilation rate, which is controllable by controlling the window apertures,  $T_p$  (control input) the heating pipe temperature and  $P$  (control input) the  $CO_2$ -enrichment flow. The variables  $C_{Co}$ ,  $RH_o$  and  $T_o$  are the outside carbon dioxide concentration, relative humidity and temperature respectively, which are uncontrollable weather inputs.

The functions  $F_{Sog}$ ,  $F_{Lga}$ ,  $F_{Hga}$ ,  $F_{Hea}$ ,  $F_{Hao}^c$ ,  $F_{Hao}^v$ ,  $F_{Lao}^v$  and  $F_{Cao}^v$  are linear and non-linear functions for the processes mentioned in table 28.

Table 28 Process descriptions for the functions in equations 71, 72 and 73

functions	process description
$F_{Sog}$	solar radiation absorbance
$F_{Lga}$	latent heat transfer by evapotranspiration from virtual unit to greenhouse air
$F_{Hga}$	heat transfer from the virtual unit to greenhouse air
$F_{Hea}$	heat transfer from heating pipes to greenhouse air
$F_{Hao}^c$	heat transfer by diffusion from greenhouse air to outside air
$F_{Hao}^v$	heat transfer by ventilation from greenhouse air to outside air
$F_{Lao}^v$	latent heat transfer by ventilation from greenhouse air to outside air
$F_{Cao}^v$	$CO_2$ transfer by ventilation from greenhouse air to outside air

#### 4.2.2.3 Bounds on inputs and quasi steady states

The control inputs  $Q$  and  $T_p$  and quasi steady states  $T_a$ ,  $RH_a$  are bounded from above and below. The control input  $P$  and quasi steady state  $C_{Ca}$  are bounded from below. These constraints are expressed by equations 62 and 63.

#### 4.2.2.4 End-constraints, initial and final conditions

The final fresh weight per head,  $y_{fw}$  and the final nitrate content per head  $y_{NO_3^-}$  are bounded from below and above respectively. These end-constraints are expressed by equation 64. The initial values of the states  $M_{Cv}$ ,  $M_{Cs}$  and  $T_g$  are captured by  $\underline{x}_0$  in equation 60. The initial and final time in equations 60 and 64 are expressed by  $t_0$  and  $t_f$ , respectively. Solutions that comply with equation 64 while taking into account equations 60, 61, 62 and 63 are difficult to find from cultivation experience, that is the inability of a lot of greenhouse lettuce growers to grow lettuce and comply

with maximum nitrate concentration levels set by the European union. However, these solutions are computed here.

#### 4.2.2.5 Running costs function and profits function

The running costs  $L$  in equation 65 is the sum of costs related to heating the greenhouse air and costs related to  $\text{CO}_2$ -addition to the greenhouse air:

$$L = F_H(T_p) + F_C(P) \quad (74)$$

The function  $\phi$  represents profits:

$$\phi(\underline{x}_f) = S(y_{fw,f}) - x_f^L \quad (75)$$

where  $x_f^L$  is the final value of the running costs and  $S$  represents lettuce sales revenues, which is an increasing function of the fresh weight per head  $y_{fw}$ .

The functions  $L$  and  $S$  are realistic functions deduced from figures presented by anonymous (2000) and anonymous (1998).

#### 4.2.2.6 Reformulation of the problem

A numerical optimisation algorithm, explained in section 4.2.3, was available to solve optimisation problems with state differential equations, end-constraints, fixed final time and bounded control input trajectories. In order to implement the optimisation problem into this algorithm and to properly deal with the algebraic equations and bounded unknowns the optimisation problem is reformulated into the following general optimisation problem.

$$\begin{bmatrix} \dot{\underline{x}} \\ \dot{\underline{v}} \end{bmatrix} = \begin{bmatrix} \underline{m}(\underline{x}, \underline{z}(\underline{x}, \underline{d}, \underline{u}), \underline{d}) \\ \underline{L}(\underline{z}(\underline{x}, \underline{d}, \underline{u}), \underline{u}) \\ \underline{w}(\underline{z}(\underline{x}, \underline{d}, \underline{u})) \end{bmatrix} = \underline{f}'(\underline{x}, \underline{d}, \underline{u}) \quad \begin{array}{l} \underline{x}(t_0) = \underline{x}_0 \\ \underline{v}(t_0) = \underline{v}_0 \end{array} \quad (76)$$

$$0 \geq \underline{c}(\underline{u}) \quad (62)$$

$$0 \leq \underline{\psi}(\underline{x}_f, \underline{v}_f) \quad \begin{array}{l} \underline{x}_f = \underline{x}(t_f) \\ \underline{v}_f = \underline{v}(t_f) \end{array} \quad (77)$$

$$\begin{array}{lllll}
 x \in \mathbb{R}^n & v \in \mathbb{R}^n & u \in \mathbb{R}^n & z \in \mathbb{R}^n & d \in \mathbb{R}^n \\
 m \in \mathbb{R}^n & L \in \mathbb{R}^n & w \in \mathbb{R}^n & \psi \in \mathbb{R}^n & c \in \mathbb{R}^n
 \end{array} \quad (78)$$

The augmented performance index that has to be maximised is:

$$J' = \phi(\underline{x}_f) + \underline{v}^T \underline{\psi}(\underline{x}_f, \underline{v}_f) + \int_{t_0}^{t_f} \underline{\lambda}^T f'(\underline{x}, \underline{d}, \underline{u}) dt \quad (79)$$

For this reformulation two aspects concerning the vector of quasi steady states  $\underline{z}$  are relevant to notice. Firstly, this vector is assumed as an explicit function of  $\underline{x}$ ,  $\underline{d}$ ,  $\underline{u}$  that is a unique, physically feasible solution of the function  $\underline{n}$  in equation 61 for the vector  $\underline{z}$ . Secondly, the controls  $P$  and  $T_p$ , and the quasi steady state  $RH_a$  are mathematically considered as the vector of quasi steady states and the control  $Q^v$  and quasi steady states  $T_a$  and  $C_{Ca}$  as the vector of controls.

The function  $\underline{w}$  is a function for recording the degree of the violation of the inequality constraint 63. Together with the initial and final values of  $\underline{v}$ , which are equal to zero, the function  $\underline{w}$  comprises isoperimetric constraints (Kirk, 1970; van Impe, 1993). The function  $\underline{f}'$  is an extension of the function  $\underline{f}$  in equation 60 and consists of functions  $\underline{m}$ ,  $L$  and  $\underline{w}$ .

#### 4.2.3 Numerical optimisation algorithm

A gradient MATLAB-algorithm developed by Bryson (1999) and extended with the adjustable control-variation weight (ACW) method was used to solve the optimal control problem iteratively. This algorithm has been proposed for optimisation problems with bounds on the inputs in conjunction with terminal constraints (Bryson, 1999; Bryson and Ho, 1975; de Graaf, Stigter and van Straten, 2004; Weinreb, 1985; Weinreb and Bryson, 1985). In this algorithm a maximum value for  $J'$  while fulfilling the end-constraints is considered to be found when the increment of  $J'$  is almost equal to zero:

$$dJ' = \left( \frac{d\phi}{d\underline{x}} + \underline{v}^T \frac{d\underline{\psi}}{d\underline{x}} - \underline{\lambda}^T \right) d\underline{x} \Big|_{t_f} + \int_0^{t_f} \left[ \left( \left( \frac{\partial f}{\partial \underline{x}} \right)^T \underline{\lambda} + \frac{d\underline{\lambda}}{dt} \right)^T \delta \underline{x} + \left( \left( \frac{\partial f}{\partial \underline{u}} \right)^T \underline{\lambda} \right)^T \delta \underline{u} \right] dt = 0 \quad (80)$$

In the algorithm the increment of  $J'$  approaches zero based on the evidence that  $\underline{\lambda}$  and  $\underline{v}$  are related for the optimal control trajectories. Together with setting to zero the coefficients of the independent increments  $d\underline{x} \Big|_{t_f}$ ,  $\delta \underline{x}$ ,  $\delta \underline{u}$  the following set of equations are used to achieve this (Bryson, 1999; Bryson and Ho, 1975; de Graaf, 2001; Weinreb, 1985):



$$\underline{\lambda} = \underline{\lambda}^* + \underline{v}^T \underline{\lambda}^v \quad (81)$$

$$\left. \underline{\lambda}^* \right|_{t_f} = \left. \frac{d\phi}{d\underline{x}} \right|_{t_f}, \quad -\frac{d\underline{\lambda}^*}{dt} = \left( \frac{\partial f}{\partial \underline{x}} \right)^T \underline{\lambda}^* \quad (82)$$

$$\left. \underline{\lambda}^v \right|_{t_f} = \left. \frac{d\psi}{d\underline{x}} \right|_{t_f}, \quad -\frac{d\underline{\lambda}^v}{dt} = \left( \frac{\partial f}{\partial \underline{x}} \right)^T \underline{\lambda}^v \quad (83)$$

In these equations  $\underline{\lambda}^*$  and  $\underline{\lambda}^v$  are adjoint variables.

These equations lead to the following equations for calculating the variation of the input-trajectories (Bryson, 1999; Bryson and Ho, 1975; Weinreb, 1985):

$$\underline{v} = Q \left\{ \frac{\partial f}{\partial \underline{u}}, \underline{\lambda}^v, \underline{\lambda}^*, K \right\}^{-1} \left\{ -g \left\{ \frac{\partial f}{\partial \underline{u}}, \underline{\lambda}^v, \underline{\lambda}^*, K \right\} + \eta \underline{\psi} \right\} \quad (84)$$

$$\delta \underline{u}(t) = -K \left[ \left( \frac{\partial f}{\partial \underline{u}}(t) \right)^T \underline{\lambda}^*(t) + \underline{v}^T \left( \frac{\partial f}{\partial \underline{u}}(t) \right)^T \underline{\lambda}^v(t) \right]^T \quad (85)$$

where  $\eta$  is a positive pre-selected constant reciprocal number of steps in reaching the end-constraints,  $g$  and  $Q$  are integral functions of  $\underline{\lambda}^*$ ,  $\underline{\lambda}^v$ ,  $\frac{\partial f}{\partial \underline{u}}$  and  $K$ .  $K$  is a time dependent diagonal matrix, which diagonal values depend on the distance between the actual control and its bounds, such that it becomes zero when one of the bounds is reached (Bryson, 1999; Bryson and Ho, 1975; de Graaf, Stigter and van Straten, 2004; Weinreb, 1985; Weinreb and Bryson, 1985).

After a number of iterations the variation of  $\underline{u}$  approaches the zero-vector, which is equivalent to reaching the optimal solution. According to the integral functions  $g$ ,  $Q$ , and equations 84 and 85,

this means that  $\underline{\psi}$  and  $\left[ \left( \frac{\partial f}{\partial \underline{u}} \right)^T \underline{\lambda}^* + (-Q^{-1}g)^T \left( \frac{\partial f}{\partial \underline{u}} \right)^T \underline{\lambda}^v \right]^T$  are close to zero.

Note that when there are no end-constraints,  $\underline{\psi}$  and  $\underline{\lambda}^v$  are empty vectors and so  $g$ ,  $Q$  and  $\underline{v}$  are empty. Equation 85 is accordingly reduced to the well-known equation for calculating the variation of  $\underline{u}$  for optimal control problems without end-constraints. In the algorithm this idea was used to solve the optimisation problem for those modes in which the end-constraints were fulfilled.

The algorithm consists of the following steps, based on the equations above:

- a. Guess  $\underline{u}(t)$  for  $t \in [t_0, t_f]$
- b. Integrate  $\dot{\underline{x}} = \underline{f}(\underline{x}, \underline{u})$  with  $\underline{x}(0)$ ,  $\underline{u}(t)$ . Store  $\underline{x}(t)$ ,  $\underline{u}(t)$  and  $\underline{\psi}(\underline{x}(t_f))$
- c. Integrate backward to compute  $\underline{\lambda}^*$ ,  $\underline{\lambda}^v$  (from  $\left(\frac{\partial f}{\partial \underline{x}}\right)^T \underline{\lambda}^*$ ,  $\left(\frac{\partial f}{\partial \underline{x}}\right)^T \underline{\lambda}^v$ ),  $Q$  and  $g$
- d. Calculate  $\underline{v}$ ,  $\delta \underline{u}$  and the new  $\underline{u}$ , which is the sum of the old  $\underline{u}$  and  $\delta \underline{u}$
- e. Repeat b to d until the stop-criterion  $\left| \int_0^{t_f} \delta \underline{u}(t) dt \right| < \varepsilon$  and  $\sum_{i=1}^k |\psi_i| < \varepsilon$  is met, where  $\varepsilon$  is a pre-selected small positive value relative to  $\phi(\underline{x}_f)$  and  $k$  is the dimension of  $\underline{\psi}$ .

#### 4.2.4 Computations and results

##### 4.2.4.1 Material and methods

Optimal open-loop trajectories of ventilation rates  $Q^v$ , CO<sub>2</sub>-concentrations  $C_{Ca}$ , greenhouse air temperatures  $T_a$ , CO<sub>2</sub>-enrichment flows  $P$  and dynamical heating pipe temperatures  $T_p$  were computed for 30 lettuce cultivations that were equally distributed over a year and affected by climate conditions that prevail in the Netherlands and Belgium. As both countries have about the same climatic conditions, computations for both countries were made using data about climate conditions measured in the Netherlands (Breuer and Van de Braak, 1989). These climate conditions consist of uncontrollable weather inputs  $S_o$ ,  $C_{Co}$ ,  $RH_o$  and  $T_o$  (disturbances). Mean values of these inputs are in table 29. Lettuce cultivation durations are also in this table.

To compute the trajectories the mathematical formulation and numerical optimisation algorithm explained in sections 4.2.2 and 4.2.3 were used. Realistic bounds on controls and quasi steady states, and realistic bounds on final values of outputs are in table 30. Values for  $M_{Cv}$  and  $M_{Cs}$  at  $t_0$  corresponded with a fresh head weight of 46 g and a nitrate content of  $4.5 \cdot 10^3$  ppm. Values of  $T_g$  at  $t_0$  were set at 10 °C.

Characteristics of optimal open-loop trajectories are compared with current common climate control setpoints. These setpoints are in table 31.

This table shows that relative humidity values are equal to or below 0.9. Taking into account outside climate conditions, relative humidity values close to 0.9 are often avoided to prevent lettuce plants from diseases or deformities. Due to this, actual relative humidity values are between 0.5 and 0.9.

Table 29: Mean values of  $S_o$ ,  $C_{Co}$ ,  $RH_o$ ,  $T_o$  and lettuce cultivation durations by season (anonymous, 1989; Breuer and Van de Braak, 1989)

	winter	spring	summer	autumn	units
$S_o$	3.5	15	14	4.5	$\text{MJ}\cdot\text{m}^{-2}\cdot\text{day}^{-1}$
$C_{Co}$	$1.3\cdot 10^{-2}$	$1.3\cdot 10^{-2}$	$1.3\cdot 10^{-2}$	$1.3\cdot 10^{-2}$	$\text{mol}\cdot\text{m}^{-3}$
$RH_o$	88	75	79	87	%
$T_o$ (maximum)	6	15	20	10	$^{\circ}\text{C}$
$T_o$ (minimum)	1	7	12	3	$^{\circ}\text{C}$
cultivation duration	60	45	30	45	days

Table 30 Realistic bounds on controls, quasi steady states and final value of outputs (from anonymous, 1989; von Elsner, et al., 2000b)

	lower bound	upper bound	units
<i>controls</i>			
$Q^v$	$7.5\cdot 10^{-5}$	$7.7\cdot 10^{-3}$	$\text{m}\cdot\text{s}^{-1}$
$C_{Ca}$	0.0	-	$\text{mol}\cdot\text{m}^{-3}$
$T_a$	5.0	40	$^{\circ}\text{C}$
<i>quasi steady states</i>			
$P$	0.0	-	$\text{mol}\cdot\text{m}^{-2}\cdot\text{s}^{-1}$
$RH_a$	0.0	0.9	-
$T_p$	$T_a$	60	$^{\circ}\text{C}$
<i>output final values</i>			
$y_{fw}$	300	-	$\text{g}\cdot\text{head}^{-1}$
$y_{NO_3^-, \text{ summer}}$	-	$3.5\cdot 10^3^*$	ppm
$y_{NO_3^-, \text{ winter}}$	-	$4.5\cdot 10^4^*$	ppm

\* These upper bounds are set by the European union

Table 31: Current common setpoints of lettuce cultivation greenhouse climate control (anonymous, 1989; Dueck, et al., 2004a; Dueck, et al., 2004b; van Henten, Bontsema and van Straten, 1997)

temperature at night	5	$^{\circ}\text{C}$
temperature at daylight	10	$^{\circ}\text{C}$
ventilation temperatures at night	$\geq 9$	$^{\circ}\text{C}$
ventilation temperatures at daylight	$\geq 12^*$	$^{\circ}\text{C}$
maximum values $\text{CO}_2$ -concentration when solar radiation intensity is high	$2\cdot 10^{-2} - 4\cdot 10^{-2}$	$\text{mol}\cdot\text{m}^{-3}$
relative humidity	$\leq 0.9$	-

\* This temperature is increased when the solar radiation intensity is high

## 4.2.4.2 Results

Characteristic patterns of computed optimal trajectories represented by values of control inputs, quasi steady states and output final values at daylight or night in specified seasons with specified climate conditions are in table 32.

Table 32 Characteristics patterns of optimal trajectories represented by values of control inputs, quasi steady states and output final values at daylight or night in specified seasons with specified climate conditions.

<i>variables</i>	<i>seasons, day versus night and climate conditions</i>	<i>values of variables</i>
<i>input controls</i>		
$Q^v$	p., s., a., at night	l.b.
	w., at night	b.b.
	all seasons, at daylight	b.b.
$C_{Ca}$	all seasons, at night	↓l.b.
	all seasons, at daylight	b.b., ↑sr*
$T_a$	w., p., a., at night, $T_o \leq 5^\circ\text{C}$	l.b.
	all seasons, at night and at daylight, $5 \leq T_o \leq 25^\circ\text{C}$	b.b.
	p., s., a., at daylight, $T_o \geq 25^\circ\text{C}$	u.b.
<i>quasi steady states</i>		
$P$	all seasons, at night	l.b.
	all seasons, at daylight	b.b., ↑sr*
$RH_a$	all seasons, at daylight, $T_a \leq 40^\circ\text{C}$	u.b.
	p., s., a., at daylight, $T_a > 40^\circ\text{C}$	b.b.
	a., w., p., at night, $0.8 < RH_o \leq 1.0$ and $T_a < 15^\circ\text{C}$	u.b.
	all seasons, at night, $RH_o < 0.8$ and $T_a > 15^\circ\text{C}$	b.b.
$T_p$	all seasons, at night, $T_a > 5^\circ\text{C}$	l.b.
	a., w., p., at night, $T_a < 5^\circ\text{C}$	b.b.
	a., w., p., from dawn till midday	b.b.
	s., at daylight and a., w., p., from midday till dusk	l.b.
<i>output final values</i>		
$y_{fw}$	all seasons	b.b.
$y_{NO_2, \text{summer}}$	p., s.	u.b.
$y_{NO_2, \text{winter}}$	w., a.	u.b.

l.b. lower bound

u.b. upper bound

b.b. between bounds

↑sr increasing with  $S_o$ 

↓l.b. decreasing to lower bound

w.

p.

s.

a.

\*

winter

spring

summer

autumn

calculated maximum value: 2000 ppm

These patterns lead to state trajectories of vacuole carbon content  $M_{Cv}$ , structure carbon content  $M_{Cs}$  and an output trajectory of lettuce fresh weight  $y_{fw}$  that increase exponentially. Ratios of  $M_{Cv}$  to  $M_{Cs}$  values fluctuate around a constant value. These fluctuations are synchronous to fluctuating (but still exponentially increasing) values of the carbon content in lettuce vacuoles  $M_{Cv}$  and are accompanied by opposite fluctuations of the nitrate concentration ( $y_{N_5}$ ). State values of the virtual unit temperature  $T_g$  fluctuate around a constant value. State values of running costs increase.

To visualize some of these patterns figures 8 to 14 are presented. Optimal time trajectories of  $S_o$ ,  $T_o$ ,  $C_{Co}$ ,  $RH_o$ ,  $Q^v$ ,  $C_{Ca}$ ,  $T_a$ ,  $P$ ,  $RH_a$ ,  $T_p$ ,  $y_{fw}$  and  $y_{N_5}$  of a winter lettuce cultivation during the whole cultivation are in figures 8 to 11. For more details, close-ups of optimal time trajectories of  $S_o$ ,  $T_o$ ,  $C_{Co}$ ,  $RH_o$ ,  $Q^v$ ,  $C_{Ca}$ ,  $T_a$ ,  $P$ ,  $RH_a$ ,  $T_p$  between days 20 to 35 are in figures 12 to 14.

#### 4.2.4.3 Interpretation

The presented characteristic patterns make sense according to the following list of physical, biological and economical interpretations.

Ventilation rates,  $Q^v$  are often on the lower bound to avoid expensive heat and  $CO_2$  loss, in case heating or  $CO_2$ -enrichment or both are needed. Ventilation rates are between bounds in case greenhouse air temperatures or relative humidity values tend to exceed their upper bounds.

Greenhouse air  $CO_2$ -concentration,  $C_{Ca}$ , decreases to the lower bound at night because  $CO_2$ -enrichment does not contribute to increasing profits. So it is of no use to make costs by dosing additional  $CO_2$ . At daylight,  $CO_2$  concentrations are at values above the lower bound that are optimal with respect to sales revenues and running costs.

Greenhouse air temperatures,  $T_a$  are not increased by heating at night in general because low temperatures help to save on running costs. An exception to this rule is made when these temperatures tend to decrease below the lower bound. At daylight, greenhouse air temperatures are at values between the bounds that are optimal with respect to sales revenues and running costs. This temperature may tend to exceed the upper bound. If this happens then the windows are opened, thus keeping the temperature at the upper bound.

Values of  $CO_2$ -enrichment flows,  $P$ , are such that optimal  $CO_2$ -concentrations can be reached.

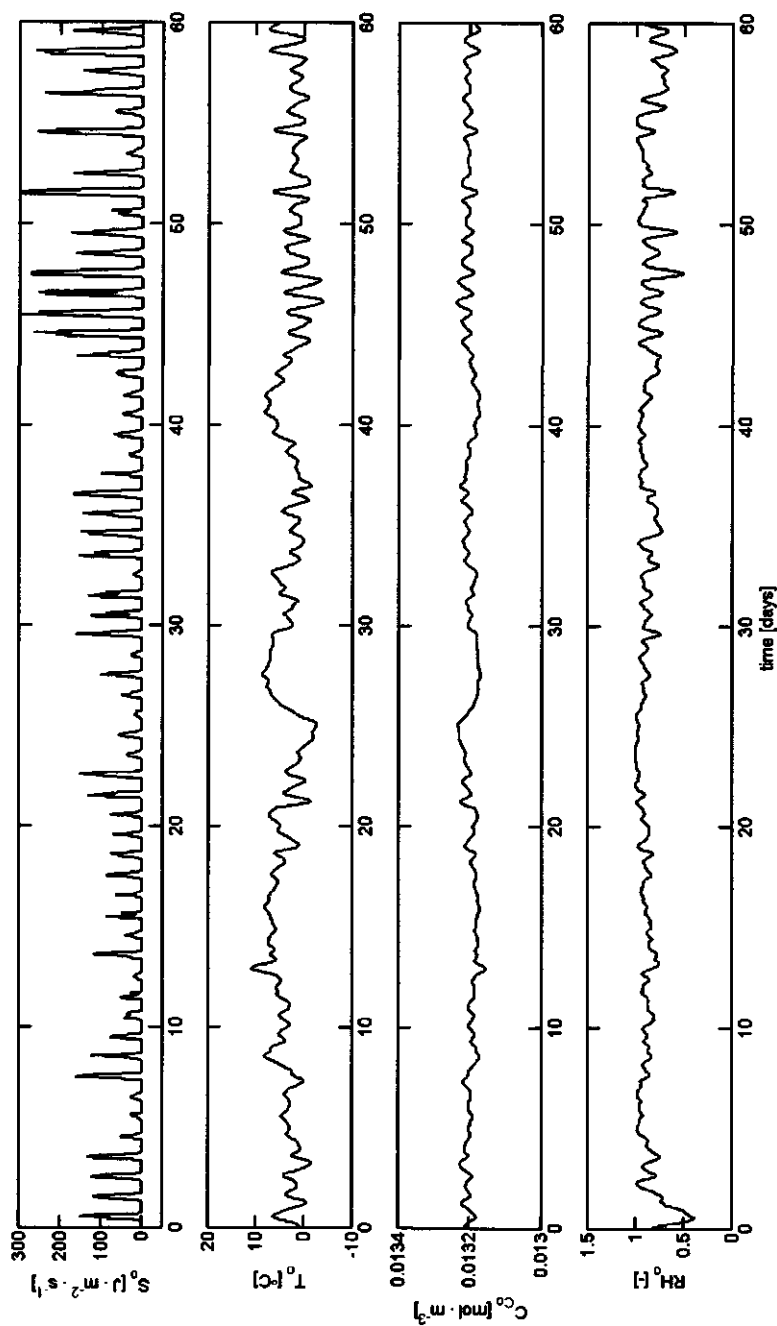


Fig. 8. Time trajectories of solar radiation intensity  $S_0$ , outside air temperature  $T_0$ , outside air  $\text{CO}_2$ -concentration  $C_{\text{CO}_2}$  and outside air relative humidity  $RH_0$  of a winter lettuce cultivation during the cultivation

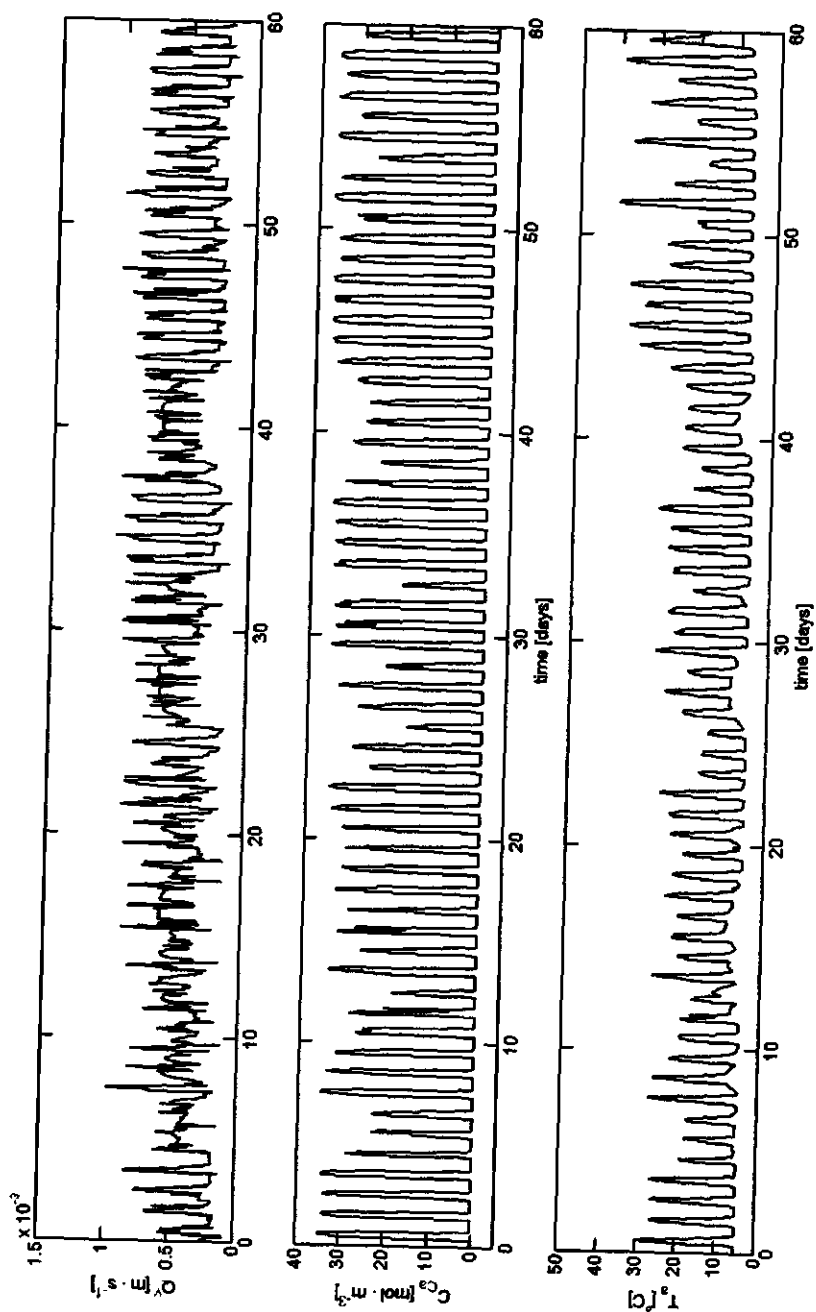


Fig. 9. Optimal time trajectories of ventilation rate  $Q'$ , greenhouse air  $\text{CO}_2$ -concentration  $C_{\text{CO}_2}$  and greenhouse air temperature  $T_a$  of a winter lettuce cultivation during the cultivation

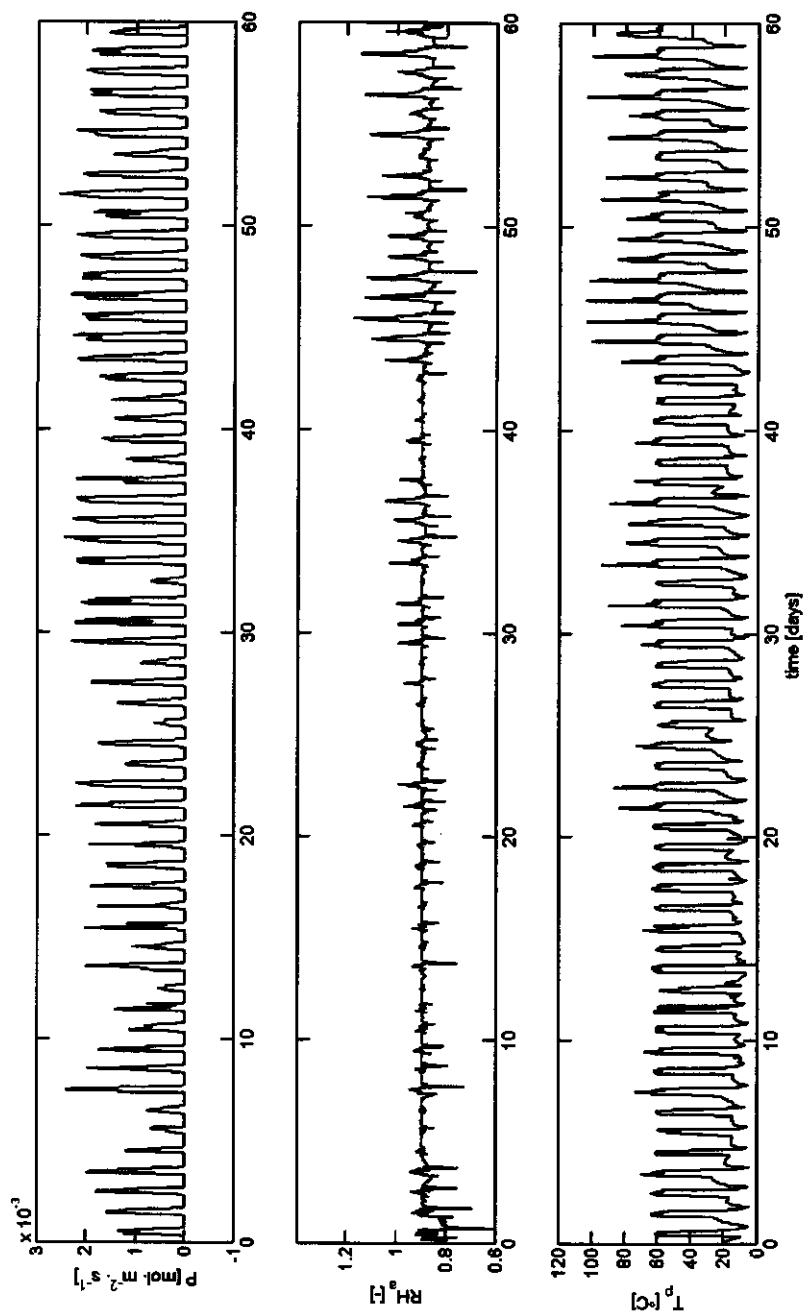


Fig. 10. Optimal time trajectories of CO<sub>2</sub>-enrichment flow  $P$ , greenhouse air relative humidity  $RH_a$  and heating pipe temperature  $T_p$  of a winter lettuce cultivation during the cultivation



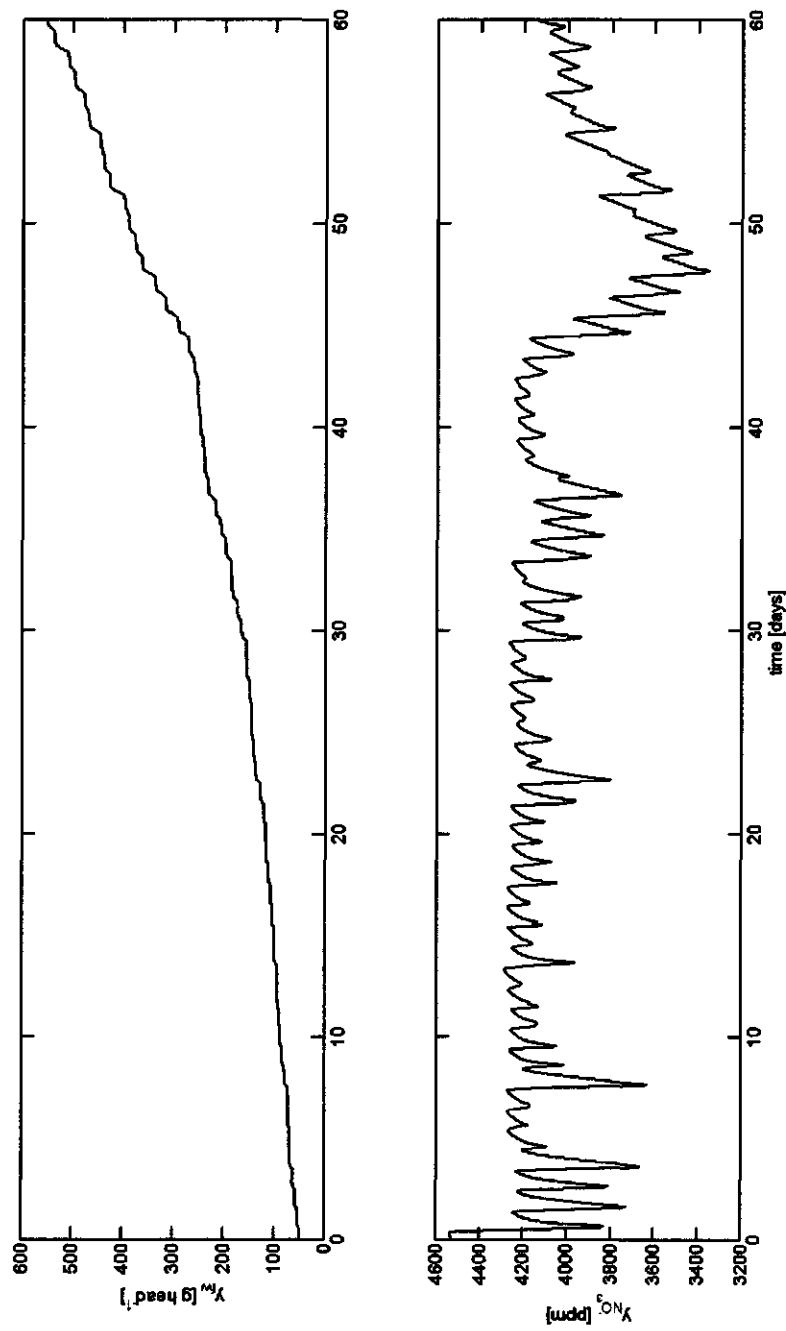


Fig. 11. Optimal time trajectories of fresh weight  $y_w$  and  $NO_3^-$  concentration  $y_{NO_3}$  of a winter lettuce concentration during the cultivation

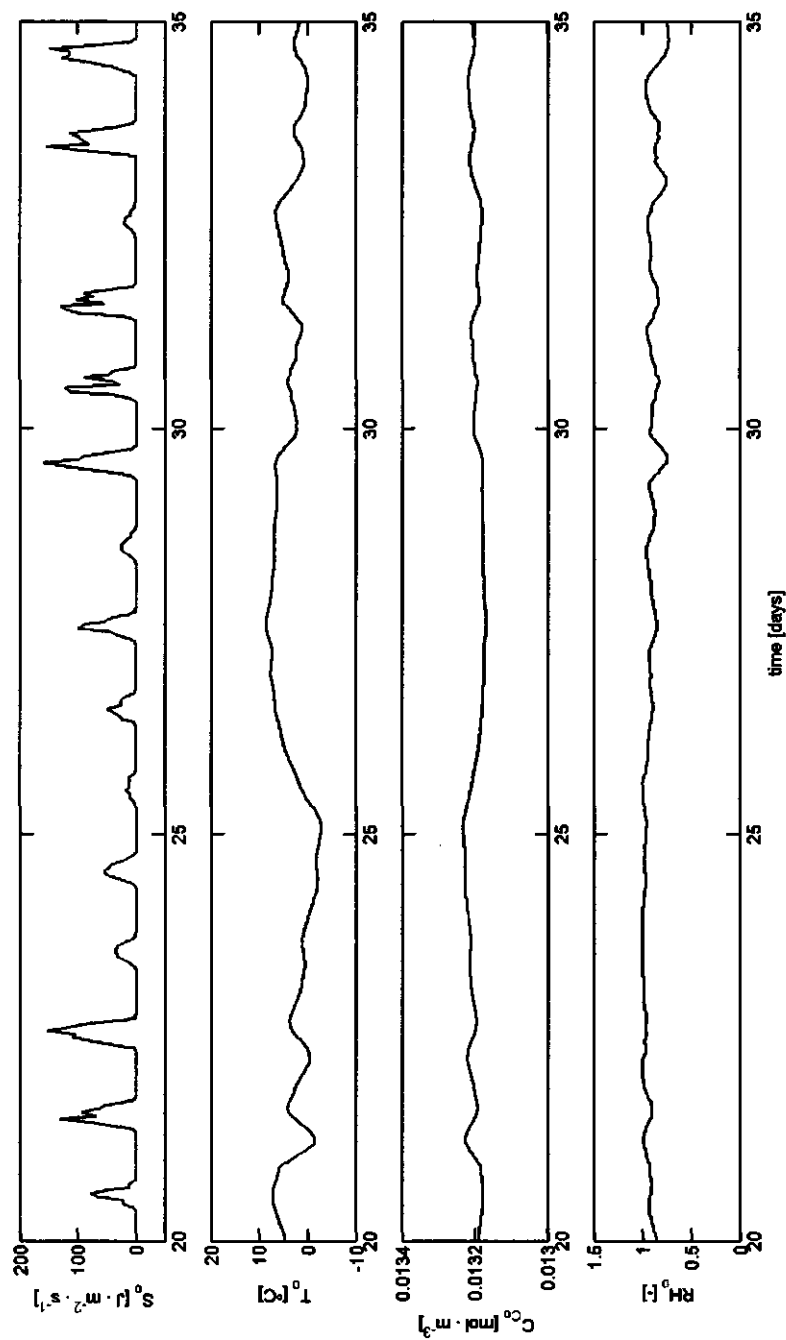


Fig. 12: Close-up of time trajectories of solar radiation intensity  $S_o$ , outside air temperature  $T_o$ , outside air  $\text{CO}_2$ -concentration  $C_o$  and outside air relative humidity  $RH_o$  of a winter lettuce between days 20 to 35.

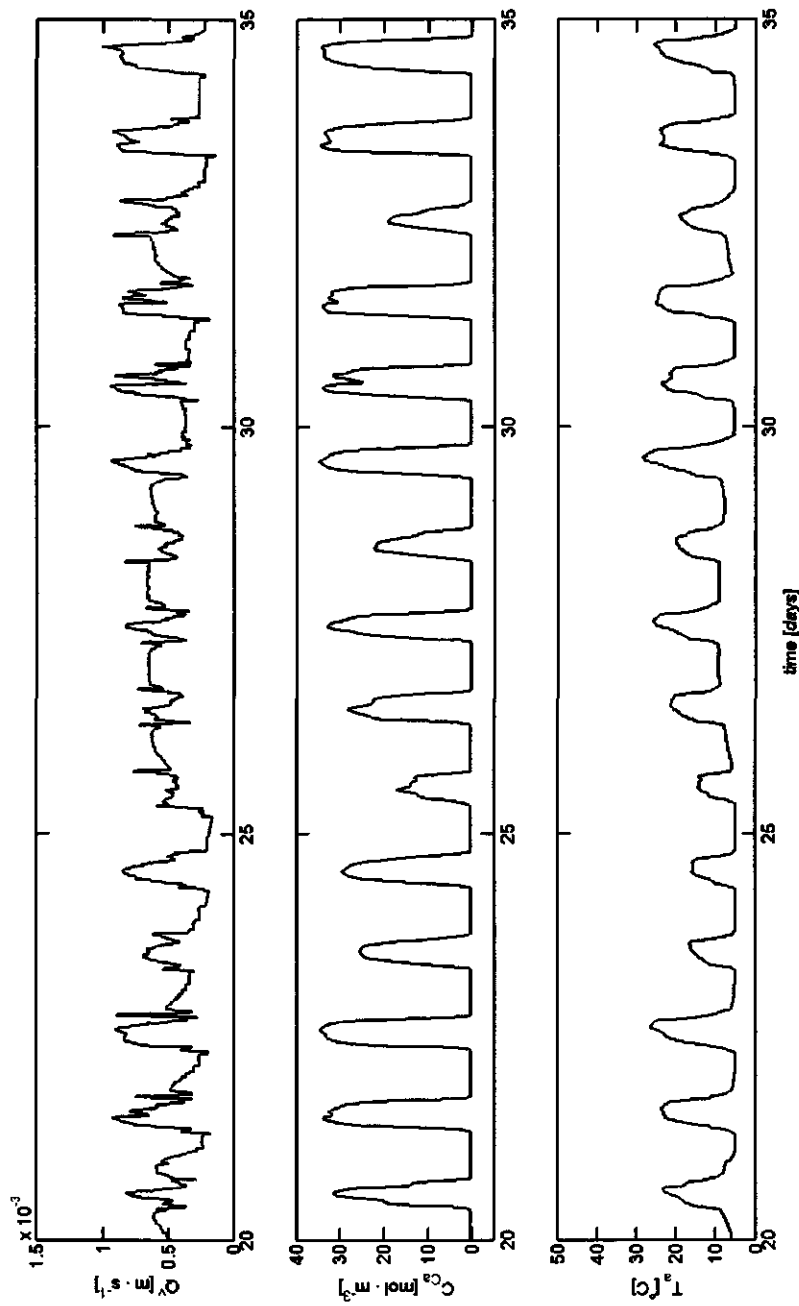


Fig. 13. Close-up of optimal time trajectories of ventilation rate  $Q$ , greenhouse air  $\text{CO}_2$ -concentration  $C_{Ca}$  and greenhouse air temperature  $T_a$  of a winter lettuce cultivation between days 20 to 35.

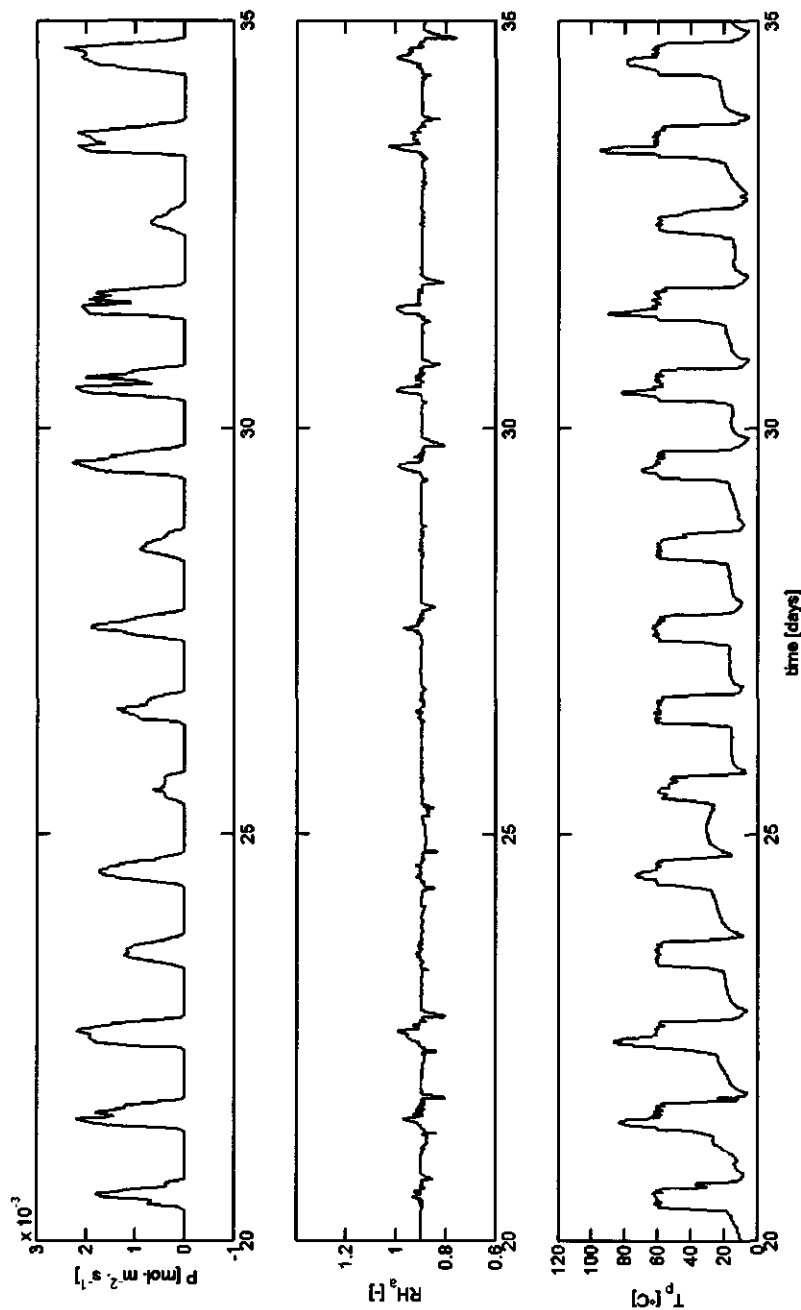


Fig. 14. Close-up of optimal time trajectories of CO<sub>2</sub>-enrichment flow  $P$ , greenhouse air relative humidity  $RH_a$  and heating pipe temperature  $T_p$  of a winter lettuce cultivation between days 20 to 35.

Relative humidity values,  $RH_a$  are controlled through controlling greenhouse air temperatures and ventilation rates and do not affect sales revenues or running costs directly. If relative humidity values tend to exceed the upper bound then greenhouse air temperatures and ventilation rates are adjusted by the algorithm such that relative humidity values are kept on the upper bound. Sometimes, this upper bound is exceeded, especially from days 40 through 60. The excess is limited, however, as can be deduced from the fact that the stop criterion of the algorithm is met. These general results are confirmed by Van Henten, Bontsema and Van Straten (1997) who found the same results for the relation between relative humidity values and ventilation rates.

Heating pipe temperatures,  $T_p$  are such that optimal air temperatures can be reached. Sometimes, the upper bound value is exceeded, especially from days 30 through 60. Just like the relative humidity excess, this excess is limited, as confirmed from the fact that the stop criterion of the algorithm is met.

Final nitrate concentrations are below or on their upper bound because climate conditions that increase profits also decrease nitrate concentrations below the upper bound.

Comparing characteristics of optimal input control and quasi steady state trajectories with current common setpoints of lettuce cultivation greenhouse climate control leads to the following observations.

Optimal  $\text{CO}_2$ -concentration trajectories are in the same range as current setpoints of  $\text{CO}_2$ -concentrations. However, increasing these setpoints may improve lettuce cultivations with respect to final nitrate concentrations and profits.

Computed optimal relative humidity values may often be closer to the upper bound at daylight than actual relative humidity values. Greenhouse growers are advised to increase their relative humidity towards the upper bound while still preventing lettuce plants from diseases and deformities. This will lead to lower ventilation rates and higher possible  $\text{CO}_2$ -concentrations that eventually will improve lettuce cultivations with respect to final lettuce nitrate concentrations and profits. It is not necessary to actually implement optimal control to benefit from this outcome: it can be applied immediately in current practice.

Optimal temperature trajectories can easily be imposed using current temperature setpoints.

#### 4.2.5 Conclusion

Nitrate concentrations that are below maximum concentrations set by the European Union can be optimally reached when applying optimal control trajectories as presented in this paper. These optimal control trajectories are such that constraints are properly dealt with. Physical, biological and economical interpretations show that characteristic patterns of computed optimal trajectories make sense. A comparison between the patterns of optimal trajectories with current common climate control setpoints reveals that optimal temperature trajectories can easily be imposed using current temperature trajectories and increasing relative humidity values towards the upper bound while still preventing lettuce plants from diseases and deformities will lead to final nitrate concentrations and higher profits. This outcome can be applied immediately in current practice.

#### References

- anonymous (1989). *De teelt van sla onder glas (Report)*, Ministerie van Landbouw, Dienst informatie, Gent, Belgium.
- anonymous (1998). *Kwantitatieve informatie voor de glastuinbouw 1998-1999*, Proefstation voor Bloemmisterij en Glasgroente, Naaldwijk, The Netherlands.
- anonymous (2000). *Land- en tuinbouwcijfers 2000*, Landbouw-economisch Instituut, Centraal Bureau voor de Statistiek, 's Gravenhage, The Netherlands.
- Breuer, J. J. G. and N. J. Van de Braak (1989). Reference year for dutch greenhouses. *Acta Horticulturae*, 248,
- Bryson, A. E. (1999). *Dynamic optimization*, Addison-Wesley Longman, Inc., Menlo Park.
- Bryson, A. E. and Y.-C. Ho (1975). *Applied optimal control; optimization, estimation and control*, Hemisphere, New York.
- de Graaf, S. C. (2001). *Test of ACW-gradient optimisation algorithm in computation of an optimal control policy for achieving acceptable nitrate concentration of greenhouse lettuce*, Haifa, Israel.
- de Graaf, S. C., J. D. Stigter and G. van Straten (2004). Test of ACW-gradient optimisation algorithm in computation of an optimal control policy for achieving acceptable nitrate concentration of greenhouse lettuce. *Mathematics and computers in simulation*, 117-126.
- Dueck, T., A. Elings, F. Kempkes, P. Knies, N. Van de Braak, N. Garcia, G. Heij, J. Janse, R. Kaarsemaker, P. Korsten, R. Maaswinkel, M. Ruijs, C. Reijnders and R. Van der Meer (2004a). *Energie in kentallen: zoek naar een nieuwe balans, nota 312 (Report)*, Plant research international B.V., Wageningen.
- Dueck, T., A. Elings, F. Kempkes, P. Knies, N. Van de Braak, N. Garcia, G. Heij, J. Janse, R. Kaarsemaker, P. Korsten, R. Maaswinkel, M. Ruijs, C. Reijnders and R. Van der Meer (2004b). *Energie in kentallen: zoek naar een nieuwe balans, nota 313 (Report)*, Plant research international B.V., Wageningen.
- Ioslovich, I. and I. Seginer (2002). Acceptable nitrate concentration of greenhouse lettuce: two optimal control policies. *Biosystems Engineering*, 83, 199-215.
- Kirk, D. E. (1970). *Optimal control theory; an introduction*, Prentice-Hall, Inc., Englewood Cliffs, New Jersey.
- Seginer, I., F. Buwalda and G. van Straten (1998). Nitrate concentration in greenhouse lettuce: a modelling study. *Acta Horticulturae*, 456, 189-197.

- Seginer, I. and G. van Straten (2001). *Simple Geenhouse Model + annotations (Report)*, Wageningen University, Wageningen.
- Stengel, R. F. (1994). *Optimal control and estimation*, Dover publications, Inc., New York.
- van Henten, E. J., J. Bontsema and G. van Straten (1997). Improving the efficiency of greenhouse climate control: an optimal control approach. *Netherlands Journal of Agricultural Science*, 45, 109-125.
- van Impe, J. (1993). *Modeling and optimal adaptive control of biotechnological processes (Report)*, Katholieke Universiteit Leuven, Leuven.
- von Elsner, B., D. Briassoulis, D. Waaijenberg, A. Mistriotis, C. von Zabeltitz, J. Gratraud, G. Russo and R. Suay-Cortes (2000a). Review of structural and functional characteristics of greenhouses in European union countries: part 2, typical designs. *Journal of agricultural engineering research*, 75, 1-16.
- von Elsner, B., D. Briassoulis, D. Waaijenberg, A. Mistriotis, C. von Zabeltitz, J. Gratraud, G. Russo and R. Suay-Cortes (2000b). Review of structural and functional characteristics of greenhouses in European union countries: part 1, design requirements. *Journal of agricultural engineering research*, 75, 1-16.
- Weinreb, A. (1985). *Optimal control with multiple bounded inputs (PhD-thesis)*, Stanford University, Stanford.
- Weinreb, A. and A. E. Bryson (1985). Optimal control of systems with hard control bounds. *IEEE Transactions on automatic control*, 30, 1135-1138.

# 5

## 5 Closed-loop optimal control

### 5.1 Closed-loop optimal control of greenhouse lettuce cultivation under measurable weather conditions

#### 5.1.1 Introduction

Cultivation of greenhouse lettuce with low nitrate concentrations while maintaining maximum profits is an issue for greenhouse lettuce growers in Netherlands and Belgium because they often have difficulties to grow lettuce with nitrate concentrations that are low enough to comply with European maximum nitrate concentration standards. On the other hand these growers have greenhouses with sophisticated climate control (von Elsner, et al., 2000a) that offer the potential to manipulate the nitrate content by suitable control. In previous sections it has already been shown that under average climate conditions at the prevailing latitudes it is possible to find control trajectories that ensure compliance with the standards and optimises cultivation profits. In this section one additional step is taken to arrive at an online closed-loop control that can be implemented in practice and solves the nitrate problem in an efficient manner. This is done by applying a closed-loop control algorithm to the lettuce cultivation problem. This algorithm computes specific ventilation rates, heating pipe temperatures and CO<sub>2</sub>-enrichment flow rates during lettuce cultivation that are (sub)optimal.

The problem is formulated as an optimal control problem with non-linear differential algebraic equations, non-affine control inputs, a non-quadratic cost function, terminal constraints and *measurable uncertain* external disturbances. These disturbances are solar radiation, outside air temperature and outside relative humidity. The involvement of them is a key issue here. Since they are measurable, they should be employed for state estimation. Moreover pre-computed climate control trajectories can be improved on-line using these measurements.

The issue of on-line adjustment of optimal control trajectories to measured uncertain disturbances has been addressed in the context of optimal greenhouse climate control by for example Van



Henten (1994), Tap (2000), Seginer and Sher (1993). The issue has also been considered in the context of other optimal physical and (bio)chemical process control problems by for example Friedland and Sarachik (1966), Rahman and Palanki (1996), Srinivasan (2002), Lee and Bryson (1989), Stengel (1994), Mayne, *et al.* (2000), and Mayne and Rawlings (2001). In principle, revisions of the optimal control trajectories can be made each time new weather data become available. MPC-algorithms and receding horizon control algorithms fall into this category of closed-loop suboptimal control algorithms. However, on-line optimisation by means of these algorithms is time consuming.

The contribution of this paper is to present a very efficient closed-loop control algorithm to control the nitrate content of lettuce. The key to achieving efficiency and (sub)optimality can be briefly stated as follows. Instead of solving a full optimal control problem *on-line* each time weather data become available, our approach uses *explicit* expressions for the control in terms of the current state, the current disturbances and the costate. These are computed *off-line*. Next these explicit expressions are evaluated *on-line* using the estimated state, the measured uncertain disturbance, and the pre-computed suboptimal costate to obtain the closed-loop suboptimal control.

The explicit expressions for the control are computed from the necessary optimality conditions and so called optimal operational modes of the system, obtained from open loop optimal control computations and simulations. Partly these computations are carried out symbolically while all of them are carried out *off-line*.

The employment of symbolic computation to determine explicit expressions for the optimal control is attractive as long as the explicit expressions obtained can be evaluated efficiently. This implies that their length should be limited. Our algorithm development meets this requirement. Although they did not use the name, the idea to use optimal operational modes of the system was introduced by (Srinivasan, Palanki and Bonvin, 2002). Roughly speaking optimal operational modes are characteristic parts of optimal control and state trajectories. They are obtained from optimal control simulations. A feature complicating the optimal control of nitrate concentration in lettuce is that the systems model contains quasi steady states that are constrained. These constraints translate into complicated control constraints in addition to their upper and lower bounds.

The outline of this chapter is as follows. Section 5.1.2 states the optimal control problem. Section 5.1.3 gives an general outline of the closed-loop control algorithm. Section 5.1.4 is about the design of the algorithm for the lettuce problem. Section 5.1.5 shows simulation results of closed-loop optimisations using the algorithm. Section 5.1.6 is the conclusion.

### 5.1.2 Mathematical formulation of the optimal control problem

The lettuce cultivation problem is formulated as an optimal control problem. For convenience this problem will be stated using the so-called Mayer formulation (Bryson, 1999; Stengel, 1994).

Given the augmented system:

$$\dot{\underline{x}} = \begin{bmatrix} \dot{\underline{x}}^m \\ \dot{\underline{x}}^L \end{bmatrix} = \begin{bmatrix} \underline{m}(\underline{x}^m, \underline{z}, \underline{u}, \underline{d}) \\ \underline{L}(\underline{x}^m, \underline{u}) \end{bmatrix} = \underline{f}(\underline{x}, \underline{z}, \underline{u}, \underline{d}) \quad \underline{x}(t_0) = \underline{x}_0 \quad (86)$$

and the constraints

$$0 = \underline{n}(\underline{x}, \underline{z}, \underline{u}, \underline{d}) \quad (87)$$

$$0 \geq \underline{c}(\underline{u}) \quad (88)$$

$$0 \geq \underline{s}(\underline{z}) \quad (89)$$

$$0 \leq \underline{\psi}(\underline{x}_f) \quad \underline{x}_f = \underline{x}(t_f) \quad (90)$$

maximise

$$J = \phi(\underline{x}_f) \quad (91)$$

where

$$\begin{array}{lllll} \underline{x} \in \mathbb{R}^{n_x} & \underline{u} \in \mathbb{R}^{n_u} & \underline{z} \in \mathbb{R}^{n_z} & \underline{d} \in \mathbb{R}^{n_d} & \underline{m} \in \mathbb{R}^{n_x-1} \\ \underline{L} \in \mathbb{R} & \underline{q} \in \mathbb{R}^{n_q} & \underline{\psi} \in \mathbb{R}^{n_\psi} & \underline{c} \in \mathbb{R}^{n_c} & \underline{s} \in \mathbb{R}^{n_s} \end{array} \quad (92)$$

Furthermore  $\underline{x}^m(t)$  is the system state vector,  $\underline{x}^L(t)$  is the running costs,  $\underline{d}(t)$  the disturbance vector and  $\underline{u}(t)$  the control input vector. The vector  $\underline{z}(t)$  is a vector of quasi steady states, which originates from the assumption that the rate of change of these variables is so fast as compared to that of other states that these variables always reach a quasi steady state. The function  $\underline{m}(\underline{x}^m, \underline{z}, \underline{u}, \underline{d})$  is the system state function,  $\underline{L}(\underline{x}^m, \underline{u})$  is the running costs function and  $\underline{n}(\underline{x}, \underline{z}, \underline{u}, \underline{d})$  is an algebraic constraint function for the calculation of the quasi steady states. Equations 88, 89 and 90 represent inequality constraints on  $\underline{c}(\underline{u})$ ,  $\underline{s}(\underline{z})$  and  $\underline{\psi}(\underline{x}_f)$ , which are functions of the states, quasi steady states and final values of the states, respectively. The function  $\phi(\underline{x}_f)$  represents the profit at final time and is maximised.

### 5.1.2.1 Outline of dynamic lettuce growth and nitrate accumulation model

The system state function  $\underline{m}$  in equation 86 partly consists of a dynamical model, developed by Seginer, Buwalda and Van Straten (1998) in which growth of lettuce and nitrate accumulation in lettuce is related to greenhouse air temperature,  $\text{CO}_2$ -concentration and solar radiation. The basis of this model is a negative correlation between sugars and nitrate in lettuce vacuoles. Sugars are produced by the photosynthesis process and are converted into lettuce structure material and energy, needed for growth and maintenance. This means that a higher production of sugars compared to conversion of sugars will lead to an increase of the sugar concentration and a decrease of the nitrate concentration in lettuce. The states of this model are the carbon content in lettuce vacuoles  $M_{Cv}$  and the carbon content in the lettuce structure  $M_{Cs}$ .

$$\frac{dM_{Cv}}{dt} = F_{Cav}(S_0, C_{Ca}, M_{Cs}, M_{Cv}) - F_{Cm}(M_{Cs}, T_a) - (1 + \theta) F_{Cvr}(M_{Cs}, M_{Cv}, T_a) \quad (93)$$

$$\frac{dM_{Cs}}{dt} = F_{Cvs}(M_{Cs}, M_{Cv}, T_a) \quad (94)$$

$F_{Cav}$ ,  $F_{Cm}$ ,  $F_{Cvr}$  are non-linear functions for photosynthesis, maintenance and growth, i.e. sugar conversion from vacuoles to structure, respectively. The parameter  $\theta$  is the growth respiration expressed as a fraction of growth.  $S_0$  is the light intensity, which is an uncontrollable weather input (disturbance), that depends on  $t$ .  $C_{Ca}$  and  $T_a$  represent the carbon dioxide concentration and air temperature in the greenhouse respectively. They are described in the next section.

The outputs of the lettuce growth and nitrate accumulation model are the fresh weight per head  $y_{fw}$  and the nitrate content per head  $y_{NO_3^-}$ , which depend on  $M_{Cs}$  and  $M_{Cv}$ .

$$\begin{bmatrix} y_{fw} \\ y_{NO_3^-} \end{bmatrix} = \underline{h}(M_{Cs}, M_{Cv}) \quad (95)$$

The negative correlation between sugars and nitrate is part of the function  $\underline{h}$ .  $\underline{\psi}$  in equation 91 is a function of  $\underline{h}$  and by substitution of equation 95, a function of the states  $M_{Cs}$  and  $M_{Cv}$ .

### 5.1.2.2 Outline of the dynamic climate model

Beside equations 93 and 94, the system state function in equation 86 contains one additional state differential equation, which is part of a dynamic climate model, developed by Seginer and Van Straten (2001).

$$\frac{dT_g}{dt} = F_{Sog}(S_0) - F_{Lga}(M_{Cs}, RH_a, T_a, S_0) - F_{Hga}(T_g, T_a) \quad (96)$$

Equation 96 is a differential equation for the temperature  $T_g$  of the virtual unit of soil, crop and apparatus in a greenhouse. Associated to equation 96 there are three algebraic equations captured by equation (87).

$$0 = F_{Hea}(T_a, T_p) + F_{Hga}(T_g, T_a) - F_{Hao}^c(T_a, T_o) - F_{Hao}^v(T_a, T_o, Q^v) \quad (97)$$

$$0 = F_{Lga}(M_{Sc}, RH_a, T_a, S_0) - F_{Lao}^v(RH_a, T_a, RH_o, T_o, Q^v) \quad (98)$$

$$0 = P - F_{Cao}^v(C_{Ca}, C_{Co}, Q^v) + F_{Cm}(M_{Cs}, T_a) - \theta F_{Cva}(M_{Cs}, M_{Cv}, T_a, C_{Ca}) - F_{Cav}(M_{Cs}, M_{Cv}, C_{Ca}, S_0) \quad (99)$$

These equations describe quasi steady state assumptions for  $C_{Ca}$ ,  $T_a$  and  $RH_a$  being the carbon dioxide concentration, air temperature and relative humidity in the greenhouse. They are algebraic equations for the sensible heat balance of the greenhouse air, for the latent heat balance of the greenhouse air and for the  $CO_2$ -balance of the greenhouse air, respectively. They originate from the assumption that the rate of change of these states is so fast compared to that of  $T_g$  that these states always reach a pseudo steady state. Furthermore  $Q^v$  (control input) is the specific ventilation rate.  $T_p$  (control input) is the heating pipe temperature,  $P$  (control input) is the  $CO_2$ -enrichment flow.  $C_{Co}$ ,  $RH_o$ ,  $T_o$  are the outside carbon dioxide concentration, relative humidity and temperature respectively, which are uncontrollable weather disturbances.

The functions  $F_{Sog}$ ,  $F_{Lga}$ ,  $F_{Hga}$ ,  $F_{Hea}$ ,  $F_{Hao}^c$ ,  $F_{Hao}^v$ ,  $F_{Lao}^v$  and  $F_{Cao}^v$  are linear and non-linear functions for the processes mentioned in table 33.

Table 33 Process descriptions for the functions in equations 96, 97, 98 and 99

functions	process description
$F_{Sog}$	solar radiation absorbance
$F_{Lga}$	latent heat transfer by evapotranspiration from virtual unit to greenhouse air
$F_{Hga}$	heat transfer from the virtual unit to greenhouse air
$F_{Hea}$	heat transfer from heating pipes to greenhouse air
$F_{Hao}^c$	heat transfer by diffusion from greenhouse air to outside air
$F_{Hao}^v$	heat transfer by ventilation from greenhouse air to outside air
$F_{Lao}^v$	latent heat transfer by ventilation from greenhouse air to outside air
$F_{Cao}^v$	$CO_2$ transfer by ventilation from greenhouse air to outside air

### 5.1.2.3 Bounds on inputs and quasi steady states

The inputs  $Q^v$  and  $T_p$  and the quasi steady states  $T_a$ ,  $RH_a$  are bounded from above and below. The input  $P$  and quasi steady state  $C_{Ca}$  are bounded from below. These constraints are expressed by equations 88 and 89.

### 5.1.2.4 End-constraints, initial and final conditions

The final fresh weight per head,  $y_{fw}$  and the final nitrate content per head  $y_{NO_3^-}$  are bounded from below and above respectively. These end-constraints are captured by equation 90. The initial values of the states  $M_{Cn}$ ,  $M_{Cs}$  and  $T_g$  are captured by  $x_0$  in equation 86.

### 5.1.2.5 Running costs function and profits function

The running costs function  $L$  in equation 91 is the sum of costs related to heating the greenhouse air and costs related to  $CO_2$ -supply to the greenhouse air:

$$L = F_H(T_p) + F_C(P) \quad (100)$$

The function  $\phi$  represents profits:

$$\phi(x_f) = S(y_{fw,f}) - x_f^L \quad (101)$$

where  $x_f^L$  is the final value of the running costs and  $S$  represents lettuce sales revenues, which is an increasing function of the fresh weight per head,  $y_{fw}$ .

The functions  $L$  and  $S$  are realistic functions deduced from figures presented by anonymous (2000) and anonymous (1998).

### 5.1.3 General outline of the closed-loop control algorithm

The design of the closed-loop control algorithm is summarized by the following steps.

Step 1: Compute different nominal optimal open loop control trajectories using different nominal trajectories of the measurable uncertain disturbances.

Step 2: Dissect these trajectories into parts where none, one or several of the constraints are active. These parts are the so-called optimal operational modes. Determine the most frequent and important modes through simulations as well as insight and experience concerning the system behavior.

Step 3: Describe these modes mathematically using the active constraints and the necessary optimality conditions for the control  $H(\underline{u}^*, \underline{x}^*, \underline{d}, \underline{\lambda}^*) \leq H(\underline{u}, \underline{x}^*, \underline{d}, \underline{\lambda}^*)$  and/or

$$\left. \frac{\partial H(\underline{u}, \underline{x}, \underline{d}, \underline{\lambda})}{\partial t} \right|_{\substack{\underline{u}=\underline{u}^*, \underline{x}^*=\underline{x}, \underline{\lambda}^*=\underline{\lambda}}} = 0 \quad \text{assuming } \underline{x}^*(t), \underline{d}(t), \underline{\lambda}^*(t), \quad t_0 \leq t \leq t_f \quad \text{to be known. Here}$$

$H(\underline{x}, \underline{u}, \underline{d}, \underline{\lambda}) = \underline{\lambda}^T \underline{f}(\underline{x}, \underline{u}, \underline{d})$  is the so-called Hamiltonian associated to the optimal control problem (86-92) and \* denotes optimality.

Step 4: Use the mathematical descriptions established in step 3 to determine  $\underline{u}^*(t)$  explicitly as a function of  $\underline{x}^*(t)$  or  $\underline{x}^*(t), \underline{d}(t)$  or  $\underline{x}^*(t), \underline{d}(t), \underline{\lambda}^*(t)$ . Employ symbolic computation if necessary.

Step 5: Develop a state-observer that exploits the measurements of the uncertain disturbances.

Step 6: From the costate trajectories computed in step 1 select an appropriate one for the on-line evaluation of the control  $\underline{u}^*(t)$  as a function  $\underline{x}^*(t), \underline{d}(t), \underline{\lambda}^*(t)$ . Alternatively decide on how to update or compute  $\underline{\lambda}^*(t)$  on-line.

Step 7: Use the results of step 1-6 to evaluate  $\underline{u}^*(t)$  on-line using the explicit expressions developed under step 4. For  $\underline{x}^*(t)$  take the current state estimate, for  $\underline{d}(t)$  take the current measurements of the uncertain disturbances and for  $\underline{\lambda}^*(t)$  take the result obtained from step 6. To do this a *decision* must be made as to which of the modes selected under step 2 is used for this computation. Also it must be decided from steps 1 and 6 how to evaluate  $\underline{\lambda}^*(t)$ .

Step 8: Check through simulations whether the behavior of the closed-loop control system is satisfactory by comparing trajectories computed in closed-loop with their optimal open loop counter parts. If the result is not satisfactory go to step 2.

Many steps of the closed-loop control algorithm described above contain heuristic parts. These heuristic parts enable the algorithm to cover a wide range of practical control problems and furthermore they allow for simplifications. Clearly a disadvantage is that these heuristic parts introduce sub optimality and require clever engineering, simulation and possibly experimentation to arrive at an implementation.

Several authors discussed topics related to steps 1-8. Algorithms to carry out step 1 are presented by for example Bryson and Ho (1975), Stengel (1994), Mehra and Davis (1972) and De Graaf, *et al.* (2004). Examples of steps 2-4 are presented by Srinivasan, *et al.* (2002), Chatzidoukas, *et al.* (2005) and Kadam, *et al.* (2005). State observer or state estimator developments (step 5) are discussed by for example Stengel (1994). Algorithms that compute costates on-line (step 6) are presented by Van Henten (1994), Friedland and Sarachik (1966), Stengel (1994) and Bryson and Ho (1975).

The result of step 4 should *preferably* be a state feedback law i.e. an explicit expression of the control  $\underline{u}^*(t)$  in terms of the current state  $\underline{x}^*(t)$ . When the uncertain external inputs  $\underline{d}(t)$  are being measured  $\underline{u}^*(t)$  may also depend explicitly on  $\underline{d}(t)$ , as in our application. Using the necessary optimality conditions mentioned under step 4, depending on the type of optimal control problem, such a feedback law *may* be determined e.g. by employing symbolic computations (Palanki, Kravaris and Wang, 1993; Palanki, Kravaris and Wang, 1994). Our implementation of the algorithm provides explicit expressions for  $\underline{u}^*(t)$  in  $\underline{x}^*(t)$ ,  $\underline{d}(t)$  and  $\underline{\lambda}^*(t)$ . The latter is another source of sub optimality because optimal values of  $\underline{\lambda}^*(t)$  are used in our applications to prevent loss of computational efficiency. Simulations of the closed-loop control system developed in this paper will reveal that taking optimal values for  $\underline{\lambda}^*(t)$  is acceptable.

#### 5.1.4 Design of the closed-loop control algorithm for the lettuce problem

##### 5.1.4.1 Step 1: Computation of open-loop optimal trajectories

Optimal open-loop trajectories of ventilation rates  $Q^v$ , CO<sub>2</sub>-concentrations  $C_{Ca}$ , greenhouse air temperatures  $T_a$ , CO<sub>2</sub>-enrichment flows  $P$  and dynamical heating pipe temperatures  $T_p$  were computed for ca. 30 lettuce cultivations that were more or less equally distributed over a year and affected by climate conditions that prevail in the Netherlands and Belgium. As both countries have about the same climatic conditions, computations for both countries were made using data about climate conditions measured in the Netherlands (Breuer and Van de Braak, 1989). These climate conditions consisted of weather inputs  $S_o$ ,  $C_{Co}$ ,  $RH_o$  and  $T_o$ . Mean values of these inputs are listed in table 34. Lettuce cultivation durations are also in this table.

To compute the trajectories the mathematical formulation and numerical optimisation algorithm explained in sections 4.2.2 and 4.2.3 were used. Realistic bounds on control inputs and quasi steady states, and realistic bounds on the terminal values of outputs are listed in table 35. Values for  $M_{Cv}$  and  $M_{Cs}$  at  $t_0$  correspond with a fresh head weight of 46 g and a nitrate content of  $4.5 \cdot 10^3$  ppm. Values of  $T_g$  at  $t_0$  were set at 10 °C.

Examples of optimal trajectories as well as their physical, biological and economical interpretations can be found in section 4.2.

Table 34 Mean values of  $S_o$ ,  $C_{Co}$ ,  $RH_o$ ,  $T_o$  and lettuce cultivation durations per season (anonymous, 1989; Breuer and Van de Braak, 1989)

	<i>Winter</i>	<i>spring</i>	<i>summer</i>	<i>autumn</i>
$S_o$ [MJ·m <sup>-2</sup> ·day <sup>-1</sup> ]	3.5	15	14	4.5
$C_{Co}$ [mol·m <sup>-3</sup> ]	$1.3 \cdot 10^{-2}$	$1.3 \cdot 10^{-2}$	$1.3 \cdot 10^{-2}$	$1.3 \cdot 10^{-2}$
$RH_o$ [%]	88	75	79	87
$T_o$ (maximum) [°C]	6	15	20	10
$T_o$ (minimum) [°C]	1	7	12	3
cultivation duration [days]	60	45	30	45

Table 35: Realistic bounds on the control inputs, the quasi steady states and the terminal values of the outputs (from anonymous, 1989; von Elsner, et al., 2000b)

	<i>lower bound</i>	<i>upper bound</i>	<i>Units</i>
<i>control inputs</i>			
$Q^v$	$7.5 \cdot 10^{-5}$	$7.7 \cdot 10^{-3}$	m·s <sup>-1</sup>
$C_{Ca}$	0.0	-	mol·m <sup>-3</sup>
$T_a$	5.0	40	°C
<i>quasi steady states</i>			
$P$	0.0	-	mol·m <sup>-2</sup> ·s <sup>-1</sup>
$RH_a$	0.0	0.9	-
$T_p$	$T_a$	70	°C
<i>terminal values of the output</i>			
$y_{fw}$	300	-	g·head <sup>-1</sup>
$y_{NO_3^-}$ , summer	-	$3.5 \cdot 10^3$ *	ppm
$y_{NO_3^-}$ , winter	-	$4.5 \cdot 10^4$ *	ppm

\* These upper bounds are set by the European union



#### 5.1.4.2 Steps 2,3,4 and 7: Dissection, selection and final design of the algorithm

The dissection is a step that is partly heuristic. To decide upon the dissection the optimal trajectories computed during step 1 have to be analysed. In performing this analysis one usually starts to build rough classifications that are refined later on. Here this process is represented by two tables. Table 36 represents a rough classification that is in the spirit of horticultural practitioners and researchers. Table 37 in the next section represents the final dissection into modes that in fact covers *all parts* of the data obtained during step 1. Moreover these dissections do not overlap one another. In other words each point in time of the trajectories obtained during step 1 is associated with precisely one mode. This still does not guarantee that all time points that occur in practice are mapped on precisely one mode. The reason being that all situations that occur in practice need not all be covered by the simulations performed under step 1. Our algorithm also provides a solution for situations that have not been simulated during step 1.

##### 5.1.4.2.1 The optimal operational modes and the flow diagram of the algorithm

A dissection of the open loop optimal trajectories into optimal operational system modes is specified in table 37. The optimal operational system modes are evaluated to compute the optimal control and the associated quasi steady states on-line. To do this it must be decided which mode of operation is active. The decision as to which mode of operation is active, is made according to the flow diagram represented by figure 15. Given the current estimated state  $\underline{x}$  and the current measured uncertain disturbances  $\underline{d}$  presumptions are made as to the values of the control inputs and the quasi steady states. These presumptions are listed in the second column of table 37. From these presumptions, using the optimality conditions and the algebraic equations the values for the remaining controls and the associated quasi steady states are computed. This is represented by the third column in table 37.

Table 36 Characteristic parts of optimal control trajectories represented by control bounds and quasi steady states.

<i>variables</i>	<i>Seasons, day versus night and climate conditions</i>	<i>values of the variables</i>
<i>control inputs at night</i>		
$Q^p$	p., s., a. w., to avoid $RH_a$ from exceeding u.b.	l.b. b.b.
$T_p$	all seasons, $T_a > 5^\circ\text{C}$ a., w., p., $T_a < 5^\circ\text{C}$	l.b. b.b.-u.b.
$P$	all seasons	l.b.
<i>quasi steady states at night</i>		
$RH_a$	a., w., p., $0.8 < RH_o \leq 1.0$ and $T_a < 15^\circ\text{C}$ all seasons, $RH_o < 0.8$ and $T_a > 15^\circ\text{C}$	u.b. b.b.
$T_a$	w., p., a., $T_o \leq 5^\circ\text{C}$ all seasons, $5 \leq T_o \leq 25^\circ\text{C}$	l.b. b.b.
$C_{Ca}$	all seasons	l.b.-b.b.
<i>control inputs at daylight</i>		
$Q^p$	all seasons, to avoid $RH_a$ or $T_a$ from exceeding u.b.	b.b.
$T_p$	a., w., p., sometimes to avoid $RH_a$ from exceeding u.b. s., to avoid $T_a$ from exceeding u.b.	b.b.-u.b. l.b.
$P$	all seasons	b.b., $\uparrow\text{sr}^*$
<i>quasi steady states at daylight</i>		
$RH_a$	all seasons, $T_a < \text{u.b.}$ p., s., a., when $T_a$ tends to exceed u.b.	u.b. b.b.
$T_a$	all seasons, $5 \leq T_o \leq 25^\circ\text{C}$ p., s., a., $T_o \geq 25^\circ\text{C}$	b.b. u.b.
$C_{Ca}$	all seasons	l.b.-b.b.

l.b. lower bound

u.b. upper bound

b.b. between bounds

 $\uparrow\text{sr}$  increasing with  $S_o$  $\downarrow\text{l.b.}$  decreasing to lower bound

w. Winter

p. Spring

s. Summer

a. Autumn

Table 37: Dissection of trajectories presumed and associated inputs and quasi steady states.

<i>Mode number</i>	<i>Presumed input and quasi steady state values</i>	<i>Associated input and quasi steady state values</i>
<i>at night</i>		
1	$T_p = \text{l.b.}, P = \text{l.b.}, Q^v = \text{l.b.}$	$RH_a, T_a, C_{Ca}$
2	Lowest feasible $T_p, P = \text{l.b.}, RH_a = \text{u.b.}$	$Q^v, T_a, C_{Ca}$
3	$RH_a$ and $T_a$ such that $T_p$ is as low as feasible, $P = \text{l.b.}$	$Q^v, RH_a, T_a, C_{Ca}$
4	$T_p = \text{l.b.}, Q^v = \text{u.b.}, P = \text{l.b.}$	$T_a, C_{Ca}, RH_a$ (values of $RH_a$ may exceed their upper bound)
<i>at daylight</i>		
5a	$\frac{\partial H}{\partial T_a} = 0, RH_a = \text{u.b.}, \frac{\partial H}{\partial C_{Ca}} = 0$	$T_p, Q^v, P$
5b	$\frac{\partial H}{\partial T_a} = 0, RH_a = \text{u.b.}, P = \text{l.b.}$	$T_p, Q^v, C_{Ca}$
6a	Feasible $T_a$ value closest to the infeasible $T_a$ value of modes 5a and 5b, $RH_a = \text{u.b.}, \frac{\partial H}{\partial C_{Ca}} = 0$	$Q^v, T_p, P$
6b	Feasible $T_a$ value closest to the infeasible $T_a$ value of mode 5a and 5b, $RH_a = \text{u.b.}, P = \text{l.b.}$	$Q^v, T_p, C_{Ca}$
7a	$RH_a$ and $T_a$ such that $RH_a$ is as high as feasible, highest feasible, $\frac{\partial H}{\partial C_{Ca}} = 0$	$Q^v, T_p, P$
7b	$RH_a$ and $T_a$ such that $RH_a$ is as high as feasible, highest feasible, $P = \text{l.b.}$	$Q^v, T_p, C_{Ca}$
8a	$T_p = \text{l.b.}, Q^v = \text{u.b.}, \frac{\partial H}{\partial C_{Ca}} = 0$	$P, T_a, RH_a$ (values of $RH_a$ may exceed their upper bound)
8b	$T_p = \text{l.b.}, Q^v = \text{u.b.}, P = \text{l.b.}$	$C_{Ca}, T_a, RH_a$ (values of $RH_a$ may exceed their upper bound)

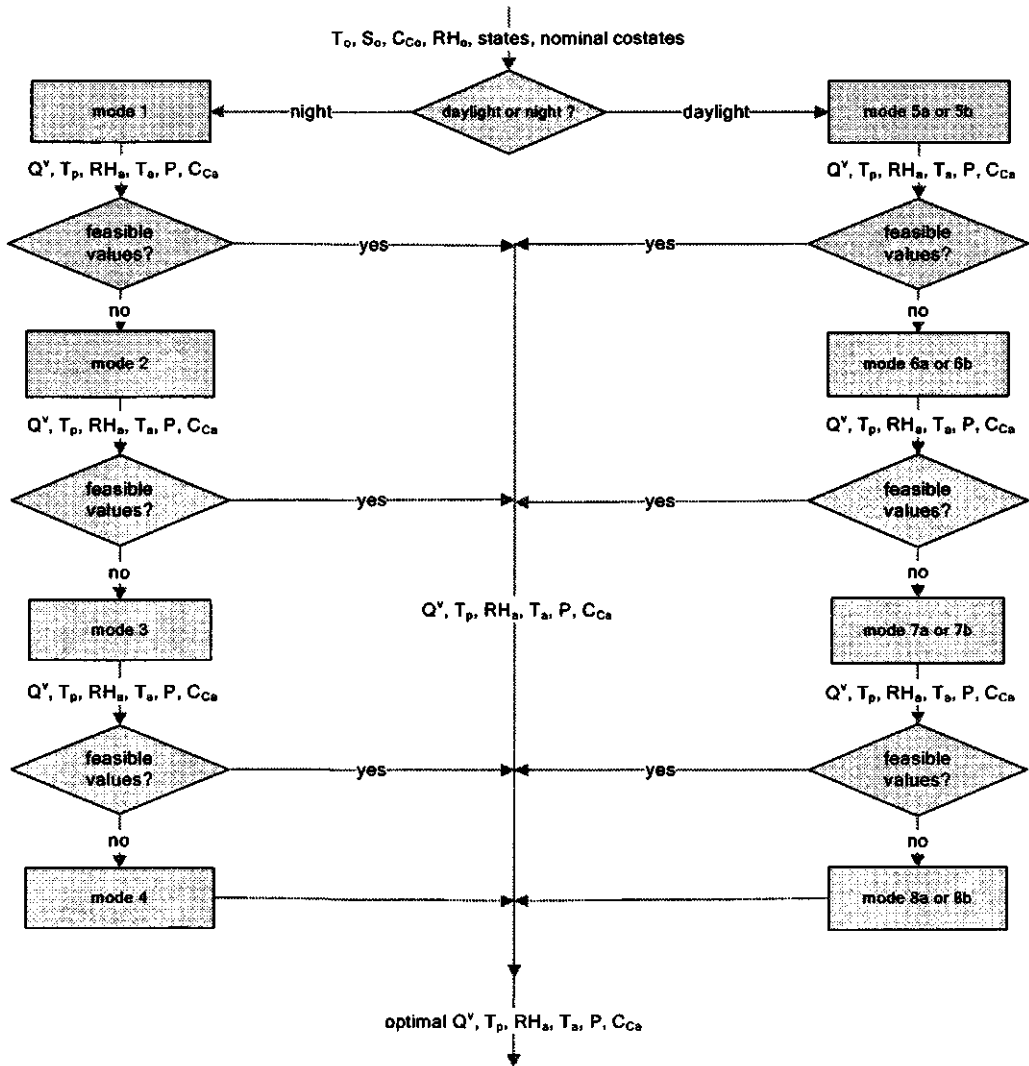


Figure 15: Flow diagram of the control algorithm

## 5.1.4.2.2 Explanation of the computations

The computation of the third column of table 37 from the first one, using the algebraic equations and the optimality conditions, is explained. The algebraic equations for this specific problem can be represented by,

$$n(\underline{x}, \underline{u}, \underline{z}, \underline{d}) = 0, n \in R^3 \quad (102)$$

$$\underline{n}'(\underline{x}, \underline{u}', \underline{z}', \underline{d}) = 0, n' \in R^2 \quad (103)$$

where,

$$\underline{u} = [P \quad Q^v \quad T_p]^T, \underline{u}' = [Q^v \quad T_p]^T, \underline{z} = [C_{Ca} \quad T_a \quad RH_a]^T, \underline{z}' = [T_a \quad RH_a]^T \quad (104)$$

Given  $\underline{x}$ ,  $\underline{d}$ , if two out of the four elements of  $\underline{u}'$  and  $\underline{z}'$  are presumed specified, the other two are computed from equation 103. Next if the additional element of either  $\underline{u}$  or  $\underline{z}$  ( $P$  or  $C_{Ca}$ ) is specified the other is computed from equation 102. Let  $R$  denote an element in the third column of table 37 which is not specified in this way. Then  $R$  follows from the optimality condition,

$$\frac{\partial H}{\partial R} = 0 \quad (105)$$

Equation 105 presumes that the outcome of  $R$  does not violate the constraints. If the outcome of  $R$  does violate the constraints or if the outcome of equations 102 and 103 violates the constraints then the solution is considered infeasible and according to the flow diagram (figure 15) we move to another mode. This does not apply to modes 4, 8a and 8b that terminate the flow diagram. These modes on the one hand ensure that the algorithm always generates a solution. On the other hand this solution need not necessarily be feasible. There may be two reasons for this. Either a feasible solution does not exist or it is not provided by the flow diagram. In the latter case this reflects the sub optimality of our algorithm. Except for one mode analytic solutions of 102, 103 and 105 are obtained using symbolic computation. Finding a feasible  $T_a$  or  $T_p$ , which is part of modes 2, 6a and 6b respectively, constitutes a line search that is performed by trying a finite number of values in between the upper and lower bounds. Finding feasible values for both  $T_a$  and  $RH_a$  which are part of modes 3, 7a and 7b respectively, constitutes a two-dimensional search that is performed by searching a grid containing a finite number of values in between the upper and lower bounds.

#### 5.1.4.2.3 Motivation and explanation of the flow diagram

Figure 15 shows that at night first the heating pipe temperature  $T_p$  and the specific ventilation rate  $Q^v$  are presumed to be at their lower bounds (mode 1). This mode is considered first because saving on heating costs is optimal at night. If the associated relative humidity  $RH_a$  and the greenhouse air temperature  $T_a$  are not feasible then mode 2 is considered, being the mode in which  $RH_a$  is presumed to be at its upper bound and  $T_p$  is as low as feasible. This mode is second best with respect to savings on heating costs. If the associated values of  $RH_a$  and  $T_a$  are infeasible then the third best mode is considered in which  $T_p$  and  $RH_a$  are in between their bounds and such that heating costs are minimal. If in summer, modes 1 through 3 do not lead to feasible values for  $T_p$ ,  $RH_a$ ,  $T_a$  and  $Q^v$ , then  $T_p$  is set at its lower bound and  $Q^v$  at its upper bound, leading to an associated value of  $RH_a$  that sometimes exceeds its upper bound (mode 4).  $\text{CO}_2$  enrichment flow rates  $P$  are always at their lower bound during the night (modes 1 through 4), because supply of  $\text{CO}_2$  is not profitable at night.

At daylight, modes 5a or 5b are considered first, being the modes in which the relative humidity value  $RH_a$  is presumed to be upper bounded and the greenhouse air temperature  $T_a$  is presumed to be in between its bounds. These modes are evaluated first because optimal values of  $T_a$  increase with solar radiation and the  $\text{CO}_2$ -concentration inside the greenhouse leading to values of  $T_a$  above the lower bound. Also these modes are considered first because  $T_a$  is needed for the evaluation of modes 6a and 6b. If modes 5a and 5b do not lead to associated values of  $Q^v$  and  $T_p$  that are feasible then modes 6a or 6b are evaluated. Modes 6a and 6b presume that  $RH_a$  is upper bounded.  $T_a$  is computed to be as close as possible to the  $T_a$  value of modes 5a or 5b and such that the associated values of  $Q^v$  and  $T_p$  are feasible. Computing such a  $T_a$  value corresponds with the application of Pontryagin's minimum principle. If the outcome of this computation produces infeasible outcomes of  $Q^v$  and  $T_p$  then Pontryagin's minimum principle is applied again in modes 7a or 7b to compute  $T_a$ . In these modes  $RH_a$  is presumed to be as close as possible to its upper bound. If in summer, modes 5a through 7b do not lead to feasible values for  $T_p$ ,  $RH_a$ ,  $T_a$  and  $Q^v$ , then the heating pipe temperature  $T_p$  is set at its lower bound and the specific ventilation rate  $Q^v$  is set at its upper bound, leading to a relative humidity value  $RH_a$  that sometimes exceeds its upper bound (modes 8a and 8b). At daylight (modes 5a through 8b), the optimal  $\text{CO}_2$  concentration in the greenhouse increases with solar radiation (modes 5a, 6a, 7a, 8a). If the computed  $P$  violates its lower bound it is put at the lower bound and the associated  $\text{CO}_2$ -concentration is computed (modes 5b, 6b, 7b, 8b).

### 5.1.5 *Simulation and performance of the closed-loop control system*

#### 5.1.5.1 Comparison

Assuming that weather conditions are fully available a-priori, and that the open loop algorithm does not contain any errors and is able to find the global optimum, then the trajectories obtained with it are optimal, whereas the closed-loop algorithm computes sub-optimal trajectories. However, if for some reason the optimum was not found then it may be possible that the closed loop algorithm helps to find a better performance, but this is not guaranteed.

In a first comparison between the trajectories computed by the closed-loop and the open-loop algorithm, both algorithms are used to compute control input trajectories under identical circumstances - i.e. the assumption of perfect a-priori knowledge of the weather. In the closed-loop algorithm this necessarily involves the use of the costates obtained from the open loop computation. If the open loop is truly optimal, one would expect the difference to be small.

As a second comparison, this time to judge the loss of performance due to imperfect a-priori knowledge of the weather, the closed-loop control system is used to compute the control trajectories under imperfectly known weather conditions. To be able to compare the results, weather conditions are not changed in the simulation but instead a different costate trajectory is used to mimic the situation of imperfect a-priori knowledge of the weather. In fact, this costate trajectory is the one computed in open loop for a cultivation that started ten days later, assuming again perfect a-priori knowledge of the weather. In the sequel, the original costate belonging to the perfect weather is called the nominal costate, and the trajectory belonging to the imperfect weather is called the non-nominal costate.

#### 5.1.5.2 Results and discussion

First the results related to a 60 days winter lettuce cultivation are shown. These results are exemplary for other cultivations.

Figure 16 shows trajectories of fresh weight per head ( $y_{fw}$ ), nitrate concentration per head ( $y_{NO_3}$ ) and the running costs against time. The trajectories are obtained from simulations of our closed-loop control system using both the nominal and a non-nominal costate trajectory. In addition, the result obtained with the open-loop control is shown. Between days 0 and 43, the trajectories in this figure show a good resemblance. The nitrate concentration trajectories show that the resemblance deteriorates between days 43 and 60. To view some of the results between day 0 and 43 in more detail, climate conditions, optimal control input trajectories and optimal quasi steady state trajectories between day 15 and 20 are shown in figure 17, figure 18 and figure 19 respectively. These figures demonstrate that all trajectories are similar.

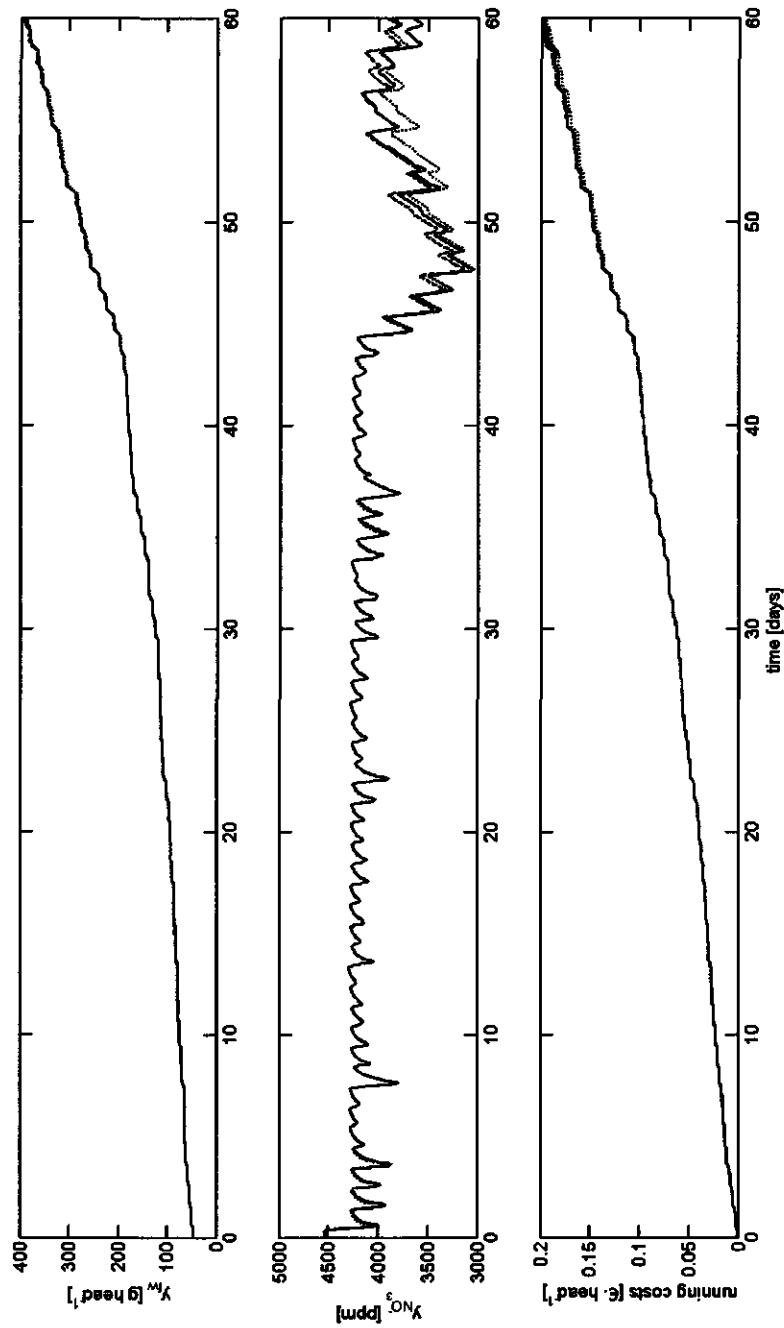


Figure 16: Trajectories of fresh head weight ( $y_{fw}$ ), nitrate concentration ( $y_{NO_3}$ ) and running costs against time (closed-loop with nominal costate trajectories —, closed-loop with non-nominal costate trajectories ---, open-loop .....)



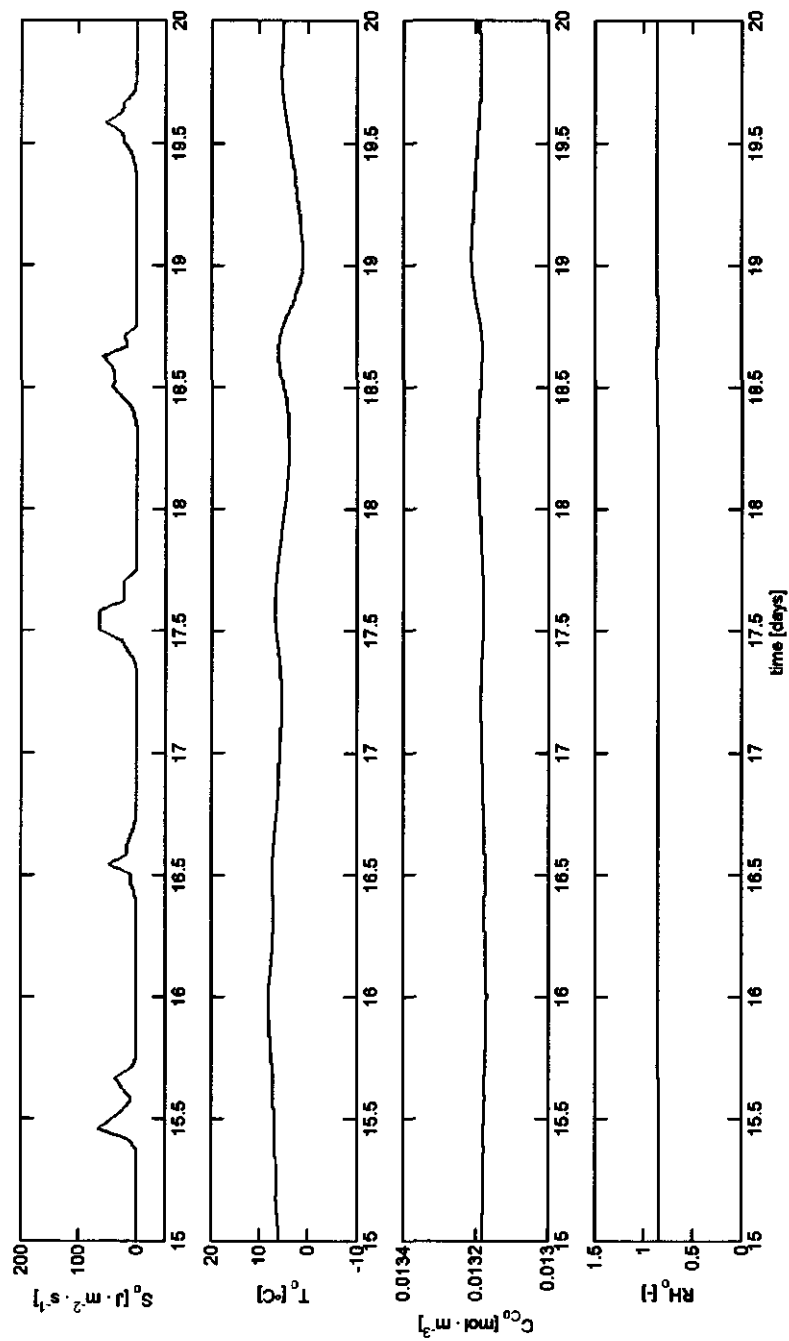


Figure 17: Details of climate conditions between days 15 to 20 (solar radiation  $S_o$ , outside air temperature  $T_o$ , outside  $\text{CO}_2$ -concentration  $C_o$ , outside relative humidity ratio  $RH_o$ ).

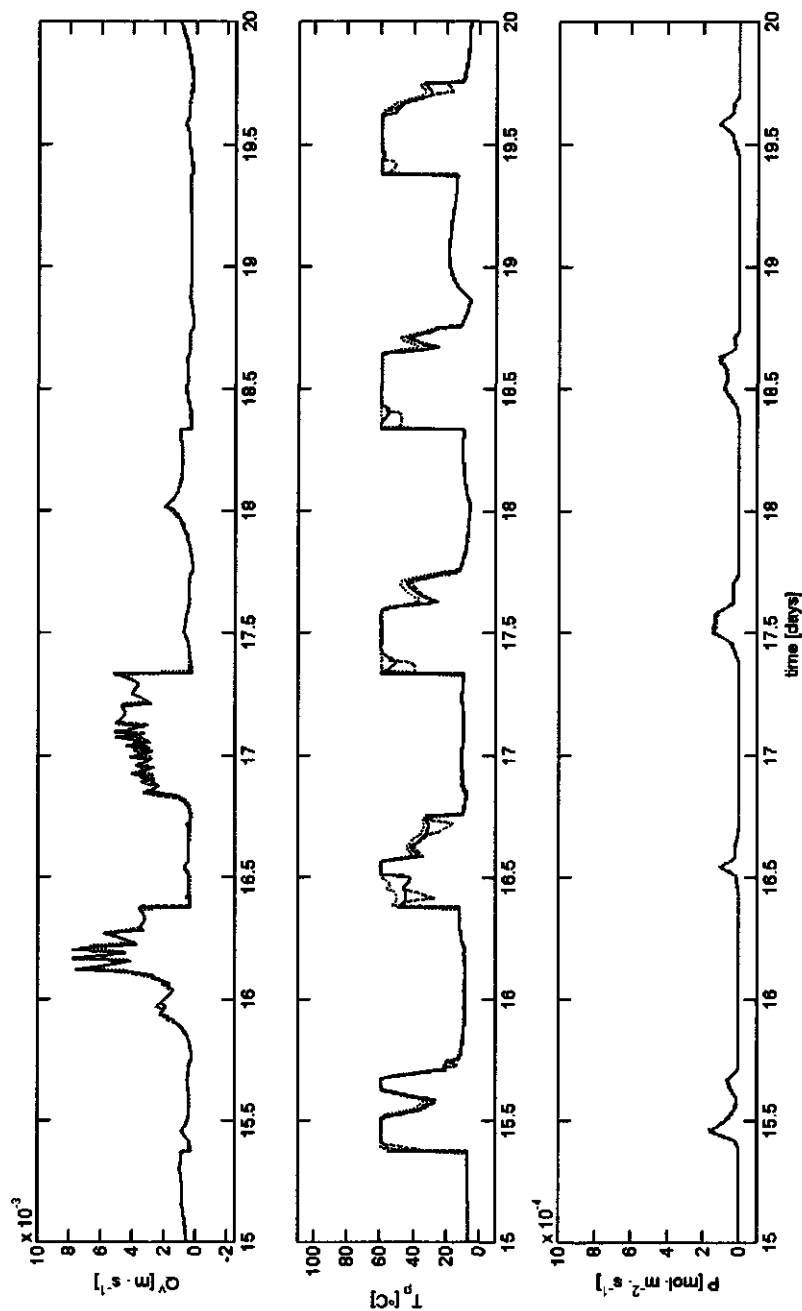


Figure 18: Details of optimal trajectories of ventilation rate ( $Q'$ ), heating pipe temperature ( $T_p$ ) and  $\text{CO}_2$ -injection rate ( $P$ ) between days 15 to 20 (closed-loop with nominal costate trajectories —, closed-loop with non-nominal costate trajectories ---, open-loop .....)

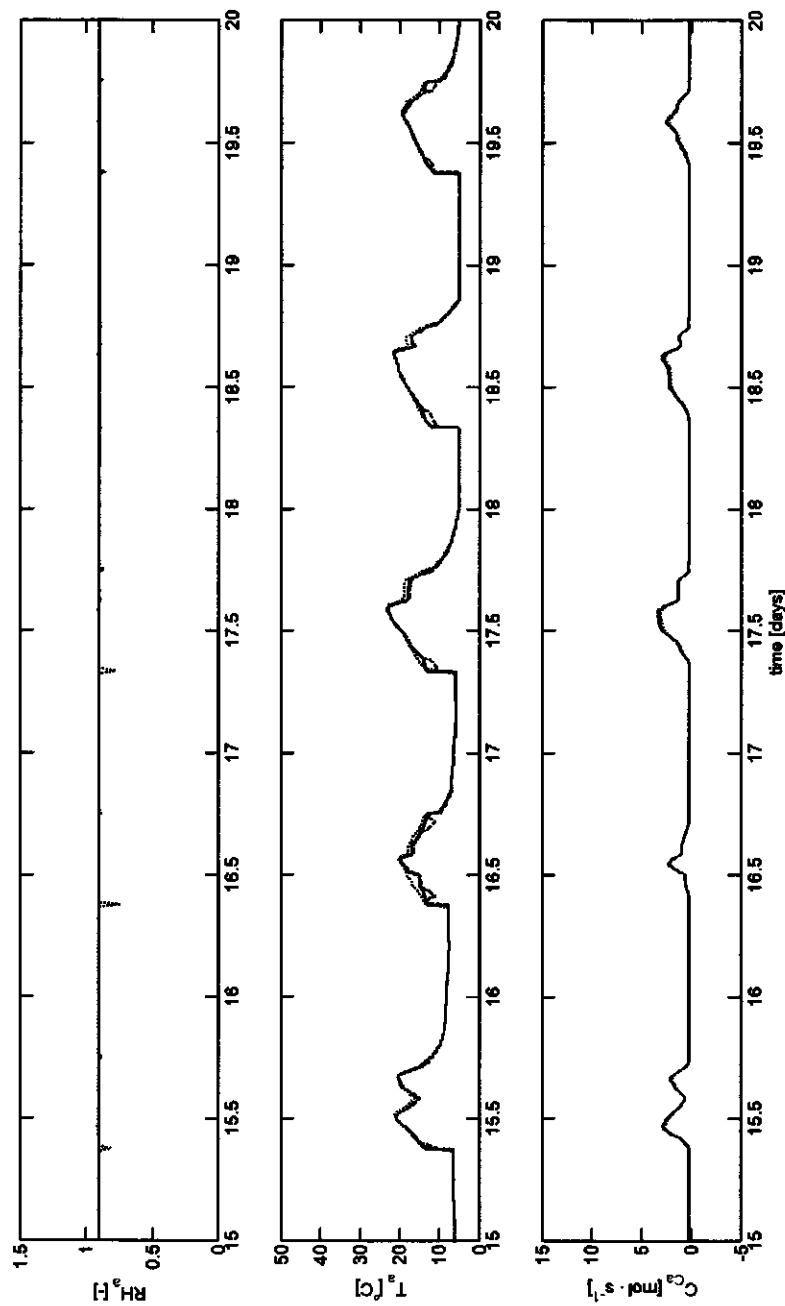


Figure 19: Example of optimal trajectories of relative humidity ( $RH_a$ ), temperature ( $T_a$ ) and  $CO_2$ -concentration ( $C_a$ ) in the greenhouse air between days 15 to 20 (closed-loop with nominal costate trajectories —, closed-loop with non-nominal costate trajectories ---, open-loop.....)

Figure 20, figure 21 and figure 22 show climate conditions, optimal control input trajectories and optimal quasi steady state trajectories respectively between days 40 and 60. These figures show that before day 43 solar radiation was relatively low compared to solar radiation after day 43. This change in solar radiation marks the start of deteriorating resemblances between the trajectories generated by the closed-loop algorithm and trajectories generated in open-loop. This holds especially for the trajectories of nitrate concentration  $y_{NO_3}$ , heating pipe temperature  $T_p$  and to a lesser extent greenhouse air temperature  $T_a$ .

The ratio of the open-loop performance ( $J_{OL}$ ) over the closed-loop performance with nominal costates ( $J_{CL,nominal}$ ) is 0.81 and the final nitrate concentrations in open-loop are 254 and 44 ppm higher than those in closed loop with nominal costates and non-nominal costates, respectively. These facts show that the open loop algorithm fails to find the global optimum, and that in this case the closed loop control algorithm results in better performance.

Control and quasi steady state trajectories computed in closed-loop with non-nominal costate trajectories are adjusted in response to unforeseen changes of weather disturbances such that control bounds and quasi steady state constraints are satisfied. Furthermore, the trajectories of fresh weight per head computed with nominal and non-nominal costate trajectories virtually coincide. This is less the case for nitrate concentration trajectories where the difference between nitrate concentrations at the final time is 210 ppm. On the other hand there is only a 1% difference in performance. As to this, note that the nitrate concentration is not part of the performance index.

To further investigate the sub-optimality of the algorithm, the loss of performance and change of nitrate concentration due to non-nominal costate trajectories, values of  $\frac{J_{OL}}{J_{CL,nominal}}$ ,  $\frac{J_{CL,non-nominal}}{J_{CL,nominal}}$  and final nitrate concentration were computed for all 32 lettuce cultivations. These are plotted against time in figures 23 and 24 respectively. Values of  $\frac{J_{OL}}{J_{CL,nominal}}$  are between 0.77 and 0.94 and open-loop computed nitrate concentrations for summer cultivations (cultivation starting days 80 to 240) exceed the upper bound of 3500 ppm at final time. These facts demonstrate once more that the open-loop algorithm falls short of finding the global optimum. Further study of the tuning parameters of the open-loop algorithm may improve these results.

The change in performance index of the closed-loop algorithm due to the use of non-nominal costates is less than 3%. This suggests that the effect of the weather uncertainty on the profit is limited. The effect on final nitrate is sometimes more pronounced, in particular during the 60 day cultivations at the end of the winter, where also the difference between open loop and closed loop is the largest.

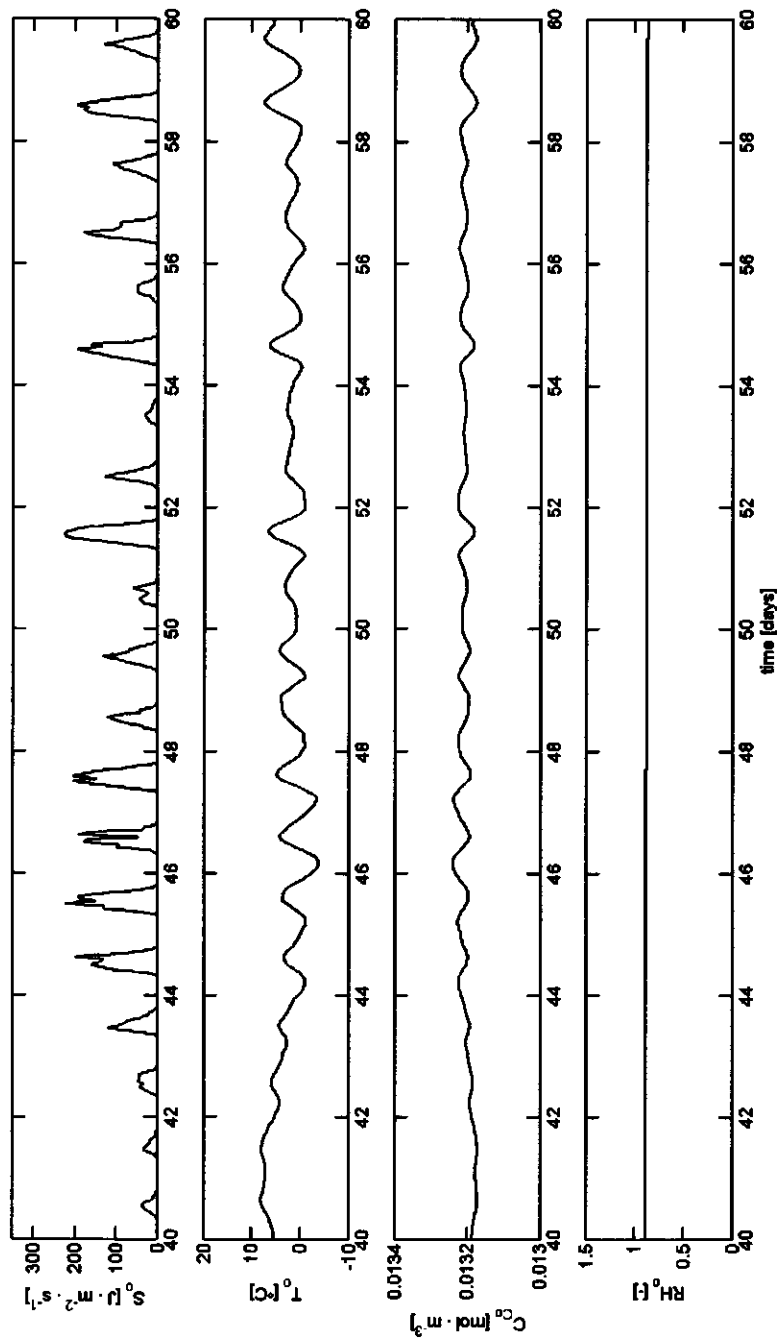


Figure 20: Details of climate conditions between days 40 to 60 (solar radiation  $S_o$ , outside air temperature  $T_o$ , outside  $\text{CO}_2$ -concentration  $C_o$ , outside relative humidity ratio  $RH_o$ ).

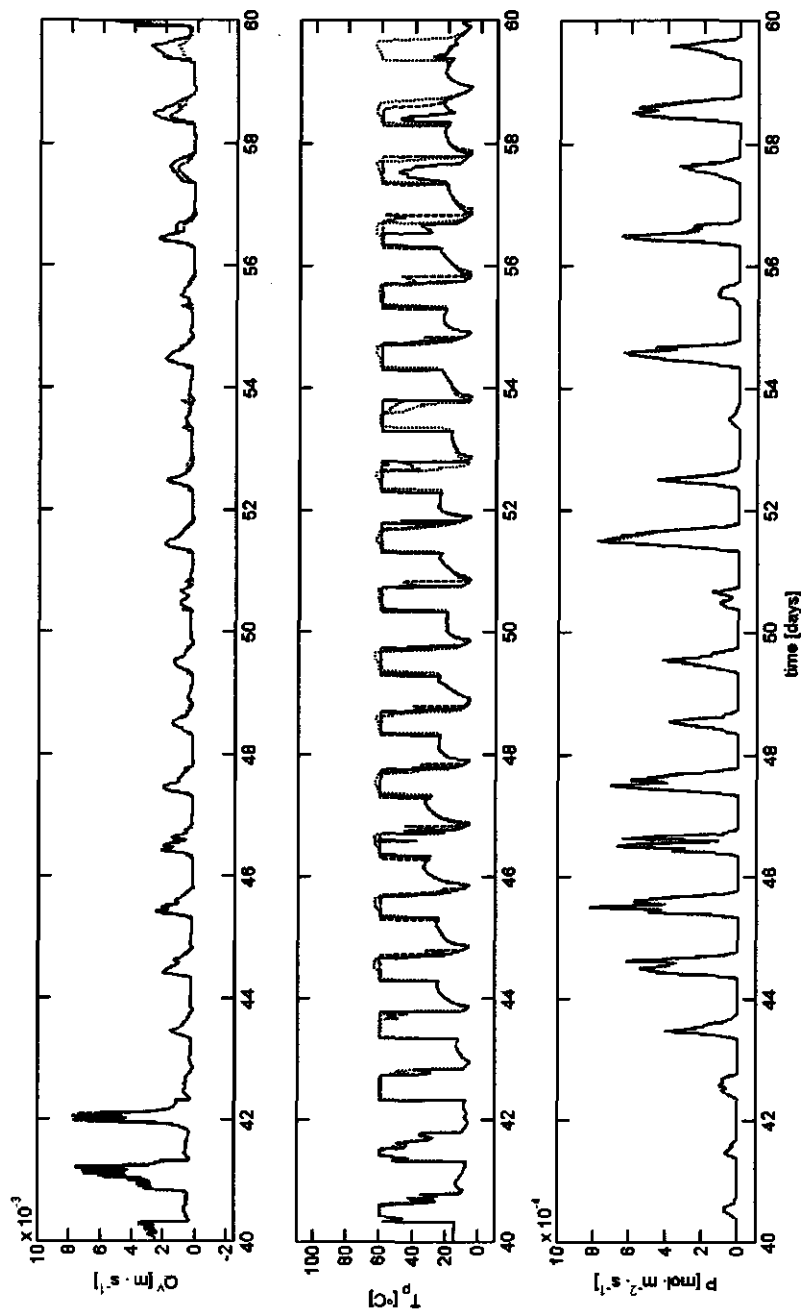


Figure 21: Details of optimal trajectories of ventilation rate ( $Q_v$ ), heating pipe temperature ( $T_p$ ) and  $\text{CO}_2$ -injection rate ( $P$ ) between days 40 to 60 (closed-loop with nominal costate trajectories —, closed-loop with non-nominal costate trajectories ---, open-loop.....)

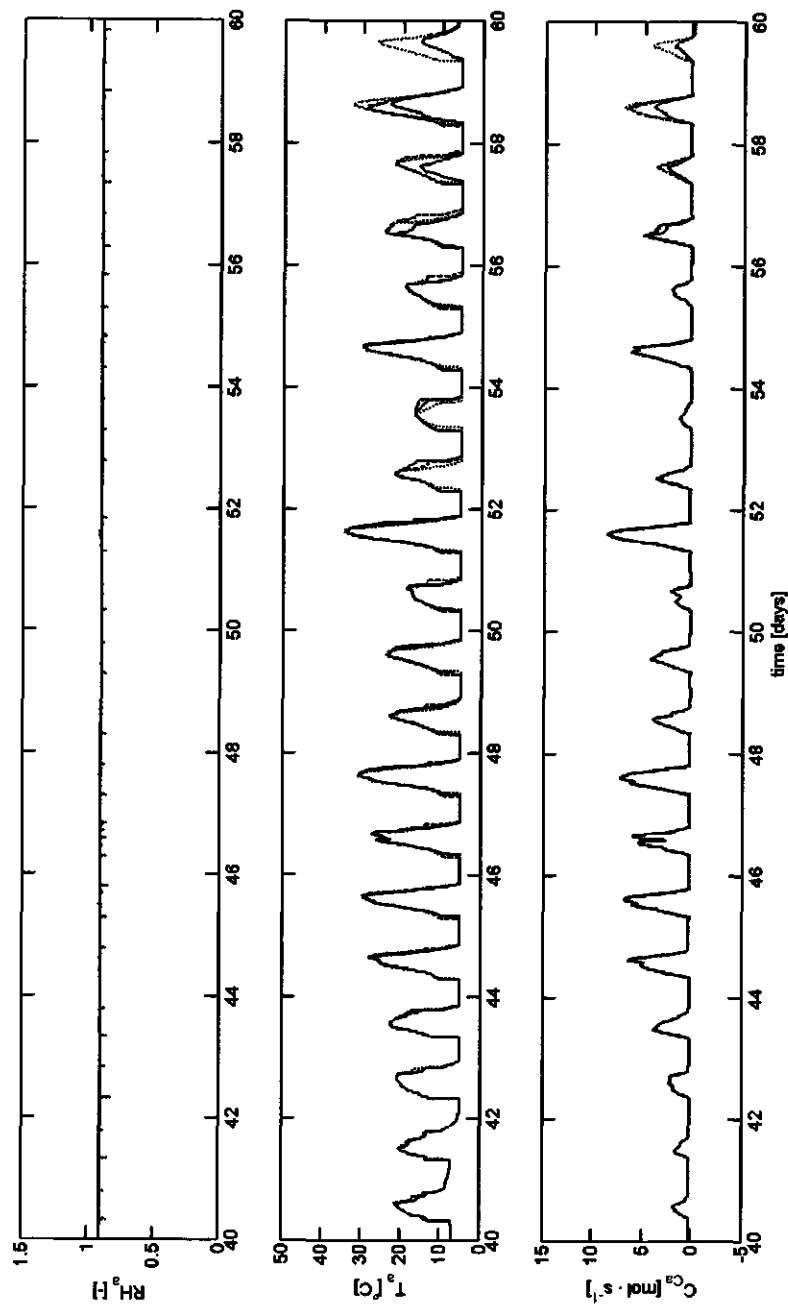


Figure 22: Details of optimal trajectories of relative humidity ( $RH_a$ ), temperature ( $T_a$ ) and  $CO_2$ -concentration ( $C_a$ ) in the greenhouse air between days 40 to 60 (closed-loop with nominal costate trajectories —, closed-loop with non-nominal costate trajectories ---, open-loop .....)

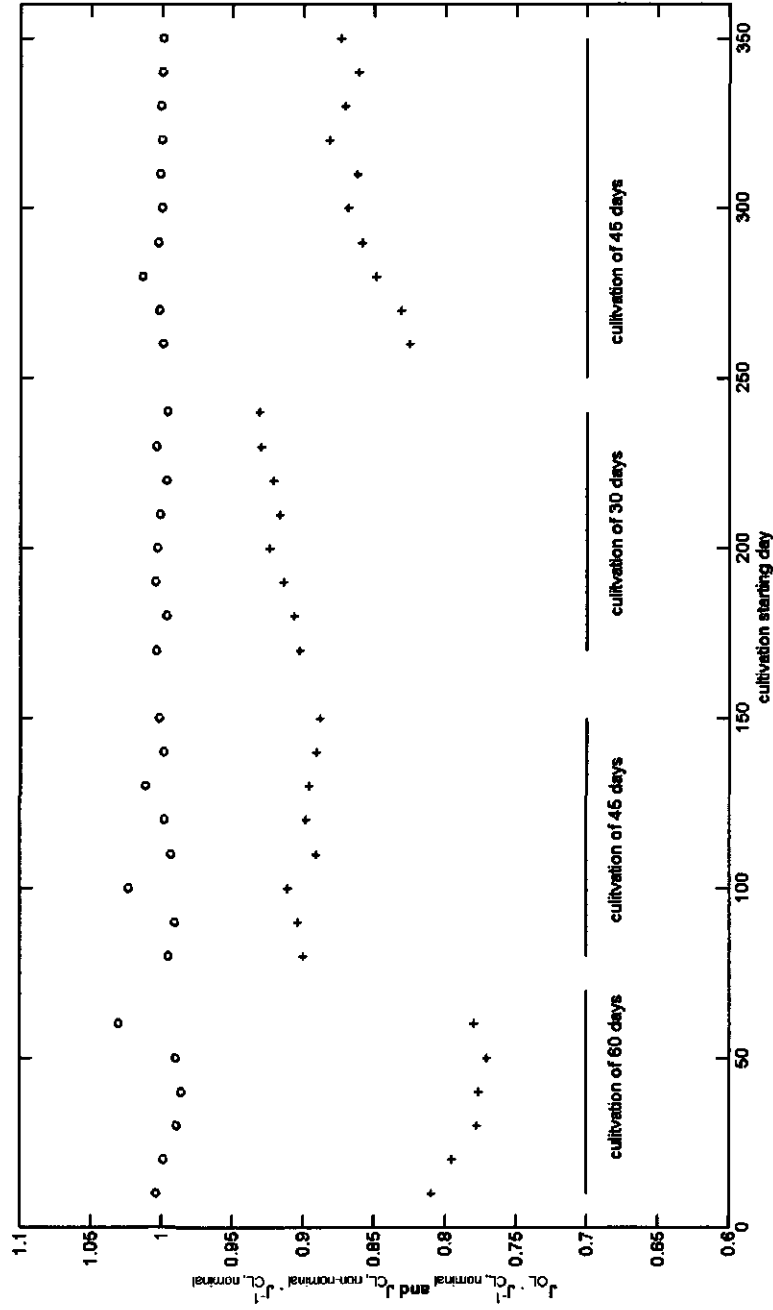


Figure 23: Values of  $\frac{J_{CL}^{opt}}{J_{CL}^{nominal}}$  (+), and  $\frac{J_{CL}^{non-normal}}{J_{CL}^{nominal}}$  (o) plotted against cultivation starting day



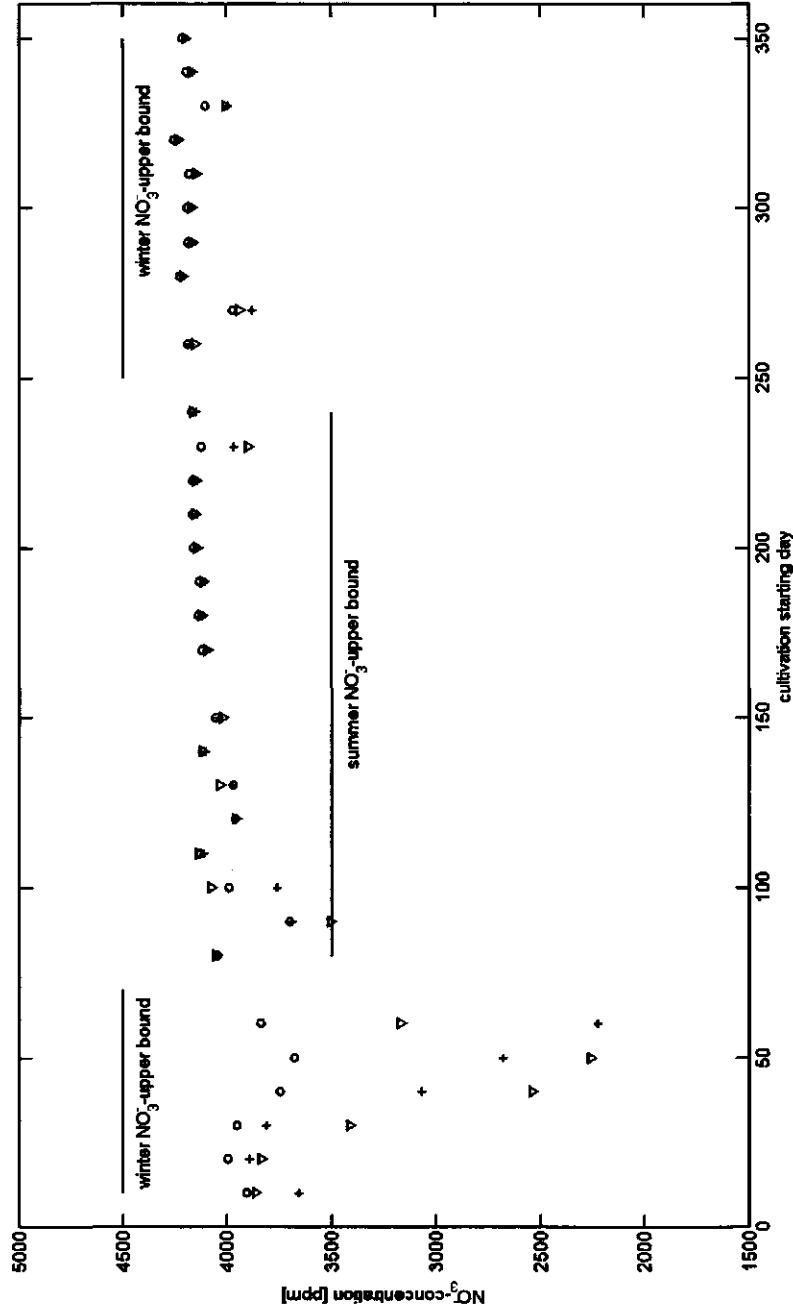


Figure 24: Final nitrate concentrations plotted against cultivation starting day (open-loop: o, closed-loop with nominal costate trajectories: +, closed-loop with non-nominal costate trajectories: ▽)

### 5.1.6 Conclusion

An efficient closed-loop suboptimal control algorithm was developed to control lettuce cultivations in greenhouses. The objectives are to maximize profit and to satisfy terminal constraints concerning the nitrate content imposed by the EU, using pre-computed non-nominal costate trajectories. The algorithm computes control values of specific ventilation rates, heating pipe temperatures and CO<sub>2</sub>-enrichment flow rates during lettuce cultivation. These values are adjusted in response to unforeseen changes of weather disturbances such that control bounds and quasi steady state constraints are satisfied.

The algorithm is computationally highly efficient because it uses so-called optimal operational modes of the system most of which can be evaluated very efficiently. These optimal operational modes are obtained through the application of necessary optimality conditions for optimal control together with optimal control computations and simulations. Also symbolic computations are employed.

In terms of the performance and the final nitrate concentration the algorithm is usually close to performance and the final nitrate concentration computed in open-loop despite the uncertainty with respect to the future weather disturbance and the partly heuristic nature of the control system design. The open-loop algorithm fails to find the global optimum, thus making it impossible to determine the true extent of sub-optimality of the closed-loop algorithm. Given the virtually identical performance of both algorithms, the extent of sub-optimality of the closed-loop algorithm can be considered to be comparable to that of the open-loop algorithm.

### References

- anonymous (1989). *De teelt van sla onder glas (Report)*, Ministerie van Landbouw, Dienst informatie, Gent, Belgium.
- anonymous (1998). *Kwantitatieve informatie voor de glastuinbouw 1998-1999*, Proefstation voor Bloemmisterij en Glasgroente, Naaldwijk, The Netherlands.
- anonymous (2000). *Land- en tuinbouwcijfers 2000*, Landbouw-economisch Instituut, Centraal Bureau voor de Statistiek, 's Gravenhage, The Netherlands.
- Breuer, J. J. G. and N. J. Van de Braak (1989). Reference year for dutch greenhouses. *Acta Horticulturae*, 248,
- Bryson, A. E. (1999). *Dynamic optimization*, Addison-Wesley Longman, Inc., Menlo Park.
- Bryson, A. E. and Y.-C. Ho (1975). *Applied optimal control; optimization, estimation and control*, Hemisphere, New York.
- Chatzidoukas, C., C. Kiparissides, B. Srinivasan and D. Bonvin (2005). *Optimisation of grade transitions in an industrial gas-phase olefin polymerization fluidized bed reactor via nco tracking*, Prague, Czech Republic.
- de Graaf, S. C., J. D. Stigter and G. van Straten (2004). Test of ACW-gradient optimisation algorithm in computation of an optimal control policy for achieving acceptable nitrate concentration of greenhouse lettuce. *Mathematics and computers in simulation*, 117-126.

- Friedland, B. and P. E. Sarachik (1966). A unified approach to suboptimum control. *Proceedings of the 3rd Congress of IFAC*, 1, 13A.11-13A.18.
- Kadam, J. V., M. Schlegel, B. Srinivasan, D. Bonvin and W. Marquardt (2005). Dynamic real-time optimization: from off-line numerical solution to measurement-based implementation. In: *Preprints of 16th IFAC World Congress* (Horacek, P., M. Simandl and P. Zitek. (Ed)). Prague, Czech Republic.
- Lee, A. Y. and A. E. Bryson (1989). Neighbouring extremals of dynamic optimization problems with parameter variations. *Optimal control applications & methods*, 10, 39-52.
- Mayne, D. Q. and J. B. Rawlings (2001). Correction to "Constrained model predictive control: stability and optimality". *Automatica*, 37, 483.
- Mayne, D. Q., J. B. Rawlings, C. V. Rao and P. O. M. Scokaer (2000). Constrained model predictive control: stability and optimality. *Automatica*, 36, 789-814.
- Mehra, R. K. and R. E. Davis (1972). A generalized gradient method for optimal control problems with inequality constraints and singular arcs. *IEEE Transactions on automatic control*, AC-17, 69-79.
- Palanki, S., C. Kravaris and H. Y. Wang (1993). Synthesis of state feedback laws for end-point optimization in batch processes. *Chemical Engineering Science*, 48, 135-152.
- Palanki, S., C. Kravaris and H. Y. Wang (1994). Optimal feedback control of batch reactors with a state inequality constraint and free terminal time. *Chemical Engineering Science*, 49, 85-97.
- Rahman, S. and S. Palanki (1996). On-line optimization of batch processes in the presence of measurable disturbances. *American Institute of chemical engineering journal*, 42, 2869-2882.
- Seginer, I., F. Buwalda and G. van Straten (1998). Nitrate concentration in greenhouse lettuce: a modelling study. *Acta Horticulturae*, 456, 189-197.
- Seginer, I. and A. Sher (1993). Optimal greenhouse temperature trajectories for a multi-state-variable tomato model. In: *The computerized greenhouse* (Hashimoto, Y., G. P. A. Bot, W. Day, H.-J. Tantau and H. Nonami. (Ed)), pp. 153-172. Academic press, San Diego, California.
- Seginer, I. and G. van Straten (2001). *Simple Greenhouse Model + annotations (Report)*, Wageningen University, Wageningen.
- Srinivasan, B., S. Palanki and D. Bonvin (2002). Dynamic optimization of batch processes: II. Role of measurements in handling uncertainty. *Computers and chemical engineering*, 27, 27-44.
- Stengel, R. F. (1994). *Optimal control and estimation*, Dover publications, Inc., New York.
- Tap, F. (2000). *Economics-based optimal control of greenhouse tomato crop production (PhD-thesis)*, Wageningen University, Wageningen, The Netherlands.
- van Henten, E. J. (1994). *Greenhouse climate management: an optimal control approach (PhD-thesis)*, Landbouwniversiteit Wageningen, Wageningen, The Netherlands.
- von Elsner, B., D. Briassoulis, D. Waaijenberg, A. Mistriotis, C. von Zabeltitz, J. Gratraud, G. Russo and R. Suay-Cortes (2000a). Review of structural and functional characteristics of greenhouses in European union countries: part 2, typical designs. *Journal of agricultural engineering research*, 75, 1-16.
- von Elsner, B., D. Briassoulis, D. Waaijenberg, A. Mistriotis, C. von Zabeltitz, J. Gratraud, G. Russo and R. Suay-Cortes (2000b). Review of structural and functional characteristics of greenhouses in European union countries: part 1, design requirements. *Journal of agricultural engineering research*, 75, 1-16.

## 5.2 Numerical feedback laws for closed-loop singular optimal control with measurable disturbances

This section is not related directly to the lettuce optimal control problem. It was added to the thesis for the general case that optimal control problems are control affine. If solutions of these problems contain non-saturated optimal control trajectories then these trajectories are singular. Singular trajectories cannot be computed directly by solving the equation  $\frac{\partial H}{\partial u} = 0$  for  $u$  as was done for the lettuce problem in section 5. In stead, for control affine problems another, more involved methods are needed to compute the singular optimal control trajectories.

This section will treat these problems while still exploiting the measurable disturbance information. It is a version of the following paper extended with theory related to measurable disturbances:

De Graaf, S.C., J.D. Stigter and G. van Straten (2005). Numerical feedback laws for closed-loop singular optimal control. *Proceedings of the 16<sup>th</sup> IFAC World Congress in Prague*

**Abstract:** Singular and non-singular optimal control trajectories of agricultural and (bio) chemical processes may need to be revised from time to time for use in closed-loop control, because of (unforeseen) changes in (measurable) disturbances, state values and system/measurement noise. Controllers designed for tracking predefined desired output trajectories are no longer optimal when these changes happen, whereas controllers that recalculate optimal trajectories by integrating state equations many times are less suitable in view of the computation time. As an alternative, efficient, numerical, nonlinear, static state feedback laws are developed in this paper for optimal control on the singular arc that can be applied in closed-loop. The efficacy of these laws is demonstrated in an example.

### 5.2.1 Introduction

Singular and non-singular control trajectories of agricultural, and (bio) chemical (semi-) batch processes may need to be revised from time to time for use in closed-loop optimal control, because of (unforeseen) changes in (measurable) disturbances, state values and system/measurement noise. In principle, adjustment can be achieved by performing an optimisation at each control interval. However, this requires numerous function calls, each implying a full integration of the state equations, which is time consuming. Other algorithms, such as MPC-algorithms are designed for tracking predefined desired output trajectories, and hence are not optimal when changes happen. Singularity of partial derivatives of the Hamiltonian with respect to inputs on singular optimal control trajectories prevents calculation of neighbouring optimal control trajectories as proposed by Lee and Bryson (1989). It is, therefore, attractive to look for alternative algorithms.

An interesting non-iterative and non-output-tracking closed-loop optimisation procedure was developed by Palanki, *et al.* (1993) and Rahman and Palanki (1996). They proposed to first determine in open loop the sequence of singular and non-singular intervals and accompanying switching times. Next, they develop symbolic static state feedback laws that fulfil the necessary conditions of singular control trajectories, while during the non-singular trajectories the minimum or maximum control values are used.

Rahman and Palanki recommend using symbolic manipulation software such as MAPLE or MATHEMATICA for the development of static state feedback laws, because of the need to compute a large number of Lie-derivatives. However, in case of complex systems, symbolic manipulation leads to expressions that are difficult to handle. Numerical calculation of optimal static state feedback laws is therefore more convenient.

Magana Jimenez (2002) developed a MATLAB5.3-ADIFOR2.0-FORTRAN<sup>compaq</sup>6.0-CONTROL (MAFC) software package that is able to synthesize numerical static state feedback laws for control-affine nonlinear systems. In the synthesis of these laws automatic differentiation is incorporated to compute the necessary Lie-derivatives numerically.

In order to be able to use this software package for optimal control, the optimisation problem needs to be cast in the form of a control-affine non-linear system. This paper shows how this can be done, and subsequently describes how numerical static state feedback laws for singular optimal control trajectories can be obtained using MAFC. The novelty of this approach lies in developing state feedback laws for the purpose of singular optimal control by using a software package that is designed for the synthesis of numerical static state feedback laws for control-affine non-linear systems. It makes it possible to implement closed-loop optimal control for complex agricultural, and (bio) chemical systems with singular trajectories, which is the main motivation for this research.

The outline of this paper is as follows. First the optimal control problem is cast in the form of a non-linear control-affine system. Next, the static state feedback laws as synthesized by the MAFC software package are presented. Finally, an example is presented that demonstrates that singular trajectories generated by a numerical static state feedback law are comparable to singular trajectories generated open-loop by a gradient method. It will also be demonstrated that a numerical static state feedback law is able to adjust singular optimal control trajectories in response to (unforeseen) changes in disturbances.

## 5.2.2 Optimal control problem

Let the system to be optimised be represented by the following control affine state equation:

$$\dot{\underline{x}} = \underline{f}(\underline{x}, \underline{d}) + \underline{g}_1(\underline{x}, \underline{d})u_1 + \dots + \underline{g}_m(\underline{x}, \underline{d})u_m \quad \underline{x}(t_0) = \underline{x}_0 \quad x \in \mathbb{R}^n, u \in \mathbb{R}^m \quad (106)$$

Assume that the performance equation that has to be minimised is:

$$J = \phi(\underline{x}_f) \quad \underline{x}_f = \underline{x}(t_f) \quad (107)$$

In these equations  $\underline{x}(t)$  is the state vector,  $\underline{d}(t)$  a vector of disturbances and  $u_1(t), \dots, u_m(t)$  are control inputs. The functions  $\underline{f}(\underline{x})$ , and  $\underline{g}_1(\underline{x}), \dots, \underline{g}_m(\underline{x})$  are smooth system state vector valued functions and  $\phi(\underline{x}_f)$  is the final weighting function.

The final values may be subject to constraints:

$$\underline{\psi}(\underline{x}_f) = 0 \quad \underline{x}_f = \underline{x}(t_f) \quad (108)$$

Note that the optimal control problem has been written in *Mayer-form* (Bryson, 1999; Stengel, 1994), which means that the problem is an end-point optimal control problem. This is not a restrictive assumption, because any non-linear optimisation problem with a performance equation of the form:

$$J = \phi(\underline{x}_f) + \int_{t_0}^{t_f} L(\underline{x}, \underline{u}) dt \quad (109)$$

where  $L(\underline{x}, \underline{u})$  represents the running costs, can be cast in the form of equations 106 and 107 by introducing an additional state differential equation for the running costs, i.e.  $\dot{\underline{x}}^L = L(\underline{x}, \underline{u})$ .

Introducing the Hamiltonian function:

$$H(\underline{x}, \underline{\lambda}, \underline{u}, \underline{d}(t)) = \underline{\lambda}^T (\underline{f}(\underline{x}, \underline{d}(t)) + \underline{g}_1(\underline{x}, \underline{d}(t))u_1 + \dots + \underline{g}_m(\underline{x}, \underline{d}(t))u_m) \quad (110)$$

we have the following necessary optimality conditions in case the inputs are not on the bounds.

$$\dot{\underline{x}} = \left( \frac{\partial H}{\partial \underline{\lambda}} \right)^T \quad \underline{x}(t_0) = \underline{x}_0 \quad (111)$$

$$\dot{\underline{\lambda}} = -\left(\frac{\partial H}{\partial \underline{x}}\right)^T \quad \underline{\lambda}(t_f) = \left(\frac{\partial \phi}{\partial \underline{x}}(t_f) + v \frac{\partial \psi}{\partial \underline{x}}(t_f)\right)^T \quad (112)$$

$$\underline{0} = \left(\frac{\partial H}{\partial \underline{u}}\right)^T \quad \forall t \in [0, t_f] \quad (113)$$

In these conditions  $\underline{\lambda}(t)$  and  $v$  are *Lagrange* multipliers for the state equations and for the final value constraint. The constant *Lagrange* multiplier  $v$  is calculated in open-loop (Bryson, 1999; Bryson and Ho, 1975; de Graaf, 2002). The conditions lead to singular trajectories because they do not define input trajectories, as the input vector  $\underline{u}$  is *not* explicit in equation 113.

In contrast, non-control-affine system representations lead to optimality conditions 113 that are explicit in the input vector  $\underline{u}$ , thus allowing the input vector  $\underline{u}$  to be written as functions of states and costates.

### 5.2.3 Non-linear system representing the optimal control problem

The control-affine optimisation problem, consisting of equations 106 and 107 needs to be (re)formulated as a non-linear system of the form

$$\dot{\tilde{\underline{x}}} = \tilde{\underline{f}}(\tilde{\underline{x}}, \underline{d}) + \tilde{\underline{g}}_1(\tilde{\underline{x}}, \underline{d})u_1 + \dots + \tilde{\underline{g}}_m(\tilde{\underline{x}}, \underline{d})u_m \quad \tilde{\underline{x}}(t_0) = \tilde{\underline{x}}_0 \quad (114)$$

$$\underline{y} = \underline{h}(\tilde{\underline{x}}) \quad (115)$$

in order to be able to synthesize static state feedback laws by the MAFC-software package. If the disturbances in the optimal control problem are assumed time-invariant then this is done by writing the Hamiltonian system (Van der Schaft, 1984):

$$\tilde{\underline{x}} = \begin{bmatrix} \underline{x} \\ \underline{\lambda} \end{bmatrix} \quad (116a)$$

$$\tilde{\underline{f}}(\tilde{\underline{x}}, \underline{d}) = \begin{bmatrix} \underline{f}(\underline{x}, \underline{d}) \\ -\left[\frac{\partial \underline{f}(\underline{x}, \underline{d})}{\partial \underline{x}}\right]^T \underline{\lambda} \end{bmatrix} \quad (117a)$$

$$\tilde{\underline{g}}(\tilde{\underline{x}}, \underline{d}) = \begin{bmatrix} \underline{g}_1(\underline{x}, \underline{d}) & \underline{g}_m(\underline{x}, \underline{d}) \\ -\left[\frac{\partial \underline{g}_1(\underline{x}, \underline{d})}{\partial \underline{x}}\right]^T \underline{\lambda} & \dots - \left[\frac{\partial \underline{g}_m(\underline{x}, \underline{d})}{\partial \underline{x}}\right]^T \underline{\lambda} \end{bmatrix} \quad (118a)$$

$$\underline{h}(\underline{\tilde{x}}, \underline{d}) = \begin{bmatrix} \underline{\lambda}^T \underline{g}_1(\underline{x}, \underline{d}) \\ \vdots \\ \underline{\lambda}^T \underline{g}_m(\underline{x}, \underline{d}) \end{bmatrix} \quad (119a)$$

In this system,  $\underline{\tilde{x}}$  is a new system state vector consisting of the system state vector  $\underline{x}(t)$  and the vector of *Lagrange* multipliers (costates)  $\underline{\lambda}$  of the optimal control problem with the same dimension as  $\underline{x}(t)$ . Here, the vector  $\underline{y}$  is the output vector, and  $\underline{\tilde{f}}(\underline{\tilde{x}}, \underline{d})$ ,  $\underline{\tilde{g}}_1(\underline{\tilde{x}}, \underline{d})$ , ...,  $\underline{\tilde{g}}_m(\underline{\tilde{x}}, \underline{d})$  and  $\underline{h}(\underline{\tilde{x}}, \underline{d})$  are smooth vector functions.

Controlling the outputs  $\underline{h}$  of this Hamiltonian system with initial values for  $\underline{x}_0$  and  $\underline{\lambda}_0$  such that the outputs are set to zero is equivalent to fulfilling the necessary optimality conditions represented by equations 110 to 113.

The equivalence holds if the initial values for  $\underline{\lambda}_0$  are selected in such a way that the optimality condition for  $\underline{\lambda}(t_f)$  is also met. Values for  $\underline{\lambda}_0$  are obtained by solving the optimal control problem (equations 1 and 2) in open-loop as will be discussed in section 5.

If the disturbances are time-varying the Hamiltonian system needs to be extended with state equations describing the dynamics of the disturbances because the Lie-derivatives calculated by MAFC (see section 5.2.4) are inadequate for time-variant disturbances (Wu and Chou, 1999):

$$\underline{\tilde{x}} = \begin{bmatrix} \underline{x} \\ \underline{\lambda} \\ \underline{d} \\ \underline{d}^1 \\ \vdots \\ \underline{d}^{p-2} \\ \underline{d}^{p-1} \end{bmatrix} \quad (116b)$$

$$\underline{\tilde{f}}(\underline{\tilde{x}}, \underline{d}) = \begin{bmatrix} \underline{f}(\underline{x}, \underline{d}) \\ -\left[\frac{\partial \underline{f}(\underline{x}, \underline{d})}{\partial \underline{x}}\right]^T \underline{\lambda} \\ \underline{d}^1 \\ \underline{d}^2 \\ \vdots \\ \underline{d}^{p-1} \\ \underline{d}^p \end{bmatrix} \quad (117b)$$



$$\tilde{g}(\tilde{x}, \underline{d}) = \begin{bmatrix} g_1(x, \underline{d}) & g_m(x, \underline{d}) \\ -\left[\frac{\partial g_1(x, \underline{d})}{\partial \underline{x}}\right]^T \underline{\lambda} & -\left[\frac{\partial g_m(x, \underline{d})}{\partial \underline{x}}\right]^T \underline{\lambda} \\ 0 & \dots & 0 \\ 0 & & 0 \\ \vdots & & \vdots \\ 0 & & 0 \\ 0 & & 0 \end{bmatrix} \quad (118b)$$

$$h(\tilde{x}, \underline{d}) = \begin{bmatrix} \underline{\lambda}^T g_1(x, \underline{d}) \\ \vdots \\ \underline{\lambda}^T g_m(x, \underline{d}) \end{bmatrix} \quad (119b)$$

In this Hamiltonian system  $\underline{d}^1, \dots, \underline{d}^p$  are the first to the  $p$ -th time-derivative vectors of the vector  $\underline{d}$ . The value of  $p$  is chosen in accordance with the information about the time derivatives of disturbances. The number of costates  $\underline{\lambda}$  and the output equation 119 are not extended because the time-invariance of disturbances only affects the second and higher time derivatives of states, costates and outputs.

#### 5.2.4 Numerical static state feedback laws synthesized by MAFC

The MAFC software package, developed by Magana Jimenez (2002) is able to synthesize numerical static state feedback laws,  $\underline{u}$  for nonlinear Hamiltonian systems represented by equations 114 to 119, and thus enables the synthesis of static state feedback laws that perform singular optimal control. The control law takes the form:

$$\underline{u} = -\underline{k}(\tilde{x}, \underline{d}, \underline{d}^1, \dots, \underline{d}^p) + \underline{l}(\tilde{x}, \underline{d}, \underline{d}^1, \dots, \underline{d}^p) \underline{y}^{sp} \quad (120)$$

where the vectors  $\underline{k}(\tilde{x})$  and  $\underline{l}(\tilde{x})$  are smooth vector functions and the vector  $\underline{y}^{sp}$  is the vector of output setpoints that acts as the new vector of inputs. These vector functions are such that the closed loop system is decoupled, which means that individual input-output channels are separated (Isidori, 1989; Nijmeijer and Schaft, 1990). This property is inherent to the theory of the synthesis of static state feedback laws. Each output is also forced to follow an  $r$ -th order linear exponential trajectory towards its setpoint value. This trajectory is defined by Kravaris (1997) and Magana Jimenez (2002):

$$\begin{aligned}
y_1 + \varepsilon_1^1 \frac{dy_1}{dt} + \dots + \varepsilon_1^{r_1} \frac{d^{r_1} y_1}{dt^{r_1}} &= y_1^{sp} \\
&\vdots \\
y_m + \varepsilon_m^1 \frac{dy_m}{dt} + \dots + \varepsilon_m^{r_m} \frac{d^{r_m} y_m}{dt^{r_m}} &= y_m^{sp}
\end{aligned} \tag{121}$$

where  $\varepsilon_{1,1}, \dots, \varepsilon_{r_m, r_m}$  are pre-selected constant tuning parameters, assigning specific eigenvalues to the output dynamics. The parameters  $r_1, \dots, r_m$  are relative degrees, i.e. the smallest integers such that the  $r^{\text{th}}$  derivative of the output  $y$  with respect to  $t$  depends explicitly on the input  $\underline{u}$ .

The vector functions  $\underline{k}(\underline{\tilde{x}}, \underline{d}, \underline{d}^1, \dots, \underline{d}^p)$  and  $\underline{l}(\underline{\tilde{x}}, \underline{d}, \underline{d}^1, \dots, \underline{d}^p)$  are defined by (Magana Jimenez, 2002):

$$\underline{k} = C^{-1} \begin{bmatrix} \varepsilon_1^{r_1} & \dots & 0 \\ \vdots & \ddots & \vdots \\ 0 & \dots & \varepsilon_m^{r_m} \end{bmatrix}^{-1} \begin{bmatrix} \sum_{j=0}^{r_1} \binom{r_1}{j} \varepsilon_1^{r_1-j} L_{\underline{f}}^{r_1-j} h_1 \\ \sum_{j=0}^{r_2} \binom{r_2}{j} \varepsilon_2^{r_2-j} L_{\underline{f}}^{r_2-j} h_2 \\ \vdots \\ \sum_{j=0}^{r_m} \binom{r_m}{j} \varepsilon_m^{r_m-j} L_{\underline{f}}^{r_m-j} h_m \end{bmatrix} \tag{122}$$

$$\underline{l} = C^{-1} \begin{bmatrix} \varepsilon_1^{r_1} & \dots & 0 \\ \vdots & \ddots & \vdots \\ 0 & \dots & \varepsilon_m^{r_m} \end{bmatrix}^{-1} \tag{123}$$

$$\text{with } \binom{r}{j} = \frac{r!}{j!(r-j)!} \quad \text{and} \quad 0! = 1$$

In these equations and  $L_{\underline{f}}^{r_1-1}, \dots, L_{\underline{f}}^{r_m-1}$  are Lie-derivative operators (Isidori, 1989; Nijmeijer and Schaft, 1990) and  $C$  is the following matrix:

$$C = \begin{bmatrix} L_{\underline{g}_1} L_{\underline{f}}^{r_1-1} h_1 & \dots & L_{\underline{g}_m} L_{\underline{f}}^{r_m-1} h_1 \\ L_{\underline{g}_1} L_{\underline{f}}^{r_1-1} h_2 & \dots & L_{\underline{g}_m} L_{\underline{f}}^{r_m-1} h_2 \\ \vdots & \ddots & \vdots \\ L_{\underline{g}_1} L_{\underline{f}}^{r_1-1} h_m & \dots & L_{\underline{g}_m} L_{\underline{f}}^{r_m-1} h_m \end{bmatrix} \tag{124}$$

Static state feedback laws cannot be obtained if the C-matrix is singular. Matrix singularity will occur if, among other things there is no  $r^{\text{th}}$  time-derivative of the output  $y$  that explicitly depends on the input  $u$ .

Note that the feedback law (equation 120) depends upon the costates of the original problem. Palanki, *et al.* (1993) develop symbolic static state feedback laws by eliminating the costates, thereby eliminating possible unstable costate-dynamics. These laws consist of Lie-brackets instead of Lie-derivatives. In contrast, MAFC calculates numerical laws using Lie-derivatives.

More details on static state feedback laws can be found in Magana Jimenez (2002), Isidori (1989) and Nijmeijer and Van der Schaft (1990).

### 5.2.5 *Synthesis and application guide of the static state feedback laws*

Following Palanki, *et al.* (1993) and Rahman and Palanki (1996) static state feedback laws are developed and applied in closed-loop optimal control according to the following procedure:

1. Calculate open-loop optimal state, costate, input and output trajectories for the optimal control problem, using expected trajectories for the measurable disturbances and optimisation methods such as gradient methods presented by, for example, Bryson (1999) and De Graaf (2001).
2. Determine which optimal trajectory intervals are singular and monitor the switching times that mark each beginning and end of these intervals. Also determine the state and costate values at each switching time that marks the beginning of an interval.
3. If needed, make the optimal control problem control-affine. Then (re)formulate the control-affine optimal control problem in a Hamiltonian nonlinear system according to equations 114 to 119. A practical choice needs to be made between inclusion and exclusion of measurable disturbance input time-derivatives, depending on the information about these derivatives. Neglect of these derivatives will lead to output deviations from setpoints (and hence to sub-optimality) if the measurable disturbances are, in fact, time-variant. However, these deviations may successfully be reduced by the force on the outputs to follow an  $r$ -th order linear exponentially trajectory by equation 121.
4. Calculate relative degrees of this nonlinear system at each switching time that marks the beginning of a singular optimal trajectory interval, using MAFC. Check whether the relative degrees change or whether the C-matrix is singular somewhere in this singular optimal trajectory interval. If this happens then stop, as static state feedback laws cannot be obtained in this case.
5. Calculate the static state feedback laws, using MAFC.
6. While on-line, observe the states and disturbances, compute the costates by simulating the process on-line with equations 114 and 115 with observed state values for  $\underline{x}_0$  and  $\underline{\lambda}_0$ , and apply in closed-loop the static state feedback laws for singular intervals and maximum or

minimum input values for the non-singular intervals. Switch from singular to non-singular intervals or vice versa at the switching times determined in open loop.

Step 6 states that costates are computed by simulating the process on-line using initial values for  $\underline{\lambda}_0$ . These values are computed in open-loop in step 1 and contain projected information about  $\underline{\lambda}(t_f)$  based on expected trajectories for the measurable disturbances. If these disturbances change then the simulation of the costates in step 6 may lead to deviations from  $\underline{\lambda}(t_f)$ . To avoid these deviations, costate-trajectories should be adjusted. This is not considered in this section, because it is not part of the feedback laws.

### 5.2.6 Validation of static state feedback laws

An example taken from Srinivasan *et al.* (2000) is used for three purposes: firstly to verify the correctness of the procedure, secondly to check the ability of the feedback law to correct the system towards a new path in case of (unforeseen) changes in (measurable) disturbances and thirdly to validate that newly calculated closed-loop behaviour is closer to optimality than just applying open-loop control.

The synthesis and application guide, presented in section 5 was used to synthesize and apply the static state feedback law.

Srinivasan *et al.* (2000) calculated optimal trajectories for one input of a non-linear system consisting of two simultaneous chemical reactions taking place in a jacket batch reactor. The optimal control problem is described by:

$$\dot{\underline{x}} = \underline{f}(\underline{x}, \underline{d}(t)) + \underline{g}(\underline{x}, \underline{d}(t))u$$

where  $\underline{f}(\underline{x}, \underline{d}(t))$  and  $\underline{g}(\underline{x}, \underline{d}(t))$  are

$$\underline{f}(\underline{x}) = \begin{bmatrix} -p_1 x_1 x_2 \\ -p_1 x_1 x_2 - p_2 x_2^2 \\ 0 \\ -p_1 x_1 x_2 x_3 \\ p_4 x_2^2 \end{bmatrix} \quad (125)$$

$$\underline{g}(\underline{x}) = \begin{bmatrix} -\frac{x_1}{x_3} & \frac{(p_3 + d) - x_2}{x_3} & 1 & 0 & -\frac{x_5}{x_3} \end{bmatrix}^T \quad (126)$$

The performance equation that has to be minimized is:

$$J = x_4(t_f) \quad (127)$$

The initial state are in table 38. The parameter and expected disturbance input values are in table 39. The input  $u$  and the final state of  $x_2$  and  $x_5$  are constrained. These constraints are in table 40.

*Step 1:* Optimal trajectories of the states, costates, input and output were calculated using the expected disturbance input and the ACW-gradient-gradient algorithm (de Graaf, 2001). These trajectories are plotted with dotted lines (----) in figures 25 to 28 and figures 29 to 32.

*Step 2:* Optimal output trajectories figures 26 and optimal control trajectories in figure 28 suggest that the optimal control trajectory consists of a singular optimal control trajectory in the time interval 25 tot 200 minutes, while outside this time-interval the input is on its upper or lower bound. In order to calculate a feedback law for the singular interval, the states and costates at the beginning of the interval (25 minutes) are required. They are in table 41.

Table 38: Initial state values

$x_1$	0.72	$x_4$	0
$x_2$	0.05	$x_5$	0
$x_3$	1		

Table 39: Parameter and expected disturbance input values

$p_1$	0.053	$p_3$	5
$p_2$	0.256	$p_4$	0.128
$d$	0.0		

Table 40: Constraints on inputs  $u$  and final values of states  $x_2$  and  $x_5$

	<i>lower bound</i>	<i>upper bound</i>		<i>lower bound</i>	<i>upper bound</i>
$u(t)$	0	$1.0 \cdot 10^{-3}$			
$x_2(t_f)$		0.025	$x_5(t_f)$		0.15

Table 41: State and costate values at 25 minutes

<i>state values</i>		<i>costate values</i>	
$x_1$	0.6422	$\lambda_1$	-0.5882
$x_2$	0.0772	$\lambda_2$	0.0012
$x_3$	1.0244	$\lambda_3$	-0.3619
$x_4$	-0.0622	$\lambda_4$	1.0000
$x_5$	0.0149	$\lambda_5$	0.7478

*Step 3:* There was no need to make the optimal control problem control-affine because the problem is already control-affine. The disturbance was assumed to be time-invariant, so extra states to describe the disturbance dynamics were not needed. The problem was reformulated as a Hamiltonian non-linear system according to equations 114 to 119a (not shown here).

*Step 4:* The relative degree of this system at 25 minutes is equal to 2 and the C-matrix is non-singular in the time interval 25 to 200 minutes. This means that a static state feedback law based on a relative degree of 2 is applicable for this singular optimal control trajectory interval.

*Step 5 and 6:* The static state feedback law was calculated and applied to calculate trajectories of the states, costates, input and output in three simulated closed-loop optimal control experiments, marked a, b and c:

*Experiment a:* To verify the correctness of the procedure, simulated state are offered as artificial observed state trajectories to the static state feedback law for the closed-loop calculation of state, costate, input and output trajectories. These trajectories are plotted with solid lines (—) in figures 25 to 28.

*Experiment b:* To check the ability of the feedback law to correct the system towards a new path, the disturbance value was perturbed deliberately. This was done by reducing the value of parameter  $p_3$  by 50% at 100 minutes, thus simulating an unforeseen change in the disturbance input value. Closed-loop calculated state, costate, input and output trajectories of this experiment are plotted with solid lines marked with dots (—•—) in figures 29 to 32.

*Experiment c:* To validate that the newly calculated closed-loop behaviour is closer to optimality than just applying open-loop control, the singular optimal control trajectory calculated in open loop was applied instead of controlling the system by the static state feedback law. These trajectories are plotted with solid lines (—) in figures 29 to 32.

### 5.2.7 Results

Figures 25 to 28 show a good resemblance between the state, costate, output and input trajectories calculated in open loop and those obtained with the static state feedback law.

Figures 29 to 32 show that in experiment b the static state feedback law changes the singular optimal control trajectory when there is a perturbation of the disturbance input at  $t=100$ , which leads to changes in state and costate trajectories. The output, being  $\frac{\partial H}{\partial u}$ , correctly returns to its setpoint value zero (figure 30). The application of the open-loop calculated optimal control trajectory in experiment c leads to an output deviation from its setpoint after 100 minutes, which means that the state, costate and input trajectories are not optimal.

### 5.2.8 Discussion

This example demonstrates that a singular trajectory generated by a numerical static state feedback law is comparable to a singular trajectory generated open-loop by a gradient method. It also demonstrates that a numerical static state feedback law is able to adjust the singular optimal control trajectories in response to (unforeseen) changes in disturbances. This result can be generalized taking into account the following remarks.

While on-line, computing costates by simulating the process on-line with equations 114 and 115 (step 6 of the state feedback law development procedure) may lead to undesirable costate trajectories. This is related to possible deviations from  $\underline{\lambda}(t_f)$  as discussed in section 5.2.5 and possible instability of the trajectories. To avoid possible deviations from  $\underline{\lambda}(t_f)$  costate trajectories can be updated from time to time through open-loop optimisations with updated disturbance input trajectories. The problem of possible instability is discussed by Kalman (1966). Specific solutions to circumvent this problem need to be found.

While on-line, switching from singular to non-singular intervals or vice versa at the switching times determined in open loop (step 6 of the state feedback law development procedure) may lead to sub-optimal control because switching times are not revised. This effect is less severe if switching times are insensitive to disturbance changes.

If measurable disturbance input time-derivatives are included in equations 114 to 119 then filters should be used to calculate these time-derivatives in order to reduce undesirable amplification of observation noise.

### 5.2.9 Conclusions and implications

Numerical, nonlinear, static state feedback laws synthesized by MAFC successfully generate singular optimal control trajectories in the presence of measurable disturbances. These laws are attractive for application in closed-loop optimal control of complex systems with measurable disturbances, because they are efficient with respect to computation time and are not designed for tracking predefined desired output trajectories that are not optimal when changes in measurable disturbances happen.

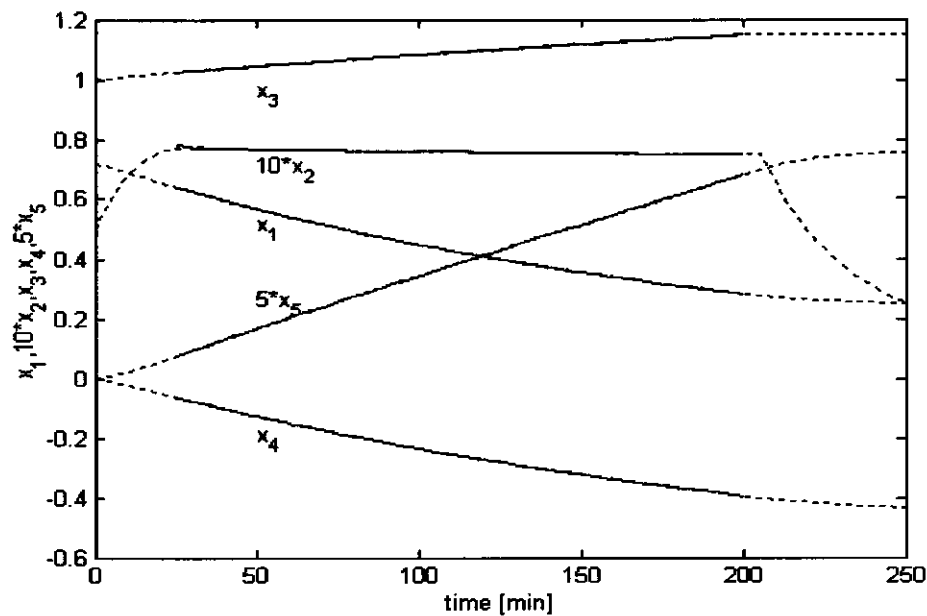


Figure 25 Optimal state trajectories calculated in open-loop (---) and in closed-loop (experiment a: —).

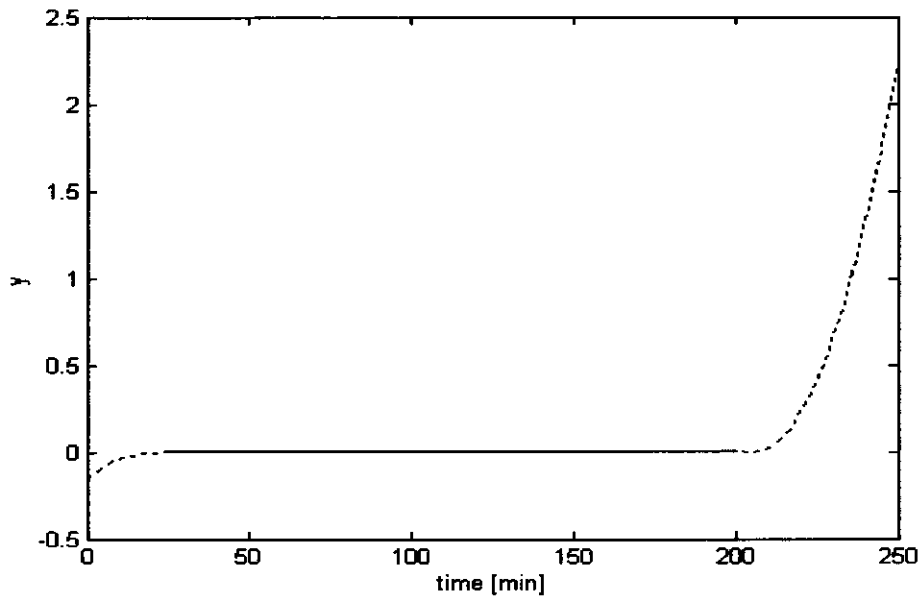


Figure 26 Optimal output trajectories calculated in open-loop (---) and in closed-loop (experiment a: —).



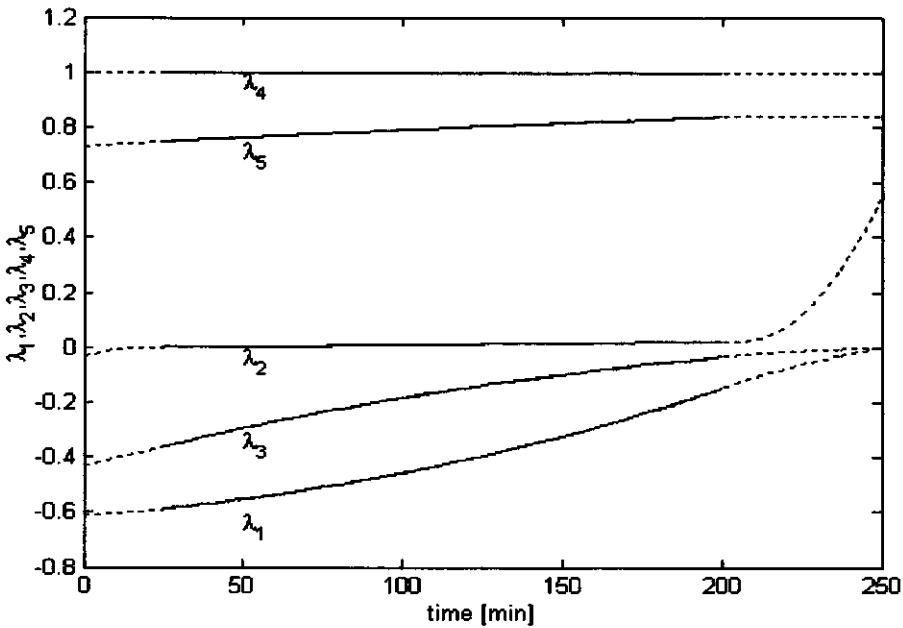


Figure 27 Optimal costate trajectories calculated in open-loop (---) and in closed-loop (experiment a: —).

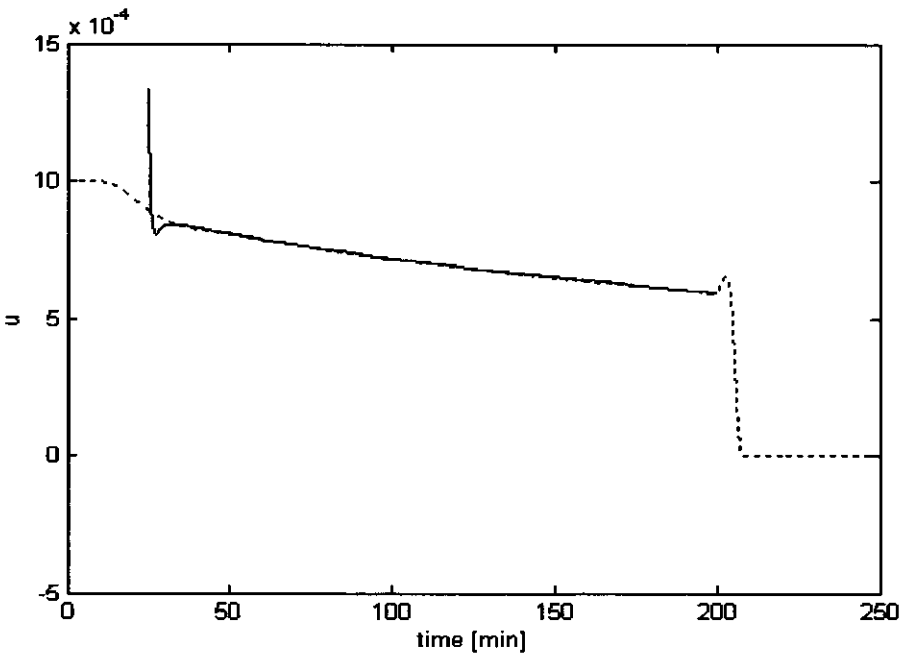


Figure 28 Optimal control trajectories calculated in open-loop (---) and in closed-loop (experiment a: —).

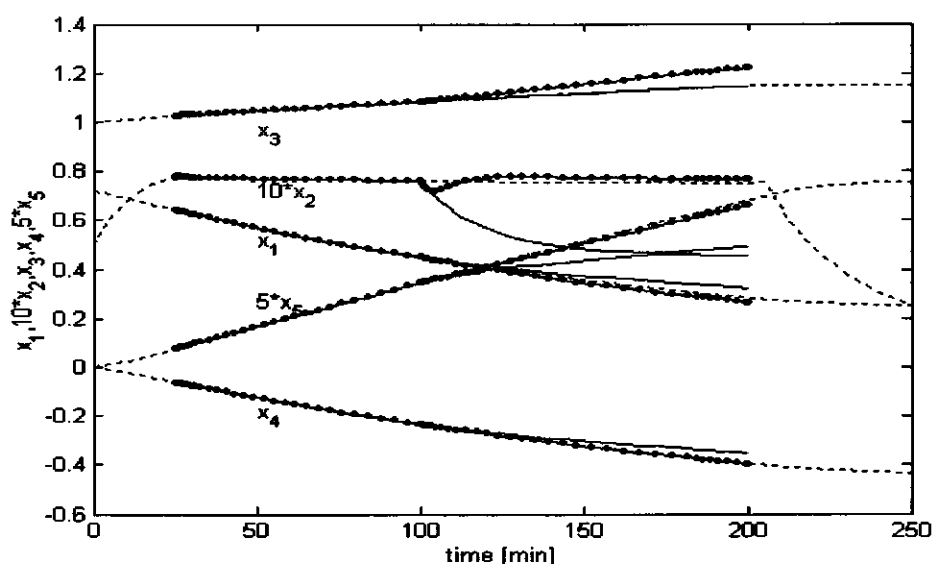


Figure 29 Optimal state trajectories without disturbance (calculated in open-loop:---), with disturbance and application of feedback law (experiment b: —●—), with disturbance and application of open-loop control (experiment c:—).

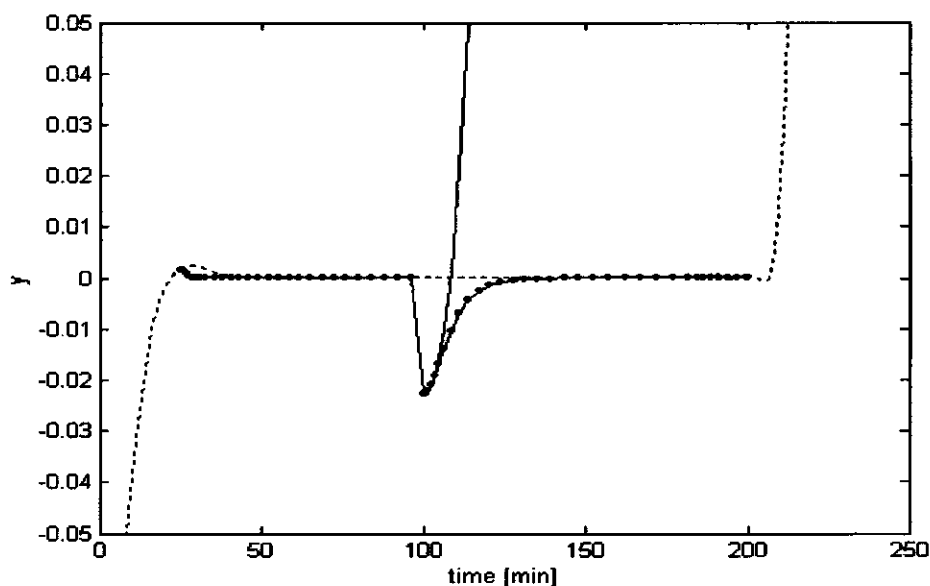


Figure 30 Optimal output trajectory without disturbance (calculated in open-loop:---), with disturbance and application of feedback law (experiment b: —●—), with disturbance and application of open-loop control (experiment c:—).

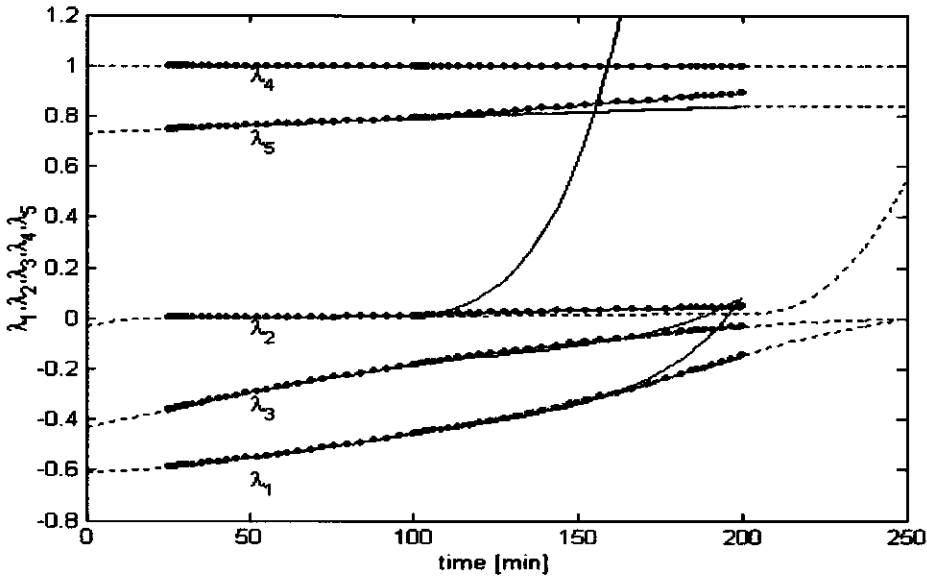


Figure 31 Optimal costate trajectories without disturbance (calculated in open-loop:---), with disturbance and application of feedback law (experiment b: —●—), with disturbance and application of open-loop control (experiment c:—).

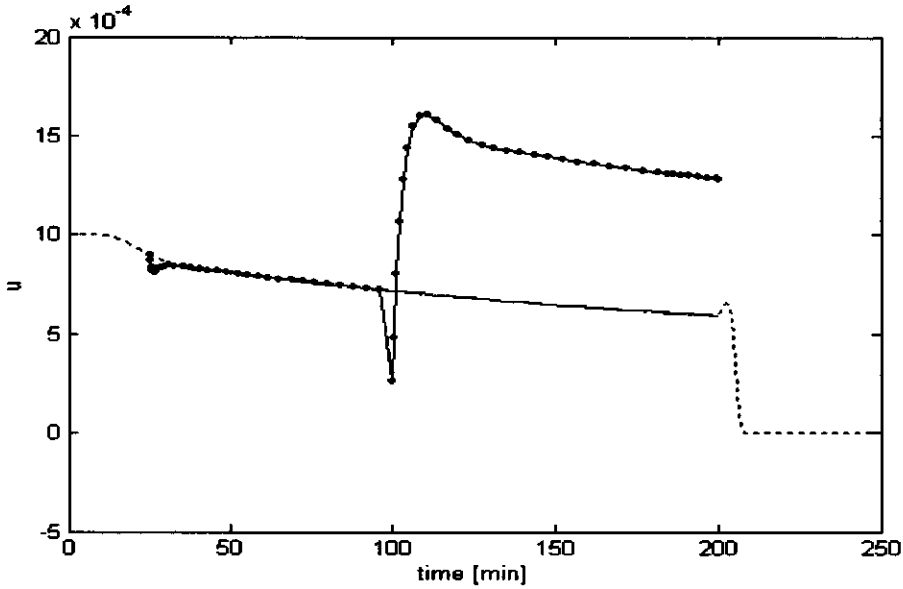


Figure 32 Optimal control trajectory without disturbance (calculated in open-loop:---), with disturbance and application of feedback law (experiment b: —●—), with disturbance and application of open-loop control (experiment c:—).

## References

- Bryson, A. E. (1999). *Dynamic optimization*, Addison-Wesley Longman, Inc., Menlo Park.
- Bryson, A. E. and Y.-C. Ho (1975). *Applied optimal control; optimization, estimation and control*, Hemisphere, New York.
- de Graaf, S. C. (2001). *Test of ACW-gradient optimisation algorithm in computation of an optimal control policy for achieving acceptable nitrate concentration of greenhouse lettuce*, Haifa, Israel.
- de Graaf, S. C. (2002). Optimal greenhouse climate control for achieving specified low nitrate concentration in lettuce. In: Wageningen University, Wageningen.
- Isidori, A. (1989). *Nonlinear control systems; an introduction*, Springer-Verlag, Berlin.
- Kalman, R. E. (1966). Toward a theory of difficulty of computation in optimal control. *Proceedings of fourth IBM scientific computing symposium*, 25-43.
- Kravaris, C., M. Niemiec, R. Berber and C. B. Brosilow (1997). Nonlinear model-based control of nonminimum-phase processes. In: *Nonlinear model based process control* (Berber, R. and C. Kravaris. (Ed)), pp. 87-141. Kluwer academic publishers, Dordrecht.
- Lee, A. Y. and A. E. Bryson (1989). Neighbouring extremals of dynamic optimization problems with parameter variations. *Optimal control applications & methods*, 10, 39-52.
- Magana Jimenez, Q. (2002). *Nonlinear control via automatic differentiation (PhD-thesis)*, Case western reserve univeristy, Cleveland.
- Nijmeijer, H. and v. d. A. J. Schaft (1990). *Nonlinear dynamical control systems*, Springer-Verlag New York Inc., New York.
- Palanki, S., C. Kravaris and H. Y. Wang (1993). Synthesis of state feedback laws for end-point optimization in batch processes. *Chemical Engineering Science*, 48, 135-152.
- Rahman, S. and S. Palanki (1996). On-line optimization of batch processes in the presence of measurable disturbances. *American Institute of chemical engineering journal*, 42, 2869-2882.
- Srinivasan, B., S. Palanki and D. Bonvin (2000). *A tutorial on the optimization of batch processes: I. Characterization of the optimal solution (Report)*, BatchPro, Gregersen, L., Danmarks Tekniske Universitet,
- Stengel, R. F. (1994). *Optimal control and estimation*, Dover publications, Inc., New York.
- Van der Schaft, A. J. (1984). *System theoretic description of physical systems*, Centre for mathematics and computer science, Amsterdam.
- Wu, W. and Y.-S. Chou (1999). Adaptive feedforward and feedback control of non-linear time-varying uncertain systems. *International journal of control*, 72, 1127-1138.

# 6

## 6 Conclusion

### 6.1 Introduction

This thesis offers possible solutions for the optimal cultivation of greenhouse lettuce. Optimal means that nitrate accumulation above maximum concentrations imposed by the EU is prevented and that profits are maximized.

This conclusion consists of two parts: a horticultural part, followed by a control-oriented part. Each can be read without reading the other.

### 6.2 Horticultural conclusion

This thesis shows that with knowledge about models and cultivation limitations, this problem can be solved mathematically through the computation of optimal trajectories of greenhouse climate variables and their affecting controls. The variables of interest are greenhouse air temperature, relative humidity ratio and greenhouse air CO<sub>2</sub>-concentration while the control inputs are heating pipe temperatures, CO<sub>2</sub>-enrichment flow rates and ventilation rates.

Next optimal trajectories of control inputs are computed with assumed known weather conditions for 30 cultivations starting at dates that are distributed evenly over the year. From the resulting greenhouse climate trajectories, characteristic patterns were identified. They are the basis of all trajectories that lead to maximum profits and final nitrate concentrations that are equal to or below the allowable maximum nitrate concentrations. Physical, biological and economical interpretations show that the obtained characteristics are realistic.

A comparison of these characteristics with current common heuristic climate control strategies shows that the current strategy finds scientific support, at least qualitatively. However, the application of optimal control offers additional benefits. For instance, while optimal CO<sub>2</sub>-

concentration trajectories are in the same range as current setpoints of  $\text{CO}_2$ -concentrations, adjusting these setpoints optimally to outside-climate conditions will improve lettuce cultivations with respect to final nitrate concentrations and profits. Also, computed optimal relative humidity values may often be closer to the upper bound at daylight than actual relative humidity values. Greenhouse growers are therefore advised to increase their relative humidity towards the upper bound, where the upper bound must be chosen as high as can be tolerated for preventing lettuce plants from diseases and deformations. This will lead to lower ventilation rates and higher possible  $\text{CO}_2$ -concentrations that eventually will improve lettuce cultivations. Finally, heuristic temperature control and heating pipe settings are replaced by optimal control leading to temperature trajectories between current minimum and maximum permitted temperatures.

The characteristic patterns obtained in open loop have been used to design an algorithm for on-line closed-loop (sub-)optimal control during lettuce cultivation. This algorithm is able to adjust the controls in response to unforeseen changes on weather input trajectories. The adjustments are such that despite the changes all process limitations are properly dealt with. Another important feature of the algorithm is that it is able to make the adjustments fast. Despite the uncertainty with respect to the future weather and the partly heuristic nature of the algorithm design, the performance of the algorithm is usually close to the performance associated to the optimal trajectories of a large number of cultivations with assumed known weather conditions.

### **6.3 Control theoretical interpretation of results presented in this thesis**

The lettuce cultivation problem was presented as an optimal control problem with external disturbances that can be exploited. Furthermore the problem contained nonlinear differential-algebraic equations, non-quadratic cost functions and constraints on control inputs and on final values of states.

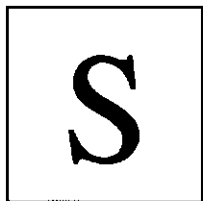
Results of open loop optimisations with assumed nominal disturbances are presented and analysed for characteristic patterns. Applying trajectories that are based on these patterns should lead to maximisation of the performance function and meeting the constraints on final values of the states.

The open-loop trajectories were computed iteratively using a gradient-algorithm that was extended with the so-called adjustable control-variation weight (ACW) construct. The ACW-gradient algorithm has been proposed in the literature for optimisation problems with bounds on the inputs in conjunction with terminal constraints.

The characteristic patterns and necessary optimality conditions were applied to obtain so-called operational modes for the design of the sub-optimal control algorithm. Symbolic computations were also employed here. The modes can be evaluated very efficiently, which makes the algorithm highly efficient computationally.

In the lettuce application, for modes where the inputs are not on the bounds, control inputs can be computed directly as the system equations are non-control affine. There are non-linear optimal control problems that are affine in the controls. In that case, the control has singular trajectories, and cannot be computed directly. In this thesis, a numerical procedure to design non-linear feedback controllers for singular trajectories is presented. The procedure is based on casting the optimal control problem in a standard control form, and applying the MAFC algorithm from the literature to obtain a numerical feedback law. This procedure is useful in case the non-linear feedback controllers cannot be designed analytically.

The algorithm is able to quickly adjust values of control inputs in response to unforeseen changes of disturbances and such that control bounds and quasi steady state constraints are satisfied. Despite the uncertainty with respect to the uncertain external disturbances and the partly heuristic nature of the algorithm design, the performance of the algorithm is usually close to the performance of the open-loop algorithm. Therefore the extent of sub-optimality of both algorithms can be considered virtually the same.



## **S. Summary**

### **S.1 Introduction**

This thesis offers solutions for the optimal cultivation of greenhouse lettuce. Optimal means that nitrate accumulation above maximum concentrations imposed by the EU is prevented and that profits are maximized. This is a horticultural problem because it is an example of how to improve crop quality via intelligent adjustment of climate conditions during cultivation. It is also a control problem because it is an example of how to control processes with a significant number of constraints while being affected by uncontrollable inputs.

This summary consists of two parts: a horticultural part, followed by a control oriented part. Each can be read without reading the other.

### **S.2 Horticultural summary**

Nitrate may have both harmful as well as beneficial effects on human health. Out of concern for harmful effects the European Union issued a directive that imposes maxima to nitrate concentrations in marketable butterhead lettuce. Greenhouse lettuce growers in temperate climate zones such as the Netherlands and Belgium often have difficulty to comply with this directive.

This thesis shows that with knowledge about models and cultivation limitations, this problem can be solved mathematically through the computation of optimal trajectories of greenhouse climate variables and their affecting controls. The variables of interest are greenhouse air temperature, relative humidity ratio and greenhouse air  $\text{CO}_2$ -concentration while the control inputs are heating pipe temperatures,  $\text{CO}_2$ -enrichment flow rates and ventilation rates.

First, three mathematical models that were used for these computations are introduced: a model of lettuce growth and nitrate accumulation, a greenhouse climate model and a model of sales revenues



and cultivation costs. These three models describe effects of outside climate conditions and control inputs on lettuce growth, nitrate accumulation, greenhouse climate, sales revenues and cultivation costs.

Next optimal trajectories of control inputs are computed with assumed known weather conditions for 30 cultivations starting at dates that are distributed evenly over the year. From the resulting greenhouse climate trajectories, characteristic patterns are identified. They are the basis of all trajectories that lead to maximum profits and final nitrate concentrations that are equal to or below the allowable maximum nitrate concentrations. Physical, biological and economical interpretations show that the obtained characteristics are realistic.

According to these characteristic patterns, ventilation rates should be kept at the lower bound in case of heating or CO<sub>2</sub>-enrichment, while ventilation between the bounds is needed in case greenhouse air temperatures or relative humidity values tend to exceed their upper bounds. Greenhouse air CO<sub>2</sub>-concentrations should be on their lower bound at night and at values above the lower bound during daylight, chosen such that they are optimal with respect to sales revenues and running costs. Greenhouse air temperatures should not be increased by heating at night except when these temperatures tend to violate their lower bound. At daylight, greenhouse air temperatures should be at values above the lower bound that are optimal with respect to sales revenues and running costs. If this temperature tends to exceed its upper bound then heating should be turned off and windows should be opened thus keeping the temperature at the upper bound. CO<sub>2</sub>-enrichment flows should be such that they lead to optimal CO<sub>2</sub>-concentrations. If relative humidity tends to exceed its upper bound then greenhouse air temperatures and ventilation rates should be adjusted in such a way that relative humidity is kept on the upper bound. Finally, heating pipe temperatures should be such that optimal air temperatures can be reached.

A comparison of these characteristics with current common heuristic climate control strategies shows that the current strategy finds scientific support, at least qualitatively. However, the application of optimal control offers additional benefits. For instance, while optimal CO<sub>2</sub>-concentration trajectories are in the same range as current setpoints of CO<sub>2</sub>-concentrations, adjusting these setpoints optimally to outside-climate conditions will improve lettuce cultivations with respect to final nitrate concentrations and profits. Also, computed optimal relative humidity values may often be closer to the upper bound at daylight than actual relative humidity values. Greenhouse growers are therefore advised to increase their relative humidity towards the upper bound, where the upper bound must be chosen as high as can be tolerated for preventing lettuce plants from diseases and deformations. This will lead to lower ventilation rates and higher possible CO<sub>2</sub>-concentrations that eventually will improve lettuce cultivations. Finally, heuristic temperature control and heating pipe settings are replaced by optimal control leading to temperature trajectories between current minimum and maximum permitted temperatures.

The characteristic patterns obtained in open loop have been used to design an algorithm for on-line closed-loop (sub-)optimal control during lettuce cultivation. This algorithm is able to adjust the controls in response to unforeseen changes on weather input trajectories. The adjustments are such

that despite the changes all process limitations are properly dealt with. Another important feature of the algorithm is that it avoids the need for time-consuming on-line optimisations. Despite the uncertainty with respect to the future weather and the partly heuristic nature of the algorithm design, the performance of the algorithm is usually close to the performance associated to the optimal trajectories of a large number of cultivations starting at different times during the year with assumed known weather conditions.

### S.3 Control summary

Closed-loop solutions are difficult to find for optimal control problems with external disturbances that can be exploited (such as sunshine in greenhouses). Nonlinear differential-algebraic equations, non-quadratic performance functions, constraints on control inputs and on final values of states make this problem even harder to solve. Such a problem is the optimal control problem of lettuce cultivation that is treated in this thesis.

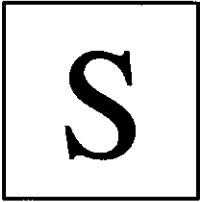
This thesis eventually presents a so-called closed-loop suboptimal control algorithm that can be used for closed-loop optimal control of greenhouse lettuce cultivations. To build this algorithm, equations, cost functions, constraints and disturbances are presented first. Then results of open loop optimisations with perfect a-priori knowledge of disturbances are presented. These results are analysed for characteristic patterns. Applying trajectories that are based on these characteristics should lead to maximisation of the performance function and meeting the constraints on final values of the states.

Open-loop trajectories were computed iteratively using a gradient-algorithm that was extended with the so-called adjustable control-variation weight (ACW) construct. The ACW-gradient algorithm has been proposed in the literature for optimisation problems with bounds on the inputs in conjunction with terminal constraints.

The characteristic patterns and necessary optimality conditions were applied to obtain operational modes for the design of the closed-loop sub-optimal control algorithm. Symbolic computations were also employed here. The modes can be evaluated very efficiently, which makes the algorithm highly efficient computationally.

In the lettuce application, for modes where the inputs are not on the bounds, control inputs can be computed directly as the system equations are non-control affine. There are non-linear optimal control problems that are affine in the controls. In that case, the control has singular trajectories, and cannot be computed directly. In this thesis, a numerical procedure to design non-linear feedback controllers for singular trajectories is presented. The procedure is based on casting the optimal control problem in a standard control form, and applying the MAFC algorithm from the literature to obtain a numerical feedback law. This procedure is useful in case the non-linear feedback controllers cannot be designed analytically.

The algorithm is able to quickly adjust values of control inputs in response to unforeseen changes of weather disturbances and such that control bounds and quasi steady state constraints are satisfied. Despite the uncertainty with respect to the uncertain external disturbances and the partly heuristic nature of the algorithm design, the performance of the algorithm is usually close to the performance of the open-loop algorithm. Therefore the extent of sub-optimality of both algorithms can be considered virtually the same.



## **S Samenvatting**

### **S.1 Introductie**

In dit proefschrift worden oplossingen voor het optimaal telen van kassla gepresenteerd. Optimaal betekent hier dat nitraatophoping in sla boven de door de EU vastgestelde maximale concentraties wordt voorkomen en dat de winst maximaal is. Dit is een teeltkundig probleem omdat het een voorbeeld is van de vraag: hoe kan de kwaliteit van gewassen verbeterd worden door kasklimaat gedurende de teelt aan te passen. Het is ook een stuurprobleem omdat het een voorbeeld is van de vraag: hoe kunnen processen met een groot aantal beperkingen en verstoringen optimaal gestuurd worden.

Deze samenvatting bestaat uit twee delen: een teeltkundig deel en een regelkundig deel. Elk deel kan afzonderlijk worden gelezen.

### **S.2 Teeltkundige samenvatting**

Nitraat kan goede en kwalijke effecten op de menselijke gezondheid hebben. Vanwege de zorg over de mogelijk kwalijke effecten heeft de Europese Unie maximum toegestane maximale nitraatconcentraties voor sla in een richtlijn vastgelegd. Kasslatelers in gebieden met een gematigd klimaat zoals Nederland en België kunnen vaak moeilijk aan deze richtlijn voldoen.

Dit proefschrift laat zien dat dit probleem met kennis van modellen en teeltbeperkingen wiskundig kan worden opgelost door optimale trajecten van klimaatomstandigheden en sturingen ervan uit te rekenen. De omstandigheden zijn kasluchttemperatuur, relatieve vochtigheid, kaslucht-CO<sub>2</sub>-concentratie en de sturingen zijn verwarmingsbuistemperatuur, CO<sub>2</sub>-doseringsdebieten en ventilatiedebieten.

Eerst worden drie wiskundige modellen die gebruikt zijn bij deze berekeningen uitgelegd: een model van slagroei en nitraatophoping, een kasklimaatmodel en een model van verkoopopbrengsten en teeltkosten. Deze drie modellen beschrijven wat de invloed is van buiten-klimaatomstandigheden en sturingen op de slagroei, nitraatophoping, kasklimaat, verkoopopbrengsten en teeltkosten.

Daarna zijn optimale stuurtrajecten van 30 slateelten berekend met bekend veronderstelde weersomstanigheden. De 30 slateelten waren gelijk over het jaar verspreid. Uit resulterende trajecten zijn karakteristieke patronen afgeleid. Deze vormen de basis van alle trajecten die leiden tot een maximale winst en nitraatconcentraties die gelijk of lager zijn dan de maximale concentraties. Fysische, biologische en economische interpretaties geven aan dat de karakteristieken reëel zijn.

Volgens de karakteristieke patronen moet het ventilatiedebiet vaak op de ondergrens liggen bij verwarming of CO<sub>2</sub>-toevoer en tussen de onder- en bovengrens wanneer de kasluchttemperatuur of relatieve vochtigheid hun bovengrenzen dreigen te overschrijden. Kaslucht-CO<sub>2</sub>-concentraties moeten 's nachts naar de ondergrens worden verlaagd en bij daglicht boven de ondergrens liggen, op waarden die optimaal zijn wat betreft verkoopopbrengsten en teeltkosten. De kasluchttemperatuur moet 's nachts niet door verwarming verhoogd worden tenzij deze temperatuur onder de ondergrens dreigt te komen. Bij daglicht moet de kasluchttemperatuur boven de ondergrens liggen, op waarden die optimaal zijn wat betreft verkoopopbrengsten en teeltkosten. Als de kasluchttemperatuur de bovengrens dreigt te overschrijden dan moet de verwarming gestopt of de ramen geopend worden, waardoor de temperatuur op de bovengrens komt te liggen. CO<sub>2</sub>-toevoerdebieten moeten leiden tot optimale CO<sub>2</sub>-concentraties. Als de relatieve vochtigheid de bovengrens dreigt te overschrijden dan moeten de kasluchttemperatuur en het ventilatiedebiet zodanig aangepast worden dat de relatieve vochtigheid op de bovengrens blijft. Tenslotte, moeten de verwarmingsbuistemperaturen leiden tot de optimale kasluchttemperaturen.

Uit een vergelijking van deze karakteristieken met huidige kasklimaat-stuurstrategieën blijkt dat kwalitatief gezien de huidige strategie wetenschappelijk ondersteund wordt. De toepassing van optimale sturingen levert echter meer op. Bijvoorbeeld, naast het feit dat optimale CO<sub>2</sub>-concentratietrajecten in dezelfde range liggen als de huidige setpoints voor CO<sub>2</sub>-concentraties, zal de optimale aanpassing van deze setpoints aan buiten-klimaatomstandigheden leiden tot een verbetering van de slateelt wat betreft nitraatconcentraties en winsten. Ook blijkt dat de berekende optimale waarden van de relatieve vochtigheid overdag vaker dichterbij de bovengrens kunnen liggen dan huidige, werkelijke waarden. Slateelers wordt daarom geadviseerd om de relatieve vochtigheid te verhogen naar een bovengrens die zo hoog is ingesteld dat ziektes en vervormingen van de slaplanten wordt voorkomen. Dit zal leiden tot lagere ventilatiedebieten en hogere CO<sub>2</sub>-concentraties wat uiteindelijk de slateelt zal verbeteren. Tenslotte kunnen heuristische optimale temperatuurtrajecten en verwarmingsbuis-temperaturen worden vervangen door optimale sturingen. Deze sturingen leiden tot temperatuurtrajecten die tussen de huidige minimaal en maximaal toegestane temperaturen liggen.

De in open-loop berekende karakteristieke patronen zijn gebruikt voor het ontwerpen van een zogenaamd sub-optimaal algoritme dat on-line klimaatomstandigheden gedurende een slateelt kan sturen. Dit algoritme is in staat om stuurtrajecten aan te passen bij onverwachte weersveranderingen. Deze aanpassingen zijn zodanig dat ondanks de veranderingen goed omgegaan wordt met alle beperkingen, vooral de beperking op de relatieve vochtigheid. Een ander belangrijk kenmerk van het algoritme is dat het in staat is om de aanpassingen snel te maken. Ondanks de onzekerheid over het toekomstige weer en het deels heuristische karakter van het algoritmeontwerp is de performance van het algoritme meestal dicht bij de performance van optimale trajecten van een groot aantal slateelten met bekend veronderstelde weersomstandigheden.

### S.3 Regeltechnische samenvatting

Closed-loop oplossingen zijn moeilijk te vinden voor een optimaal sturingsprobleem met verstoringen die nuttig kunnen worden aangewend (zoals zonlicht in kassen). Niet-lineaire differentiaalvergelijkingen, niet-kwadratische doelfuncties, beperkingen op sturingen en op toestandseindwaarden maken dit probleem nog lastiger om op te lossen. Zo'n probleem is het slateelt-optimalisatieprobleem dat in dit proefschrift wordt behandeld.

Dit proefschrift presenteert uiteindelijk een zogenaamd sub-optimaal algoritme dat gebruikt kan worden voor het closed-loop, optimaal sturen van slateelt kassen. Om tot dit algoritme te komen, worden eerst de vergelijkingen, doelfuncties, beperkingen en verstoringen gepresenteerd. Daarna worden resultaten gepresenteerd van open-loop optimalisaties die uitgevoerd zijn met bekende nominale verstoringen. Deze resultaten worden geanalyseerd op karakteristieke patronen. De toepassing van trajecten die gebaseerd zijn op deze patronen zou moeten leiden tot een maximalisatie van de doelfunctie terwijl er wordt voldaan aan de beperkingen op de toestandseindwaarden.

De open-loop trajecten werden iteratief berekend met een gradiënt-algoritme dat was uitgebreid met de zogenaamde adjustable control-variation weight (ACW) functie. Het ACW-gradiënt algoritme werd in de literatuur aangeraden voor optimalisatieproblemen met beperkingen op sturingen en op toestandseindwaarden.

De karakteristieke patronen en de noodzakelijke optimalisatievoorwaarden werden gebruikt om procedures te verkrijgen voor het ontwerp van het sub-optimaal algoritme. Symbolische berekeningen zijn hier ook toegepast. De procedures kunnen erg efficiënt geevalueerd worden, wat het algoritme rekentechnisch efficiënt maakt.

In de slatoepassing, voor tijdsintervallen waarin de sturingen zich niet op de grenzen bevinden, kunnen de sturingen direct berekend worden omdat de systeemvergelijkingen niet control-affine zijn. Er zijn niet-lineaire optimalisatieproblemen die control-affine zijn. In dit geval, bestaan stuurtrajecten uit singuliere trajecten die niet direct berekend kunnen worden. In dit proefschrift wordt een numerieke procedure voor het ontwerpen van niet-lineaire feedback regelaars voor

singuliere trajecten gepresenteerd. De procedure is gebaseerd op het formuleren van het optimale sturingsprobleem in een standaard vorm en het toepassen van het MAFC-algoritme uit de literatuur om een numeriek feedback-regelaar te krijgen. Deze procedure is handig wanneer niet-lineaire feedback regelaars niet analytisch ontworpen kunnen worden.

Het algoritme is in staat om stuurtrajecten snel aan te passen bij onverwachte verstoringen. Deze aanpassingen zijn ook zodanig dat voortdurend rekening wordt gehouden met opgelegde beperkingen. Ondanks de onzekerheid over de verstoringen en het deels heuristische karakter van het algoritmeontwerp is de performance van het algoritme meestal dicht bij de performance het open-loop algoritme. De mate van sub-optimaliteit van beide algoritmes kan daarom als gelijk worden beschouwd.



## A. Appendix A

### A.1 Rationale of the negative correlation between lettuce nitrate concentration and the ratio of photosynthesis time-integrals and growth time-integrals

Results of Vanthoor (2002) presented in figure 33 show decreasing lettuce nitrate concentrations with increasing ratio of photosynthesis time-integrals and growth time-integrals. These ratios can be interpreted as dimensionless numbers that combine effects of global solar radiation intensity values, temperatures and CO<sub>2</sub>-concentrations during the last 14 cultivation days on lettuce nitrate concentrations at harvest time. They were calculated according to the equation:

$$R = \frac{\int_0^{t_f} \frac{\epsilon I \sigma C_{Ca}}{\epsilon I + \sigma C_{Ca}} dt \cdot \left( \int_0^{t_f} \nu k e^{(t_s - t)} dt \right)^{-1}}{\quad} \quad (128)$$

Parameters and inputs in this equation are specified in table 42.

This relationship is an extension of results presented by Drews, *et al.* (1995) and Seginer, *et al.* (1998). Drews found a good relation between nitrate concentration at harvest and medium sum of daily radiation over last 14 cultivation days (or  $2.9 \cdot 10^7$  seconds) before harvest. Seginer stated that the nitrate concentration is approximately inversely proportional to the *balance* between supply of carbohydrates by photosynthesis and demand of carbohydrates by growth and maintenance. These results were combined and reformulated into: The nitrate concentration is approximately inversely proportional to the *ratio* of photosynthesis rate over last 14 cultivation days before harvest and growth rate over last 14 cultivation days before harvest. As the rates of photosynthesis and growth are functions of global solar radiation intensity, temperature and CO<sub>2</sub>-concentration inputs (see table 10 in section 3.2.1), the ratio combines the effects of these inputs during the last 14 cultivation days on lettuce nitrate concentrations at harvest time.



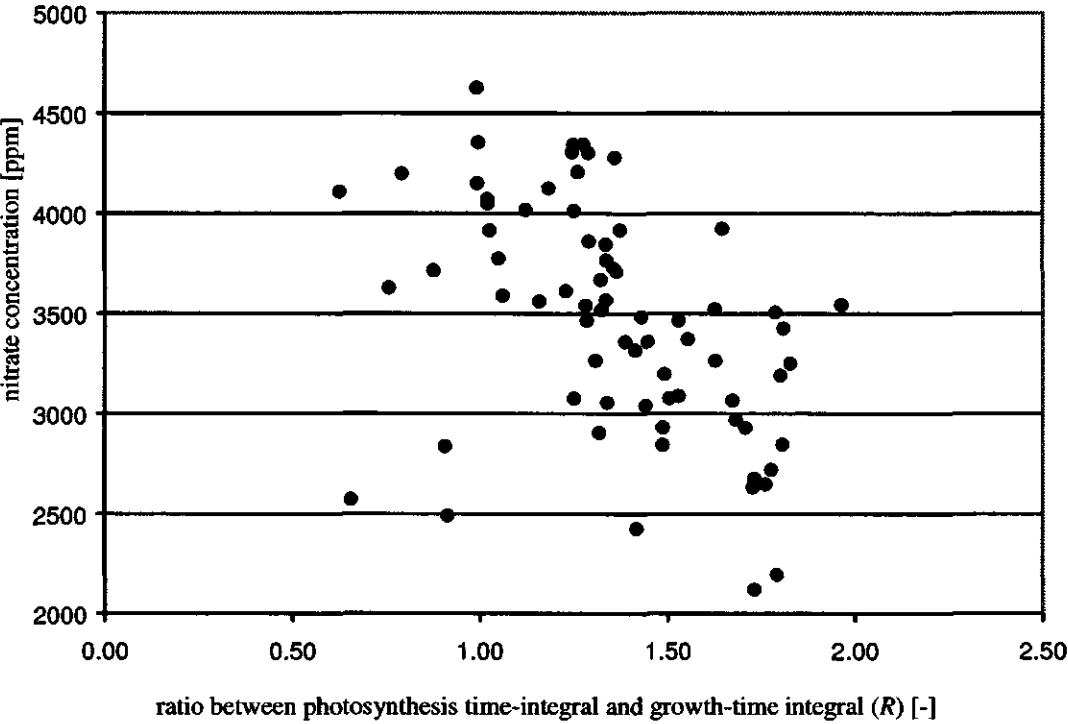


Figure 33: Lettuce nitrate concentrations plotted against ratios between photosynthesis time-integrals and growth time-integrals

Table 42: Specification of parameter and inputs used in equation 128

<i>name</i>	<i>symbol</i>	<i>value</i>	<i>units</i>
<i>parameters</i>			
final time	$t_f$	$1.2 \cdot 10^6$	s
photosynthesis efficiency	$\varepsilon$	0.07	$\text{mol [C]} \cdot \text{mol}^{-1} \text{ PAP}$
leaf conductance of $\text{CO}_2$	$\sigma$	$1.2 \cdot 10^{-3}$	$\text{m} \cdot \text{s}^{-1}$
growth yield	$v$	18.7	$\text{mol [C]} \cdot \text{m}^{-2}$
specific maintenance rate coefficient	$k$	$0.25 \cdot 10^{-6}$	$\text{s}^{-1}$
temperature effect parameter	$c$	0.0693	$^{\circ}\text{C}^{-1}$
reference temperature	$T^{\circ}$	20	$^{\circ}\text{C}$
<i>inputs</i>			
solar radiation intensity	$I$		$\text{mol [C]} \cdot \text{mol}^{-1} \text{ PAP} \cdot \text{m}^{-2} \cdot \text{s}^{-1}$
$\text{CO}_2$ -concentration in the greenhouse air	$C_{\text{Co}}$		$\text{mol} \cdot \text{m}^{-3}$
greenhouse air temperature	$T_a$		$^{\circ}\text{C}$

## A.2 Simple procedure to estimate climate changes that lead to lettuce nitrate concentrations of ca. 3500 and 4500 ppm

According to figure 33 it is save to assume that in general a ratio  $R_{3500}$  of 1.7 will lead to a nitrate concentration of 3500 ppm and a ratio  $R_{4500}$  of 1.0 to a nitrate concentration of 4500 ppm. Greenhouse growers can adjust these values by computing their own ratios and linking these values to measured lettuce nitrate concentrations.

To estimate quantitative changes of solar radiation intensity, temperature and  $\text{CO}_2$ -concentration that each lead to a nitrate concentration of 3500 or 4500 ppm through changes of ratios  $R$ , figures 34, 35 and 36 were created. These figures show one or more relations between values of solar radiation intensity, day-length or mean daily temperature plotted on the x-axis and a y-value that determines the ratio on the y-axis.

The steps of the estimation procedure are:

1. Define current values of solar radiation intensity, day-length, mean daily temperature and  $\text{CO}_2$ -concentration.
2. Determine which line in figure 34 is related to the  $\text{CO}_2$ -concentration.
3. Using this line and the solar radiation intensity value, determine an  $y_1$ -value.
4. Determine an  $y_2$ -value using figure 35 and the mean daily temperature value.
5. Determine an  $y_3$ -value using figure 36 and the day-length value.

6. If a nitrate concentration of 3500 is preferred then compute  $y_1^*$ ,  $y_2^*$ ,  $y_3^*$  by:  $y_1^* = \frac{R_{3500}}{y_2 \cdot y_3}$ ,

$$y_2^* = \frac{R_{3500}}{y_1 \cdot y_3} \text{ and } y_3^* = \frac{R_{3500}}{y_1 \cdot y_2}$$

If a nitrate concentration of 4500 is preferred then compute  $y_1^*$ ,  $y_2^*$ ,  $y_3^*$  by:  $y_1^* = \frac{R_{4500}}{y_2 \cdot y_3}$ ,  $y_2^* = \frac{R_{4500}}{y_1 \cdot y_3}$

$$\text{and } y_3^* = \frac{R_{4500}}{y_1 \cdot y_2}$$

7. Using figure 34, determine what change of  $\text{CO}_2$ -concentration or what change of maximum solar radiation intensity is needed to change  $y_1$  into  $y_1^*$ .
8. Using figure 35, determine what change of mean daily temperature is needed to change  $y_2$  into  $y_2^*$ .
9. Using figure 36, determine what change of day length is needed to change  $y_3$  into  $y_3^*$ .

Table 43 shows an example that illustrates the procedure for a preferred nitrate concentration of 3500 ppm.

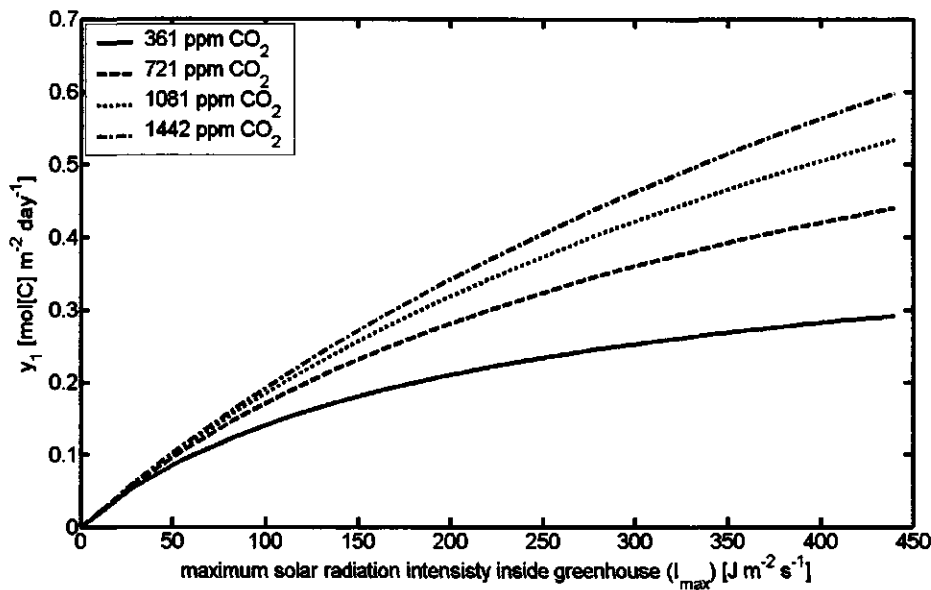


Figure 34:  $\gamma_1$ -factor plotted against the maximum shortwave or solar radiation intensity ( $I_{max}$ ) inside a greenhouse

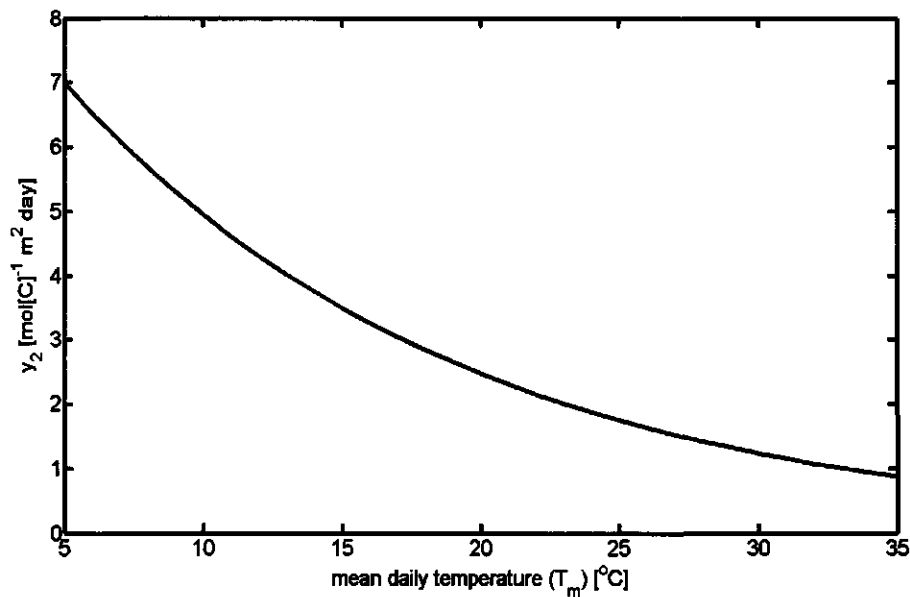


Figure 35:  $\gamma_2$ -factor plotted against mean daily temperature ( $T_m$ )

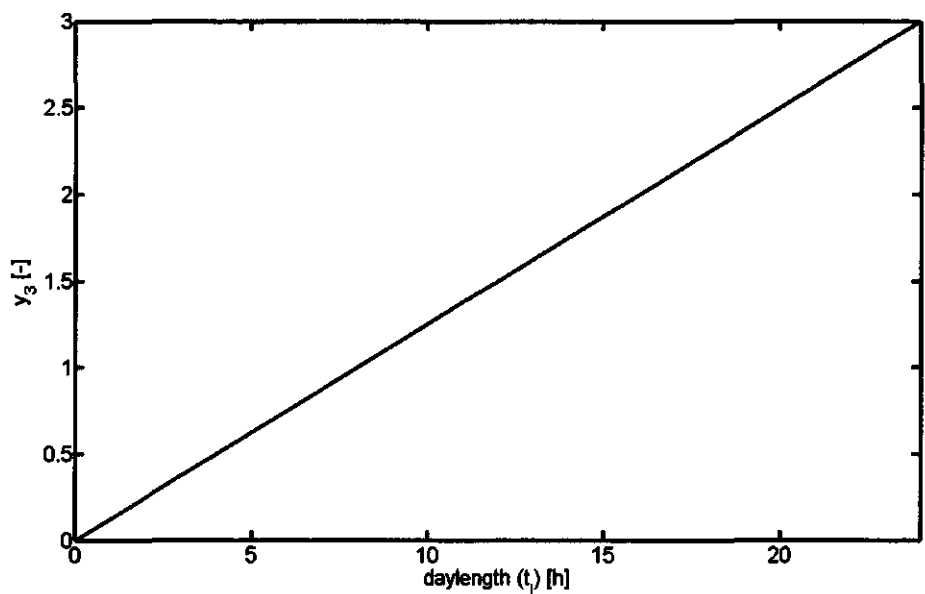


Figure 36:  $y_3$ -factor plotted against day length ( $t_i$ )

Table 43: Example that illustrates the procedure for a preferred nitrate concentration of 3500 ppm.

steps		results of steps
1	maximum inside global radiation ( $J \cdot m^{-2} \cdot s^{-1}$ ) CO <sub>2</sub> -concentration (ppm) mean daily temperature (°C) day-length (h) line legend in figure 1	4.5·10 <sup>2</sup> 361 27 14 — 361 ppm CO <sub>2</sub>
3	y <sub>1</sub> -value in figure 1	0.28
4	y <sub>2</sub> -value in figure 2	1.5
5	y <sub>3</sub> -value in figure 3	1.8
6	y <sub>1</sub> <sup>*</sup> -value y <sub>2</sub> <sup>*</sup> -value y <sub>3</sub> <sup>*</sup> -value	0.6 4.4 4.0
7	change of CO <sub>2</sub> -concentration (ppm) change of maximum solar radiation intensity	361 → 1442 ppm change impossible, because 0.3 is the maximum y <sub>1</sub> -value for a CO <sub>2</sub> -concentration of 361 ppm
8	change of mean daily temperature (°C)	27 → 12
9	change of day length (h)	change impossible, because 3.0 is the maximum y <sub>3</sub> -value.

This procedure is based on the computation of a ratio  $R$  by multiplication of factors  $y_1$ ,  $y_2$  and  $y_3$ . The factors are computed according to:

$$y_1 = n_d \int_0^{t_d} \frac{\epsilon I \sigma C_{ca}}{\epsilon I + \sigma C_{ca}} dt \quad n_d = 14, \quad t_d = 2.8 \cdot 10^4 \text{ s} \quad I = I_{\max} \sin\left(\frac{t}{t_d} \pi\right) \quad 129$$

$$y_2 = \frac{1}{\int_0^{t_f} v k e^{-(t_r - t')} dt} \quad t_f = 1.2 \cdot 10^6 \text{ s} \quad 130$$

$$y_3 = \frac{t_1}{t_8} \quad 131$$

After computing the factors  $y_1$ ,  $y_2$  and  $y_3$ , the ratio  $R$  is computed by:

$$R = y_1 y_2 y_3 \quad 132$$

## References

- Drews, M., I. Schonhof and A. Krumbein (1995). Nitrat-, Vitamin C-,  $\beta$ -Carotin- und Zuckergehalt von Kopfsalat im Jahresverlauf beim Anbau im Gewächshaus (*Lactuca sativa* L.). *Gartenbauwissenschaft*, 60, 180-187.
- Seginer, I., F. Buwalda and G. van Straten (1998). Nitrate concentration in greenhouse lettuce: a modelling study. *Acta Horticulturae*, 456, 189-197.
- Vanthoor, E. (2002). *Relation photosynthesis, growth and nitrate in Beitem experiments (Report)*, Wageningen University, Wageningen.